RIO TINTO WINU PTY LTD

Surplus Water Management PFS

Winu Copper Gold Project

Document no. Rev 0: 311012-01475-REP-HG-038

02 July 2025

Level 14, 240 St Georges Terrace
Perth WA 6000
Australia

T: +61 8 9278 81118111
Worley Consulting Pty Ltd
ABN 50 098 008 818

worley.com

Synopsis

The Winu Copper Gold Project (the Project) is predicted to produce surplus water from dewatering over the course of its life. The total life of mine (LoM) P50 and P90 surplus volume estimates from Project's water balance are 13.6 and 47.3 GL (or 23 and 47 L/s) respectively, with peak surplus in Year 9 (3.7 and 4.0 GL/a respectively).

The Project considered, as part of this study, the options of disposing of surplus water into two large infiltration ponds constructed in the surficial sand (currently unsaturated), and/or into a managed aquifer recharge (MAR) borefield nominally consisting of 15 injection sites into the deeper-lying sandstone aquifer (partly saturated). Small-scale field infiltration trials carried out in 2024 and 2025 within the footprints of the two planned ponds established an understanding of the short-term aquifer response to infiltration/injection and the connectivity between the shallow (surficial sand) and deep (sandstone aquifers).

A numerical model in MODFLOW-USG was developed to simulate the long-terms effects of surplus water disposal over the life of mine. The model is calibrated to observed effects of the infiltration trials and predictive simulations indicate that both disposal options may be viable. Some water is predicted to recirculate back into the open pit which is situated 2 to 2.5 km from the surplus water infrastructure.

Due to relatively deep-seated water levels, the risk associated with groundwater mounding and establishment of temporary groundwater dependent ecosystems (GDEs) is limited to the immediate surroundings of infiltration ponds.

Disclaimer

02 July 2025

Level 14, 240 St Georges Terrace
Perth WA 6000
Australia

T: +61 8 9278 81118111
Worley Consulting Pty Ltd
ABN 50 098 008 818

the overall capabilities of Worley to undertake the Work proposed and must be destroyed upon completion of those purposes.

Details on how personal information provided to Worley is processed can be found at https://www.worley.com/site-services/privacy.

PROJECT 311012-01475 - Rep-HG-038: Surplus Water Management PFS - Winu							
Rev	**Description**	**Originator**	**Reviewer**	**Worley Approver**	**Revision Date**	**Customer Approver**	**Approval Date**
Rev B	Draft for comments	LC/MS	MS	SA	05 June 2025		
Rev 0	For Client Use	LC/MS	MS	SA	02 July 2025		

-

Table of contents

Appendices

List of tables

List of figures

Acronyms and Abreviations

Acronyms and abbreviations	Definition
BoD	Basis of Design
GDEs	Groundwater Dependent Ecosystems
HSU	Hydrostratigraphic Unit
LoM	Life of Mine
mAHD	metres Australian Height Datum
mBGL	metres Below Ground Level
MAR	Managed Aquifer Recharge
Mtpa	Million tonnes per annum
MCA	Multi Criteria Analysis
PFS	Pre-Feasibility Study
PSD	Particle Size Distribution
RMS	Root Mean Squared
SoW	Scope of Works
SPT	Standard Penetration Testing
SWL	Static Water Level
TDS	Total Dissolved Solids

1. Introduction

The Winu copper-gold project, herein referred to as The Project, is located approximately 320 km east of Port Hedland in the Pilbara region of Western Australia.

The Project involves the development of a below-water table open-cute mining operation with a mineral processing plant located adjacent to the proposed mine and ore production. For the purpose of surplus water management, the results from water balance modelling using a nominal processing rate of 10.0 Million tonnes per annum (Mtpa) have been applied, noting that this may differ from Mineral Resource/Ore Reserve estimates (Worley, 2025a). The median results from this modelling show the mine will be in a water surplus from years 1 to 16 (Figure 1-1), with additional periods of excess water management likely required during sporadic high rainfall events occurring throughout the life of mine (LoM). The volumes of excess water per year to be included in the design of the surplus management strategy have been adopted from the P50 and P90 quantities in Figure 1-1 from the 2025 Water Balance modelling.

The options for surplus water management investigated in this report include infiltration into predominantly unsaturated surficial sands via infiltration ponds (**pond option**) or into a partially saturated Permian Sandstone aquifer situated underneath surficial sands and silcrete (the latter forming an intervening low permeability layer – aquitard).

The latter option requires boreholes to be drilled through the aquitard into the sandstone aquifer and is referred to as the **reinjection (MAR) option**. A combination of the two options is also investigated with a previously considered quarry option excluded.

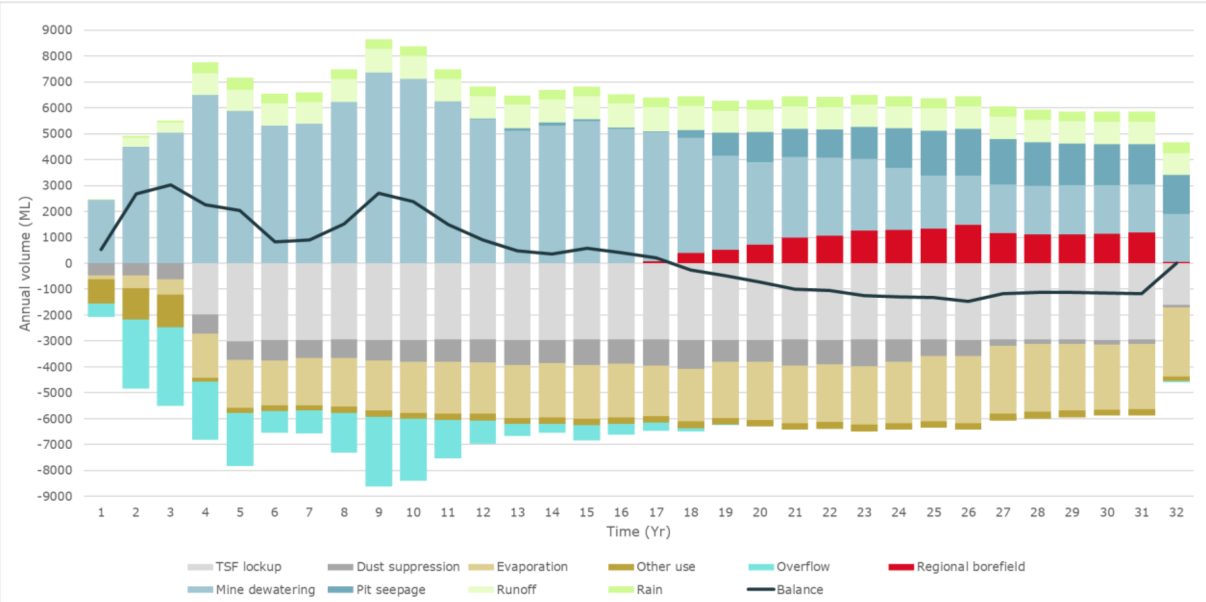

Figure 1-1: Median annual site water balance (ML/year) from 10 Mtpa processing capacity water balance modelling (Worley 2025a)

1.1 Scope of Work

The Scope of Work (SoW) is detailed in the 2024/2025 Infiltration Pond Pre-Feasibility Study Phase and aims to form a basis of design (BoD) for surplus water management for a base case 10.0 Mtpa processing capacity. Developing this BoD requires:

- Interpretation of the geotechnical and geophysical data from the geotechnical field program,
- Calibrating the depth of sand, silcrete and sandstone layers and a weathering profile from geophysics surveys and develop an updated conceptualisation of near-surface geology and incorporating it into the whole site geological conceptualisation,
- Use this updated conceptualisation to produce relevant lithological layers that can be used as input to update the numerical groundwater model,
- Interpretation and analysis of infiltration testing data from site investigation of the two test pond locations and selection of aquifer parameters for the shallow surficial sands and deep Permian sandstone aquifer needed for excess water management options,
- Update the existing numerical groundwater model with the updated conceptualisation layers and hydraulic parameters,
- Highlight within the BoD:
  - Groundwater mounding thresholds (depth below ground surface and extents),
  - Heritage and environmentally sensitive areas to be avoided when constructing and,
  - Groundwater inflows to pit including flow paths and travel times.
- Test using the numerical groundwater model and base case water rates from latest water balance modelling for 10.0 Mtpa processing capacity, assess and compare the following two (currently) preferred options for surplus water management:
  1. 2 x infiltration ponds into sand,
  2. 2 x infiltration ponds into sand and Managed Aquifer Recharge (MAR) bores through silcrete into sandstone.
- Using a Multi Criteria Analysis (MCA) approach determine the cost and impacts of each option and select the preferred option for the PFS.
- For the preferred option, test the model sensitivity to:
  - Higher excess water flow rates extracted from water balance modelling,
  - Hydraulic conductivity of sand,
  - Leakage through aquitard, and
  - Hydraulic conductivity of sandstone.
- Use results of sensitivity analysis to select the model scenario that forms the basis of the preferred option design.
- Solute transport modelling to determine the mixing qualities of injected water in the partially saturated sandstone aquifer and the impact of total dissolved solids (TDS) within the aquifer.

Table 1-1: Excess water (ML/yr) from water balance modelling (Worley, 2025a)

Year	Min	P10	P20	P50	P80	P90	Max
1	507	519	524	536	558	569	615
2	2649	2665	2668	2683	2707	2720	2772
3	2981	2997	3001	3015	3040	3052	3104
4	1555	1834	1962	2262	2989	3325	4008
5	1124	1458	1627	2041	2866	3201	4116
6	0	250	363	830	1775	2075	3186
7	0	300	441	890	1850	2131	3251
8	485	888	1036	1526	2589	2860	4057
9	1696	2041	2236	2694	3680	4025	5196
10	1370	1759	1910	2389	3375	3752	4877
11	547	868	1005	1486	2446	2805	3931
12	0	272	431	893	1836	2145	3231
13	0	0	50	479	1322	1616	2668
14	0	0	0	354	1325	1583	2832
15	0	10	151	574	1594	1849	2993
16	0	0	0	402	1262	1553	2668
17	0	0	0	299	1160	1420	2547
18	0	0	0	135	868	1096	1998
19	0	0	0	43	615	833	1546
20	0	0	0	0	415	572	1185
21	0	0	0	0	334	480	1014
22	0	0	0	0	311	459	993
23	0	0	0	0	216	376	782
24	0	0	0	0	136	274	620
25	0	0	0	0	89	214	542
26	0	0	0	0	31	135	439
27	0	0	0	0	108	253	663
28	0	0	0	0	148	290	711
29	0	0	0	0	143	290	723
30	0	0	0	0	143	292	719
31	0	0	0	0	126	274	703
32	0	0	0	58	523	740	1203

2. Geophysical Investigation Outcomes

A total of nineteen (19) seismic refraction geophysics survey lines have been conducted across the two proposed infiltration pond locations. The survey lines cross-cut the area and target shallow geology (<60m) to provide more data on the depth of the unsaturated surficial sands, the lateral extent of the silcrete aquitard and the thickness of the partially saturated sandstone aquifer or depth to mudstone.

Geotechnical investigation bores at the two test pond locations and along the lines of survey were used to correlate the geophysics results and assign lithologies. The investigation included the drilling, logging and standard penetration testing (SPT) of nineteen (19) diamond bores. The geotechnical investigation results have been presented in a separate report (Knight Piésold, 2024) and will not go into detail here.

Comparing the shear wave velocity results presented in cross section to logged lithologies enabled a geology to be assigned to a specific range of shear wave velocities and this has been used to update the geological conceptualisation and Leapfrog model. Near surface shear velocities have been divided into three (3) ranges to classify geology. Low range of 300 to 450 m/s which are representative of surficial sands, typically 0 to 20 m deep, a mid-range of 450 to 700 m/s which incorporates the grouping of sandstone and weathered silcrete, and a high range of 700 to 1000 m/s that classifies fresh silcrete, competent sandstone and basal mudstones. Figure 2-1 demonstrates how the geophysics results have been used to develop the infiltration pond geological model, with the complete survey and leapfrog model geologies available in Appendix A. These results show the competent sandstones and silcrete are not laterally extensive throughout the model domain.

The survey lines relative to the infiltration pond and test bore locations are shown below in Figure 2-2.

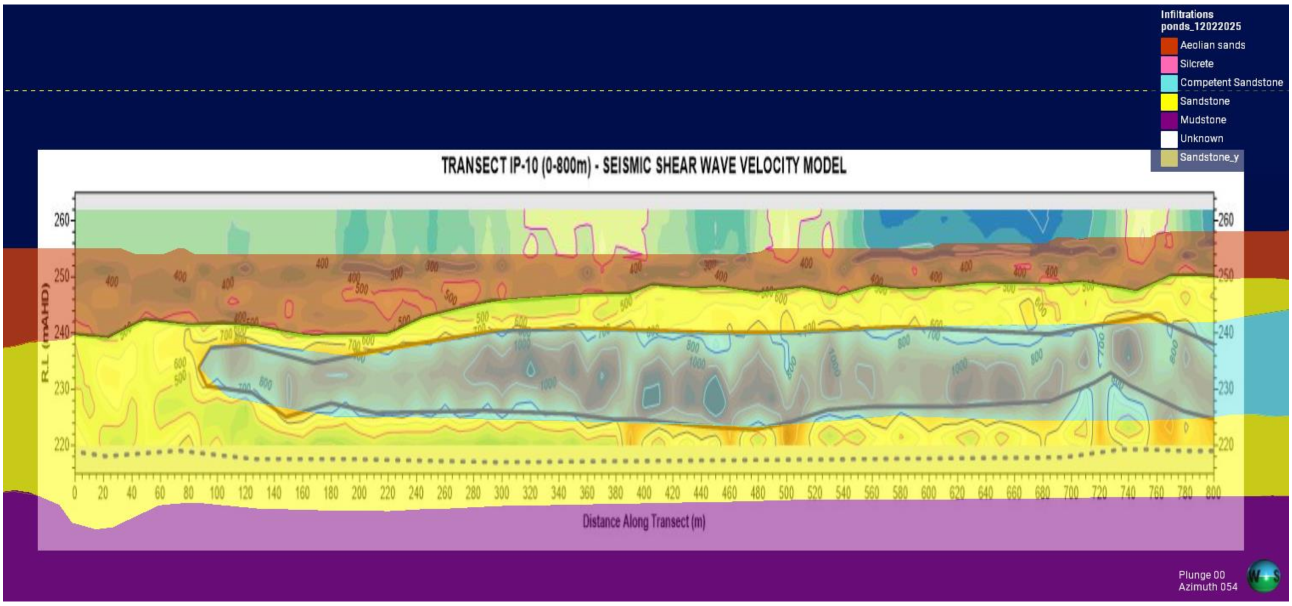

Figure 2-1: Geophysics cross section and assigned geology in Leapfrog geological model

worley consulting

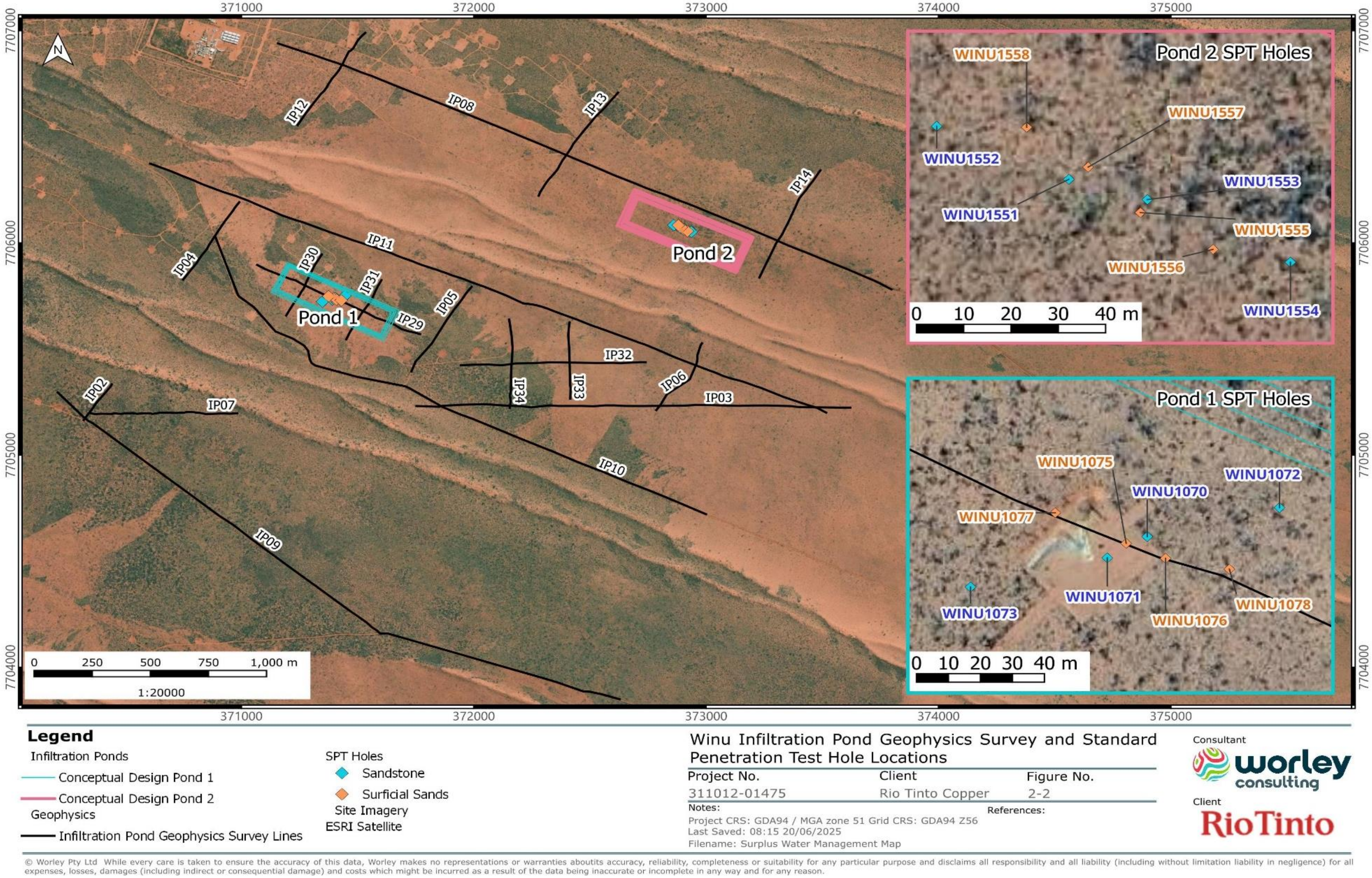

Figure 2-2: Locations of Geophysics survey lines and SPT holes across the pond study areas

3. Leapfrog Model

Previous numerical modelling (Advisian, 2023) of infiltration options distinguished between surficial (aeolian) sand, silcrete and sandstone as separate layers. The geophysical surveys, geotechnical and hydrogeology bores from the infiltration pond studies along with infiltration testing at the infiltration pond locations have provided a new dataset to improve the geological conceptualisation of the shallow geology (<60m).

These results led to an update of the Leapfrog-derived geological model, focusing on the aeolian sands and silcrete contact, the sandstone and mudstone contacts as well as the implementation of a new layer of competent sandstone which informs the hydrostratigraphic unit (HSU) structure of the numerical modelling update.

Observations of the sandstone lithology from drill core and chip cuttings show a heterogeneity with depth and between the two pond locations. Figure 3-1 and Figure 3-2 show the variation in the composition of the sandstone at the two pond locations. The sandstone at pond 2 is typically more weathered, with a larger grain size and weaker cementation expected to result in higher porosity and hydraulic conductivity. This difference in observed geology forms the basis to implement the new competent sandstone layer.

Depth to mudstone between the two sites differs by approximately 8 m, pond 1 the sandstone-mudstone contact average depth is 42.9 m compared to 50.9 m at pond 2. This impacts the water table at both locations, average static water level (SWL) at pond 1 is 42.22 mBGL (212.55 mAHD) with a saturated thickness of up to 3.66 m compared to pond 2 SWL of 38.92 mBGL (210.86 mAHD) and a saturated thickness of up to 12 m. The thicker water table at pond 2 has likely increased the amount of water throughflow and degree of weathering of the sandstone over time and increased the permeability of the deeper sandstone at this location.

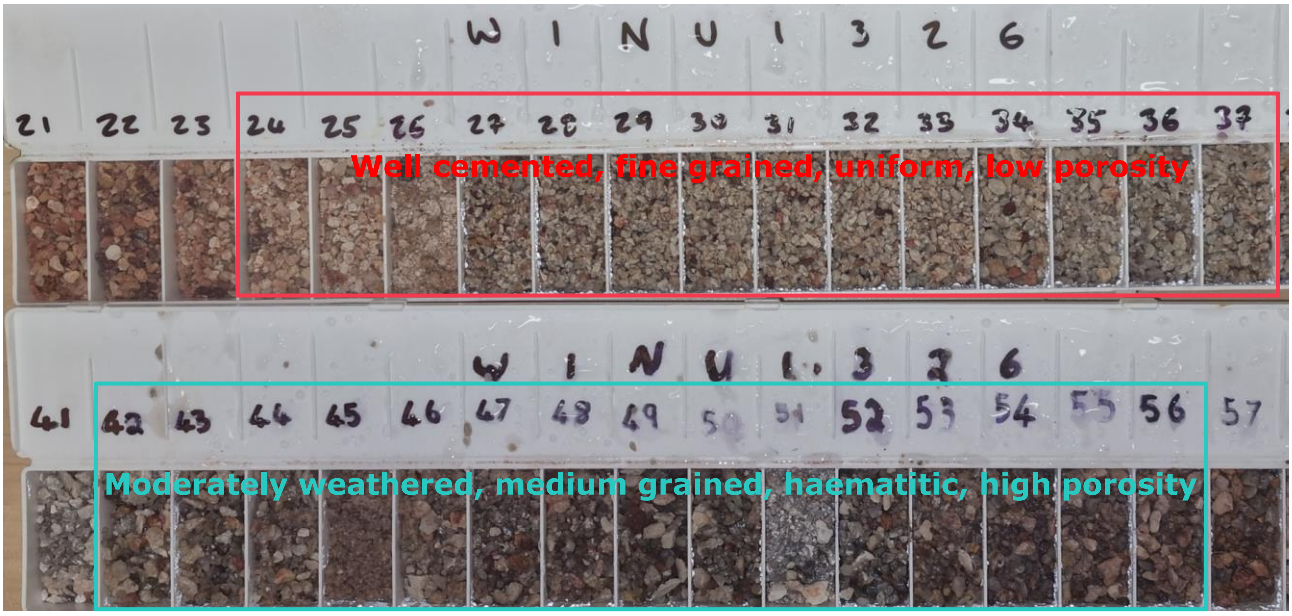

Figure 3-1: WINU1326 infiltration bore drill chip samples from Pond 2

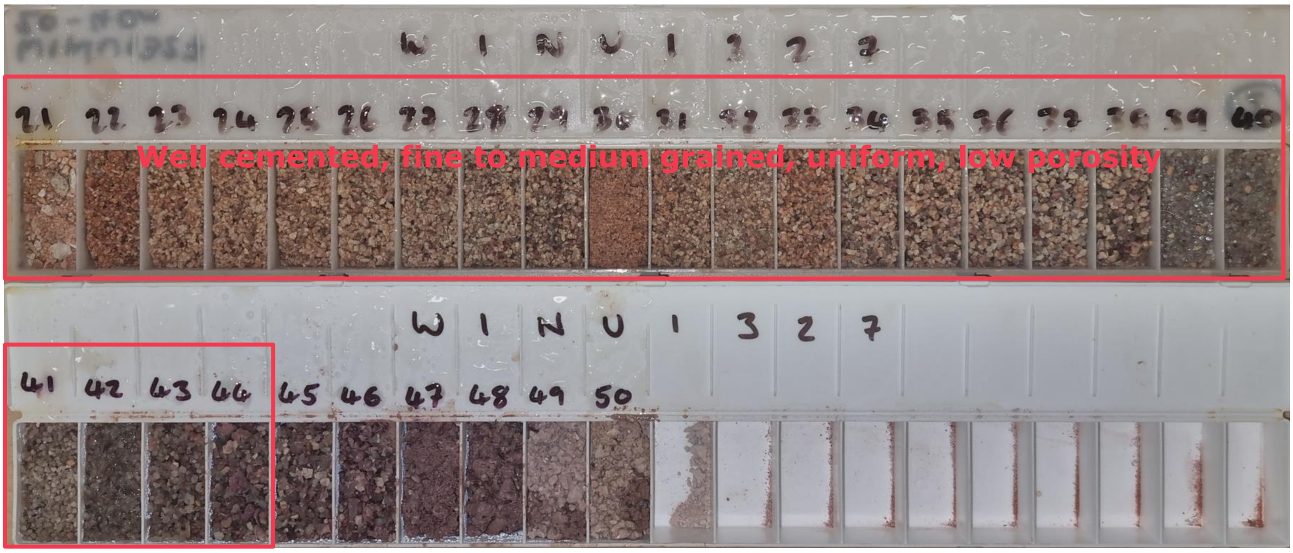

Figure 3-2: WINU1327 infiltration bore drill chip samples from Pond 1

The geophysics results show little difference in shear wave velocities between well cemented, low porosity sandstone and fresh silcrete and for the purpose of this model have been grouped into one layer referred to as 'Competent Sandstone'. Weathered silcrete has a similar shear wave velocity to the larger grain size and more porous sandstone and is grouped together into one 'Sandstone' layer. All geophysical cross sections used to assign lithologies and develop the geological model can be viewed in Appendix A.

3.1 Surficial Sand Cover

The geophysics surveys have provided a more laterally extensive dataset to refine model layers and depth of surficial sands around the pond locations than previous models relying on point data from drillhole logs. This layer has been merged with a surficial sand surface from the pit drill area where there is a large amount of lithology data to interpret and produce a contact surface with sandstone.

The previous conceptualisation assumed the average site-wide thickness and depth of Aeolian sands to be 10 to 15 m, where now it is understood to be closer to 8 to 12 m. The thickness of the regional surficial sand cover is now reduced based on this updated conceptualisation and has been used to interpolate the base of surficial sands to the model boundaries where there is a lack of drillhole and geophysics data.

The top of the surficial sands is constrained by topography with a north increasing gradient of approximately 0.01°. The sandstone and mudstone contact dips to the north at approximately 0.23°, increasing the depth between mudstone and topography which is accounted for by increasing the thickness of the surficial sands HSU.

3.2 Sandstone Contacts

In areas where the silcrete is highly weathered and determined likely to transmit water based from the geotechnical core logging, it is grouped with sandstone and can be in direct contact with the surficial sands. The presence of highly weathered silcrete has been interpolated from the geophysics cross sections

The depth to mudstone is reasonably understood across the Winu project area from drillhole lithology data. It shows an undulating surface which has been captured in detail within the drill area where most drillhole data is available. The mudstone generally dips to the north-west at gradient of approximately 0.23° which has been used to extrapolate the depth of the mudstone to the model boundaries where there is a lack of drilling information.

3.3 Competent Sandstone

A new modelled layer of competent sandstone has been implemented from field observations of diamond core, hydraulic testing and geophysical survey test results. Silcrete observed around the project is often associated with Ferricrete, while the properties differ slightly, for the purpose of this model and for the remainder of this report they shall be grouped together and referred to as silcrete. Where the silcrete is slightly weathered to fresh it is grouped with the competent sandstone. Field observations show heterogeneity in the weathering intensity and competency of both the silcrete and sandstone lithologies that has been modelled as a laterally in-extensive and undulating sedimentary layer (Figure 2-1).

The competent sandstone is modelled as an intrusional surface to capture the non-uniform stratigraphic sequence and varied extent of the lithology. The geophysical surveys have allowed a more detailed interpolation of the competent sandstone layer up to 1,300 m from the pond areas with a simple extrapolation applied beyond this area.

4. Hydraulic Testing

4.1 Approach

The aim of infiltration testing was to determine the available storage of the unsaturated surficial sands and the partially saturated sandstone across the two (2) proposed infiltration pond locations and provide a calibration dataset for the numerical modelling optimisation. A total of six (6) production bores were drilled, two screened in the surficial sands and four (4) in the sandstone aquifer, two of which fully penetrate and the remaining two partially penetrate the sandstone aquifer. The test locations and details are summarised in Table 4-1.

A constant head was applied to the test bores and the flow rate required to maintain the head was recorded for the duration to monitor the rate of infiltration. Water was supplied from the nearest production bore in the metasediment aquifer which is hydraulically separated from the tested aquifers by the mudstone HSU aquitard. Relative locations of the proposed infiltration ponds and the test locations are shown in Figure 2-2.

A total of 16 monitoring bores were installed in the diamond drilled holes used as part of the Geotechnical SPT study of the pond areas discussed in Section 2 and reported in Knight Piésold (2024). Each pond test location incorporates eight monitoring bores, four each in the surficial sands and the sandstone aquifer, with screens installed to the base of the tested aquifer.

The monitoring bores are arranged in an approximately linear design centred around the production bore to monitor the lateral movement of water and quantify water table mounding. All bore construction and lithology logs are available in Appendix B.

Table 4-1: Summary of infiltration test bores and test dates

Bore ID	Screened aquifer	Start date of pumping	End date of pumping	Infiltration flow rate (L/s)
Pond 1				
WINU1327 (10" PB)	Fully penetrating sandstone	22/01/2025	03/02/2025	0.5 to 3.0
Sump Test	Surficial sand	21/02/2025	18/03/2025	1.8 to 2.2
WINU1325 (10" PB)	Partially penetrating sandstone	25/03/2025	08/04/2025	1.1 to 2.5
WINU1070 (2" MB)	Fully penetrating sandstone	10/04/2025	17/04/2025	0.8 to 5.7
Pond 2				
WINU1326 (10" PB)	Fully penetrating sandstone	29/10/2024	21/11/2024	6.0 to 9.0
Sump Test	Surficial sand	24/11/2024	14/12/2024	3.0 to 5.2

4.2 Test design

The general infiltration test design consisted of five bores in a linear arrangement with an injection bore located in the centre with two monitoring bores spaced equally on either side on the injection bore, Figure 4-1 and Figure 4-2.

The injection bores are 10" PVC installs with 1.75 mm screens installed in the base of the tested aquifer. The sandstone aquifer deep injection bores contain either a bentonite seal or a fully grouted surface seal set into the silcrete layer to prevent vertical movement of water through the annulus between the two tested aquifers.

The monitoring bores are 2" blank PVC with 1.00 mm slotted lengths to the base of the tested aquifer that have been installed in PQ3 diameter diamond holes, drilled as part of the geotechnical program. The completed bore designs can be seen in Appendix B.

Observations from the infiltration tests form the calibration dataset for the updated numerical model developed for this study.

4.2.1 Surficial Sands

The shallow surficial sands monitoring bores are drilled approximately 7 m and 30 m either side of the injection bore. Initial falling head tests conducted while developing the injection bores to remove drilling muds demonstrated very low flow rates (<0.1 L/s) would be achieved during the test.

Subsequently a sump test was devised as an alternative method of testing the infiltration capacity of the surficial sands. The test sumps are trapezoidal prisms with approximate dimensions of 10.3 x 3.5 x 1.9 m and a total volume of 33.7 m^3. The sump was dug as central to the monitoring network and as close to the shallow infiltration bore as possible based on limitations of the cleared pad footprint and proximity to other bore locations.

The surficial sands test was designed to apply a constant head of 1.7 m within the sump (0.2 m BGL). The flow rate required to maintain this head was monitored for the duration of the test. Pond 2 sump test used the automatic valve head control unit to control water level within the sump which resulted in some variability in the flow data and a float valve system was used during the Pond 1 test which produced a more consistent flow rate.

4.2.2 Sandstone Aquifer

The deep sandstone monitoring bores are located approximately 15 m and 60 m away from the central injection bores. The bore locations for the tests can be seen in Figure 4-1 and Figure 4-2, with test results detailed below.

Field observations during drilling and initial testing of the production bores required the modification of some aspects of the test approach. Sandstone chips showed an increase in grain size and weathering while cementation decreased with depth, particularly in the bottom five metres of the sandstone. Therefore, partially penetrating production bores were also installed to enable the testing of vertical hydraulic conductivity of the sandstone aquifer.

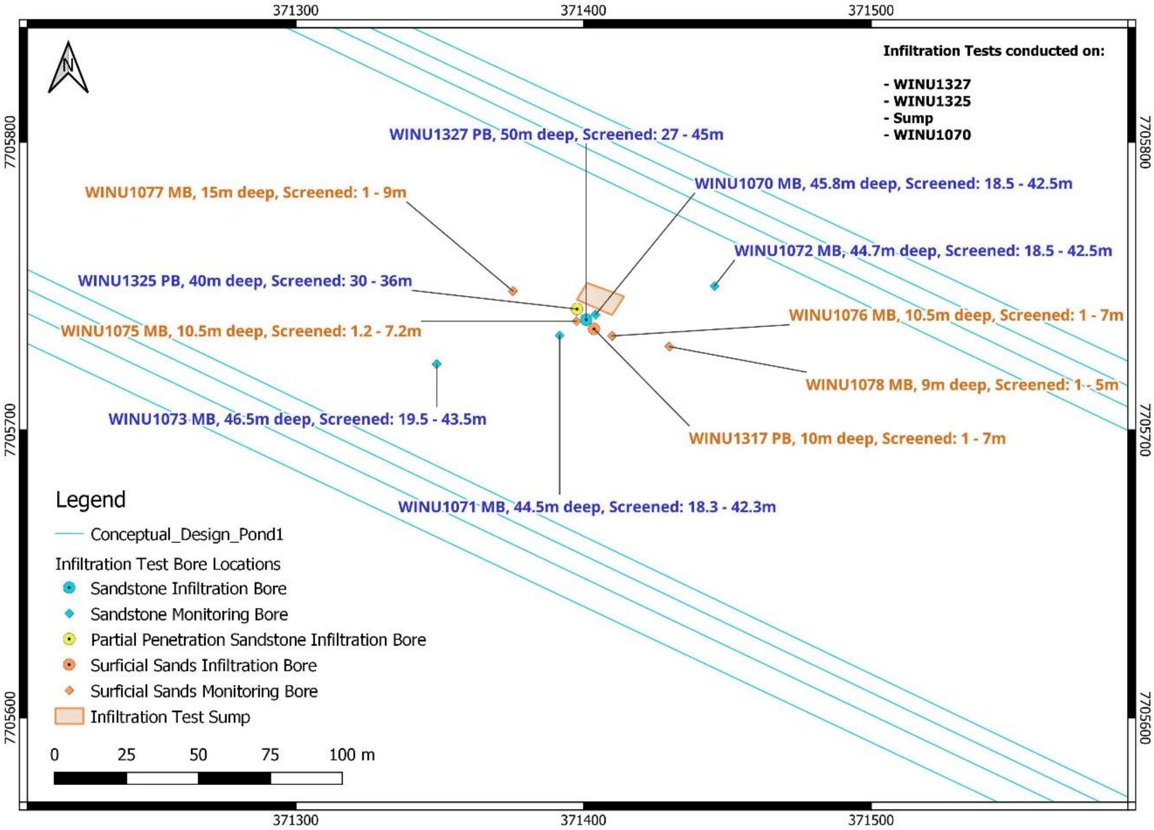

Figure 4-1: Pond 1 infiltration test setup

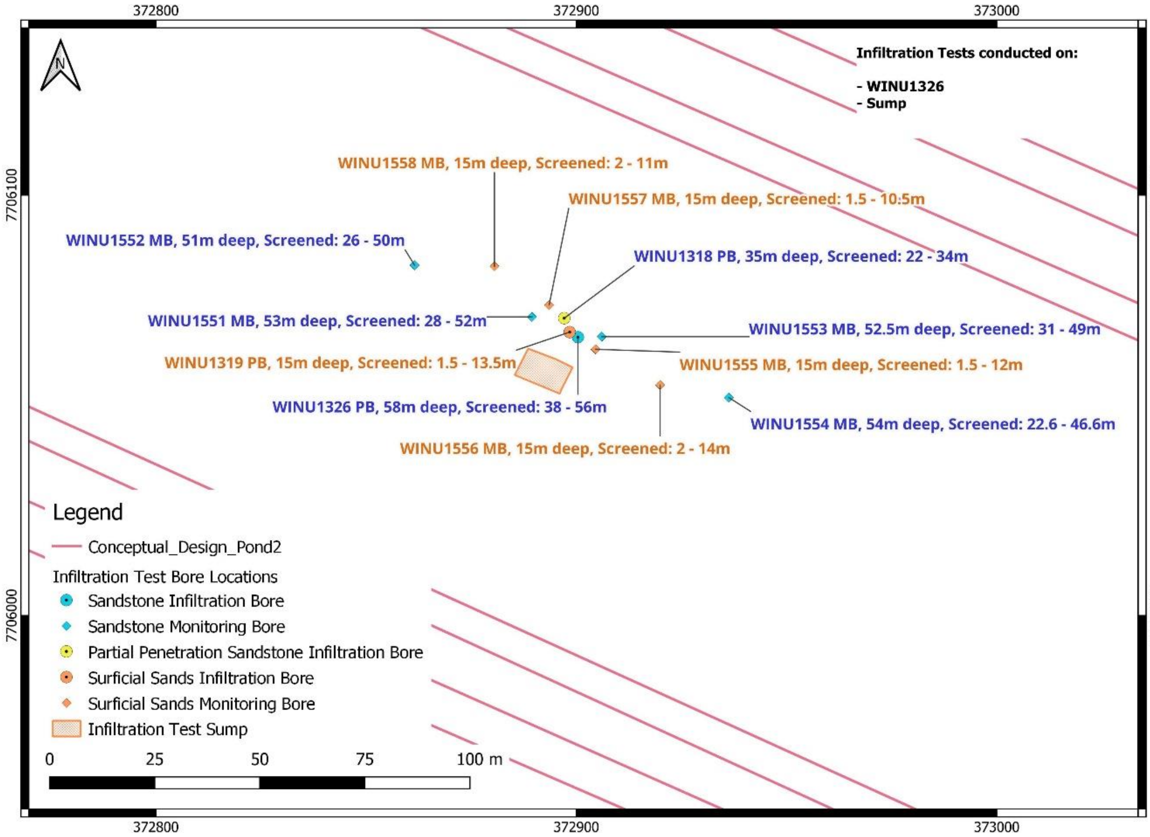

Figure 4-2: Pond 2 infiltration test setup

4.3 Surficial Sands Infiltration Testing

Low infiltration rates of the bores located in the surficial sands, likely resulting from low well efficiencies and difficulties conditioning and removing drilling muds from boreholes in an unsaturated aquifer required an alternative testing methodology. Subsequently a sump was dug as central to the monitoring network as practicable, and a constant head applied to induce infiltration into the surficial sands. The volume of water required to maintain the constant head can then be used to calculate the rate of infiltration.

4.3.1 Pond 1 Sump Test

Infiltration rates for the duration of the test gradually rose from 1.75 to 2.2 L/s with the water level in the sump controlled at a constant 1.65 m using a float valve. The three shallow monitoring bores installed in the surficial sands and within 10 m of the sump showed a response to the infiltrating water and those beyond 20 m showed no water level response. Figure 4-3 shows once the water supply to the sump was turned off the water levels reacted and started falling within 3.5 hours, returning to static water level (SWL) within 45 hours as summarised in Table 4-2.

Of the deep monitoring bores installed in the sandstone four (4) of the five (5) bores showed an increase in water level in response to the sump test, the first of which WINU1070 started rising late on day 16 (403.5 hours into the test). This indicates the surficial sands and sandstone aquifer are connected through the silcrete aquiclude. Figure 4-4 shows the water levels in the deep bores continued to rise for up to 5 days once pumping ceased showing the impact of release from storage in the surficial sands continuing to infiltrate down to the sandstone aquifer.

Table 4-2: Summary of pond 1 sump test borehole observations. Pumping duration 605 hrs (25.2 days)

Bore ID	Screened aquifer	Distance from sump (m)	Time WL start to rise (hrs)	Max WL rise (m)	Time to recover to SWL post pumping (hrs)
WINU1317	Surficial sand	6.94	60.6	1.68	44.77
WINU1075	Surficial sand	7.46	49.8	1.2	34.02
WINU1076	Surficial sand	7.27	67.0	1.18	42.02
WINU1077	*Surficial sand*	*22.49*	*Dry*	*Dry*	*Dry*
WINU1078	*Surficial sand*	*22.77*	*Dry*	*Dry*	*Dry*
WINU1325	*Partially Penetrating Sandstone*	*3.44*	*Dry*	*Dry*	*Dry*
WINU1070	Sandstone	2.2	403.5	1.61	*N/A**
WINU1327	Sandstone	5.16	432.1	1.46	*N/A**
WINU1071	Sandstone	13.90	501	0.76	*N/A**
WINU1072	Sandstone	31.64	531.8	0.46	*N/A**
WINU1073	*Sandstone*	*53.64*	*Dry*	*Dry*	*Dry*

**Due to scheduling the entirety of recovery monitoring could not be concluded*

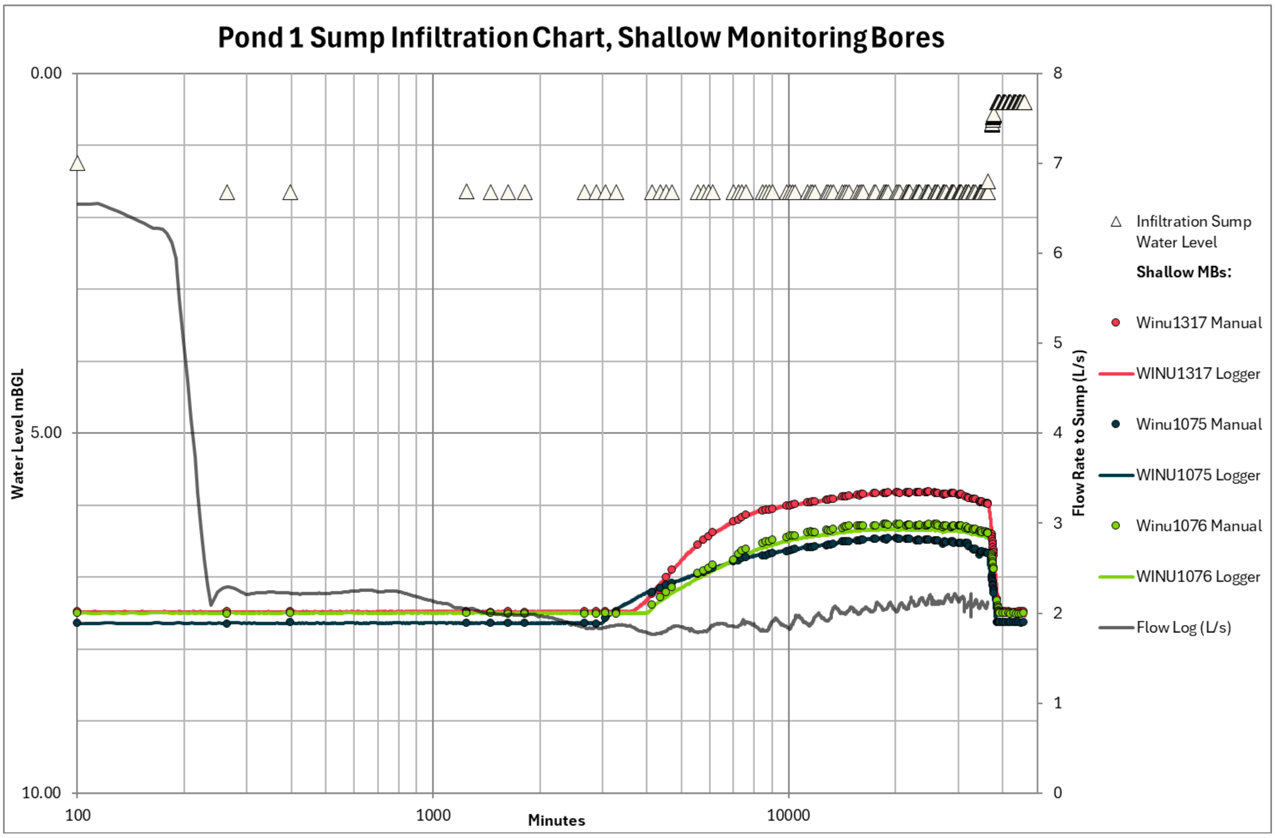

Figure 4-3: Pond 1 Sump test shallow monitoring bore water levels

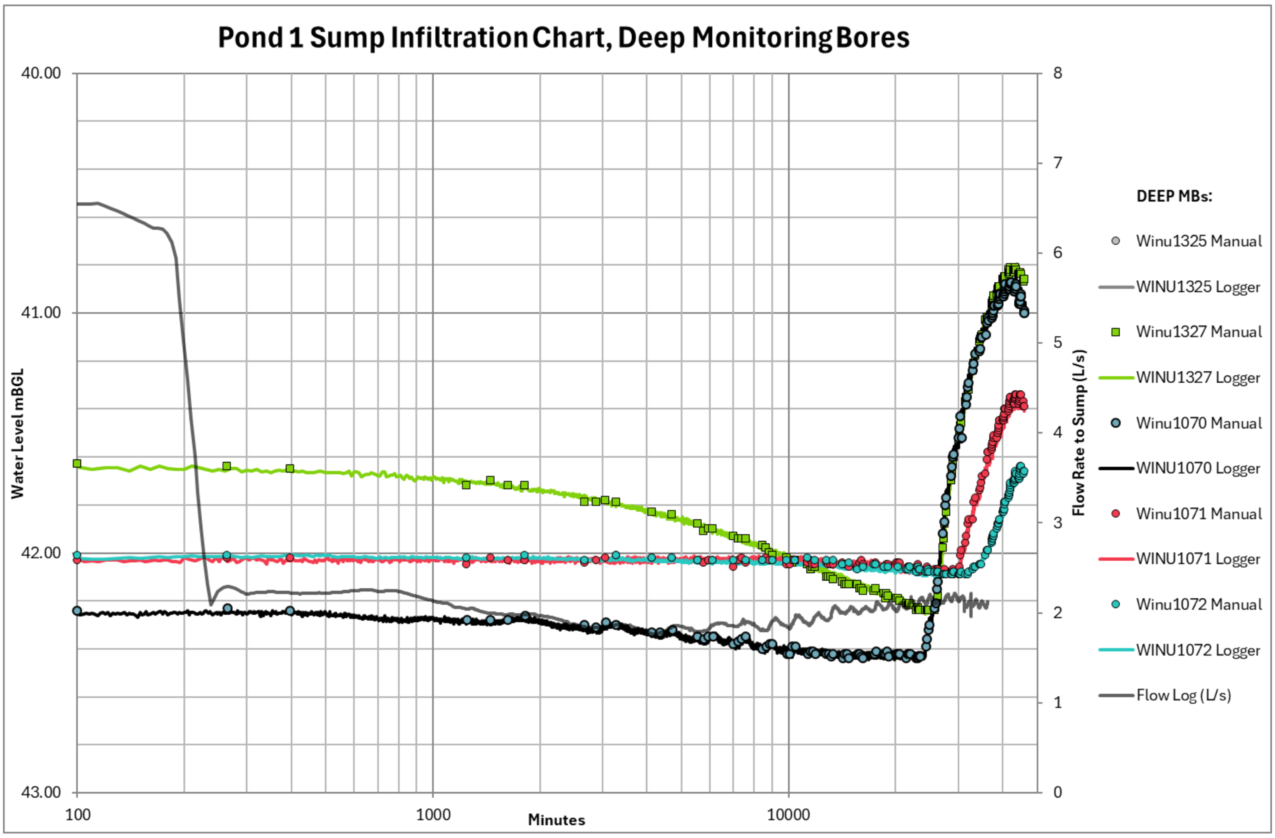

Figure 4-4: Pond 1 Sump test deep monitoring bore water levels

4.3.2 Pond 2 Sump Test

Injection rates increased from 3 to 5.2 L/s over the duration of the test, with the water level in the sump controlled at a constant 1.7 m using a pressure transducer linked to the pump control unit. The three closest monitoring bores in the surficial sands showed a response and mounding to infiltrating water, with the two monitoring bores beyond 20 m not reacting to the test.

The five deep monitoring bores show no initial water level response until 10.8 days (259 hours) into the test after which all bores recorded an increasing water level trend. This confirms leakage through the silcrete aquiclude from the surficial sands to the sandstone aquifer. A rapid rise in water level in WINU1318 after 64 hours is attributed to a fault in the installation allowing water down the annulus of the bore.

Water level recovery in the shallow monitoring bores back to SWL was relatively fast compared to the deep monitoring bores (Table 4-3). Deep monitoring bore WINU1553 took the longest time to return to SWL taking 30.1 days to return to baseline, more than twice the time for initial water level rise to be observed. Due to the apparent fault in construction WINU1318 measures the water levels in both aquifers and has been used to interpret water level recovery post test. The change in gradient of water levels as indicated in Figure 4-6 highlights the release of water from storage and subsequent drainage from the surficial sands, creating a secondary water source to the sandstone aquifer post pumping.

Table 4-3: Summary of Pond 2 sump test borehole observations, pumping duration 480 hrs (20 days)

Bore ID	Screened aquifer	Distance from sump (m)	Time WL start to rise (hrs)	Max WL rise (m)	Time to recover to SWL (hrs)
WINU1319	Surficial sand	7.2	38.2	2.88	342.17**
WINU1555	Surficial sand	8.1	43.1	4.71	53.08
WINU1557	Surficial sand	11.5	97.1	3.36	37.33
WINU1558	*Surficial sand*	*21.2*	*Dry*	*Dry*	*Dry*
WINU1556	*Surficial sand*	*21.3*	*Dry*	*Dry*	*Dry*
WINU1318*	Partially penetrating sandstone	6.67	64.7*	18.57*	606.17*
WINU1326	Sandstone	7.00	259.3	0.41	478.5
WINU1551	Sandstone	9.46	347.7	0.40	507.83
WINU1553	Sandstone	10.08	276	0.47	723.17
WINU1552	Sandstone	33.54	412.2	0.28	*N/A*
WINU1554	Sandstone	37.87	388.4	0.27	*N/A*

**Water level rise understood to be a fault in construction allowing water to flow down the annulus*

***Bore contains drilling muds which decrease the bore efficiency and delay the time to return to SWL*

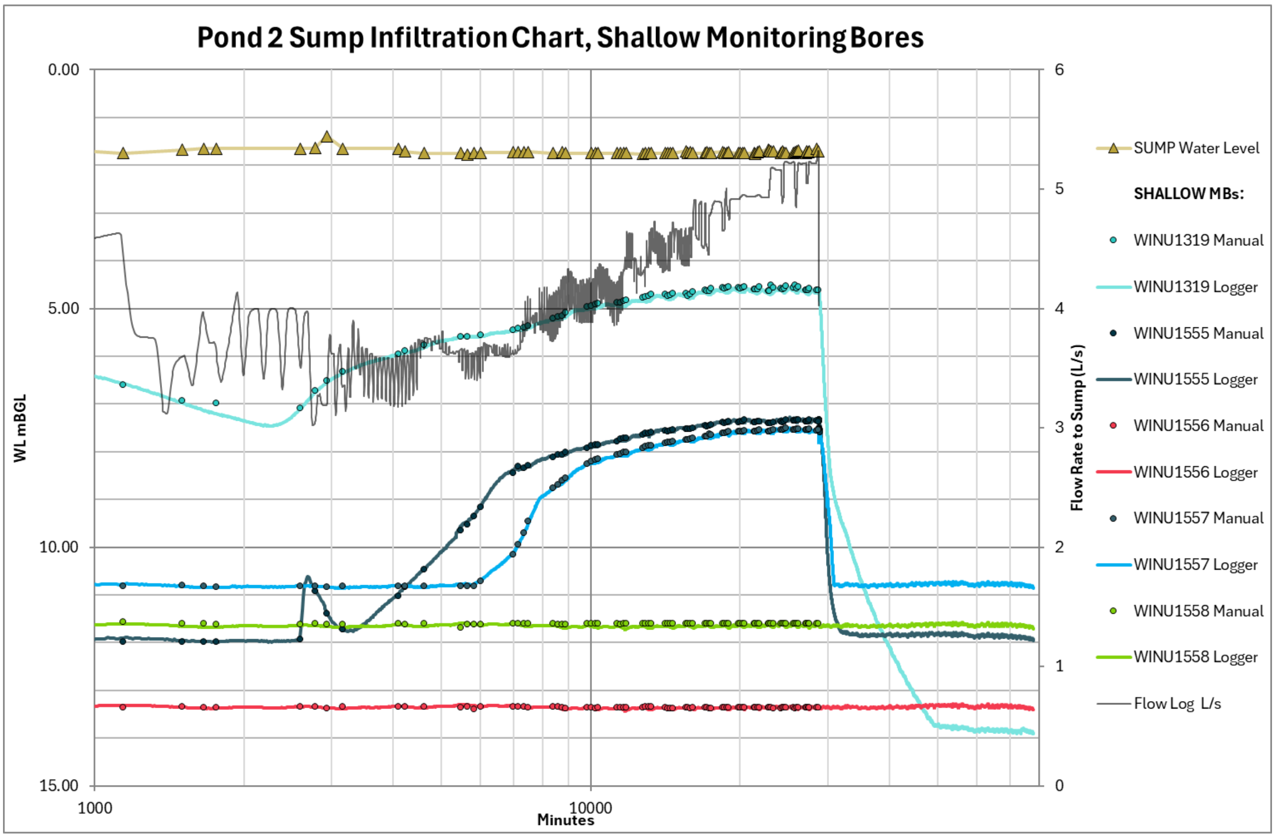

Figure 4-5: Pond 2 Sump test shallow monitoring bore water levels

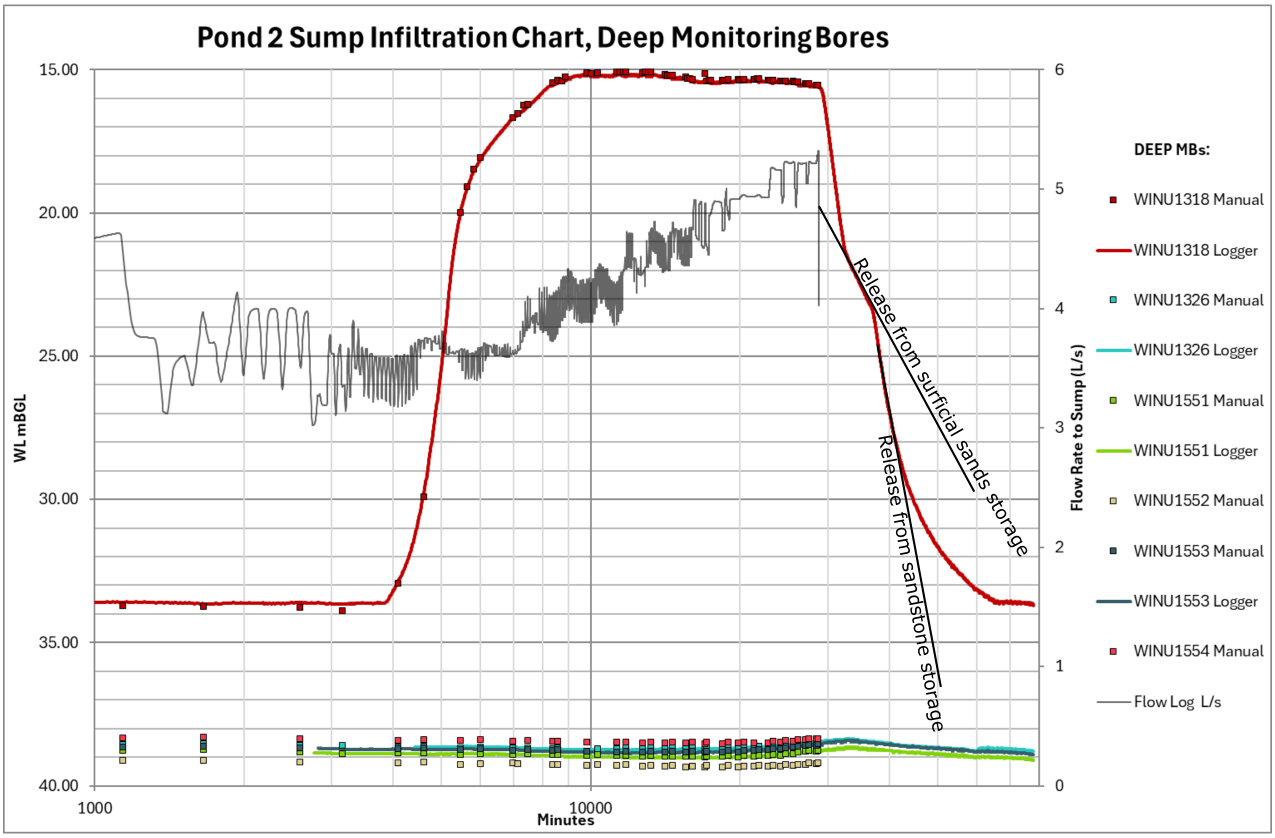

Figure 4-6: Pond 2 Sump test deep monitoring bore water levels

4.4 Sandstone Infiltration Testing

Of the four 10 inch injection bores drilled, three were used for infiltration testing to test the high variability in the geological properties of the sandstone aquifer, WINU1318 at pond 2 had initial infiltration flow rates less than 0.5 L/s and therefore testing was cancelled. The two bores installed in competent sandstone (WINU1325 and WINU1327) recorded initial infiltration rates of 2 L/s, sufficient to induce mounding greater than 1 m in the sandstone aquifer. Decreasing flow rates as these tests progressed to 1 L/s or less became insufficient to maintain water level mounding in the aquifer and water levels would gradually decrease for the remainder of the test.

Subsequently, an additional infiltration test was conducted on WINU1070, a 50 mm monitoring and diamond drilled bore to test the impact of drilling methodology on infiltration rate. WINU1070 responded to all tests at Pond 1 indicating good hydraulic connection to the other bores in the test monitoring network and potential for high infiltration flow rates.

4.4.1 Pond 1, Bore Injection Testing

Three boreholes, two fully penetrating and one partially penetrating the sandstone aquifer were used to test the infiltration capacity of the aquifer. Drilling logs from these bores show the sandstone encountered is typically very fine to fine, competent and low porosity, Appendix B. Table 4-4 summarises the tests conducted at Pond 1.

Table 4-4: Summary of Pond 1 Sandstone test observations

Bore ID	Screened aquifer	Infiltration rate (L/s)	No. of bores with water level rise	Maximum water level rise of non PB (m)
		Pond 1		
WINU1327 (10” PB)	Fully penetrating sandstone	3.0 to 0.5	2	1.82
WINU1325 (10” PB)	Partially penetrating sandstone	2.5 to 1.1	4	1.1
WINU1070 (2” MB)	Fully penetrating sandstone	5.7 to 0.8	3	9.1

4.4.1.1 WINU1327 fully penetrating bore

Infiltration rate decreased from 2.4 to 0.23 L/s over the first five days of testing while maintaining a constant head of 2.5 mBGL in the injection bore (Figure 4-7). During the early stages of the test when flow rates were 2.25 L/s, water level mounding up to 1.82 m was induced in WINU1070 and WINU1071 as shown in Figure 4-8. As the flow rate decreased below 2.25 L/s the water levels gradually started to decrease, and no water level response was observed in the far monitoring bores Table 4-5.

Table 4-5: Summary of Pond 1 WINU1327 sandstone test bore observations, pumping duration 286.5 hrs (11.9 days)

Bore ID	Screened aquifer	Distance from injection bore (m)	Time WL start to rise (hrs)	Max WL rise (m)
WINU1327 Injection Bore	Sandstone	0	0	38.63
WINU1070	Sandstone	3.7	7.1	1.82
WINU1071	Sandstone	10.8	22.3	0.91
WINU1325	Partially penetrated sandstone	4.9	*N/A*	0
WINU1072	Sandstone	46.1	*N/A*	0
WINU1073	Sandstone	54.2	*N/A*	0

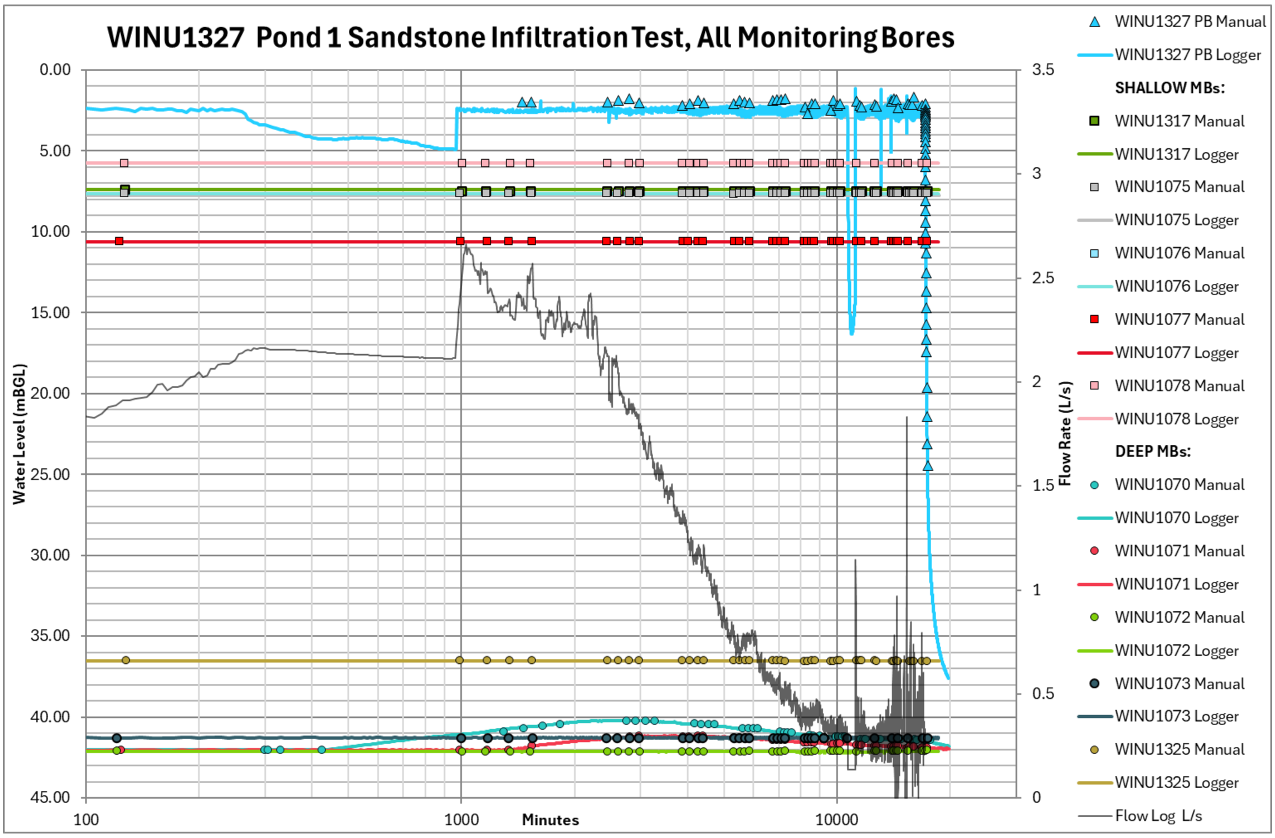

Figure 4-7: Pond 1 WINU1327 PB Sandstone test all monitoring bore water levels

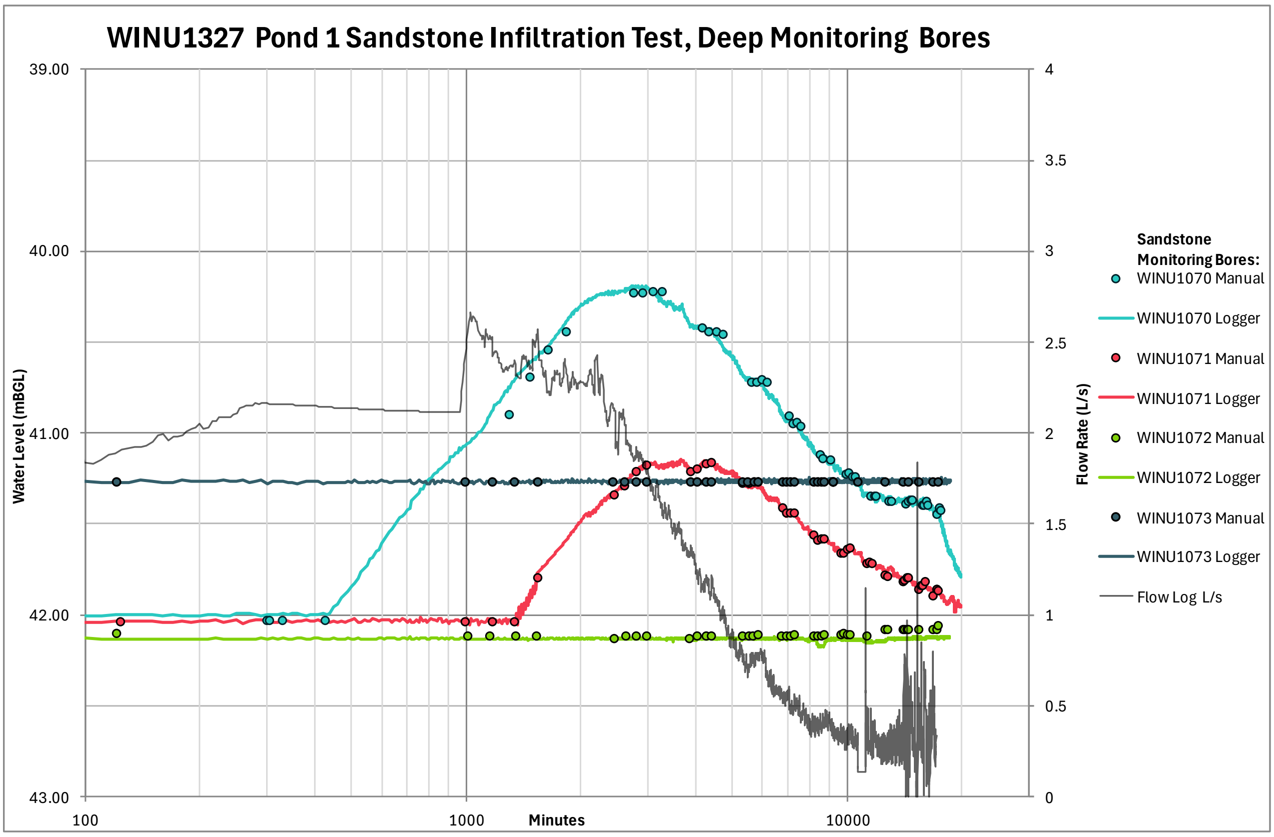

Figure 4-8: Pond 1 WINU1327 PB Sandstone test deep monitoring bore water levels

4.4.1.2 WINU1325 partially penetrating bore

From 26 hours onwards in the test the flow rates gradually decreased from 2.4 L/s to 1.1 L/s which impacted the rate and degree of water level mounding. The water level in the injection bore is varied and ranges from 0 – 4 mBGL due to a malfunction in the automatic head control unit and switching to manual flow rate control. The initial higher flow rates are potentially resulting from filling available storage in the competent sandstone or from clogging of pore spaces by remnant drilling muds present in the borehole and mobilized by the injected water.

Table 4-6: Summary of Pond 1 WINU1325 sandstone test bore observations, pumping duration 336 hrs (14 days)

Bore ID	Screened aquifer	Distance from injection bore (m)	Time of start WL rise (hrs)	Max WL rise (m)	Time to recover to SWL (hrs)
WINU1325 Injection Bore	Partially penetrated Sandstone	0	0	34.89	*N/A*
WINU1070	Sandstone	6.7	0.16	1.06	*N/A*
WINU1327	Sandstone	10.5	1.67	1.1	44.8
WINU1071	Sandstone	11.0	2.1	0.81	44.8
WINU1072	Sandstone	48.5	33.3	0	*N/A*
WINU1073	Sandstone	52.4	*N/A*	0	*N/A*

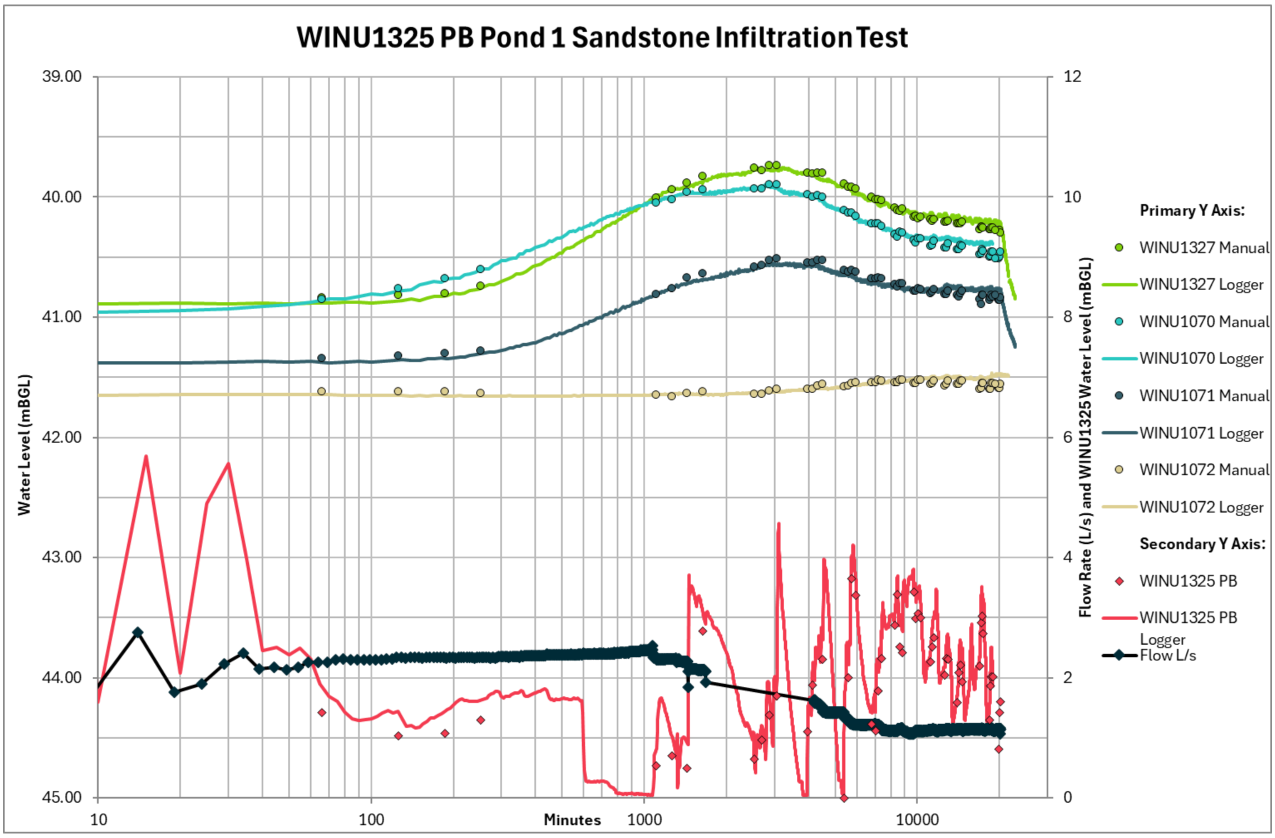

Figure 4-9: Pond 1 Partial Penetration Sandstone WINU1325 PB Infiltration Test

4.4.1.3 WINU1070 diamond drilled monitoring bore

Infiltration testing of WINU1070 was conducted to determine the impact of drilling methodology on infiltration rates. Flow rates were at their highest at 5.7 L/s for the first 25 hours of the test before they started to subsequently decrease over the remainder of the test. Water level response in WINU1327 showed over 9 m of mounding at these flow rates but immediately started to fall with decreasing infiltration rates. An equilibrium water level mounding of 4.16 m when flow rate stabilised at 3 L/s before a further reduction of flow rate occurred.

Table 4-7: Summary of Pond 1 WINU1070 sandstone test bore observations, pumping duration 168 hrs (7 days)

Bore ID	Screened aquifer	Distance from injection bore (m)	Time of start WL rise (hrs)	Max WL rise (m)	Time to recover to SWL (hrs)
WINU1070 Injection Bore	Sandstone	0	0	31.95	*N/A*
WINU1327	Sandstone	3.7	3.5	9.26	75
WINU1325	Partially penetrated Sandstone	6.7	*N/A*	0	*N/A*
WINU1071	Sandstone	14.4	9.2	0.8	75.5
WINU1072	Sandstone	42.5	43.25	0.16	*N/A*
WINU1073	Sandstone	57.8	*N/A*	0	*N/A*

Initial flow rates in the diamond hole despite the smaller hole diameter had the highest flow rates of all Pond 1 tests before sequentially decreasing to 1 L/s. The quick response in water levels to cessation of pumping (Figure 4-10) shows the sandstone aquifer has a larger capacity for infiltration than the bore can provide. While taking water level measurements during the test some boreholes showed the presence of drilling muds within the bore, impacting the well efficiency and potentially becoming mobilized, blocking pore space and reducing conductivity and infiltration rates over time.

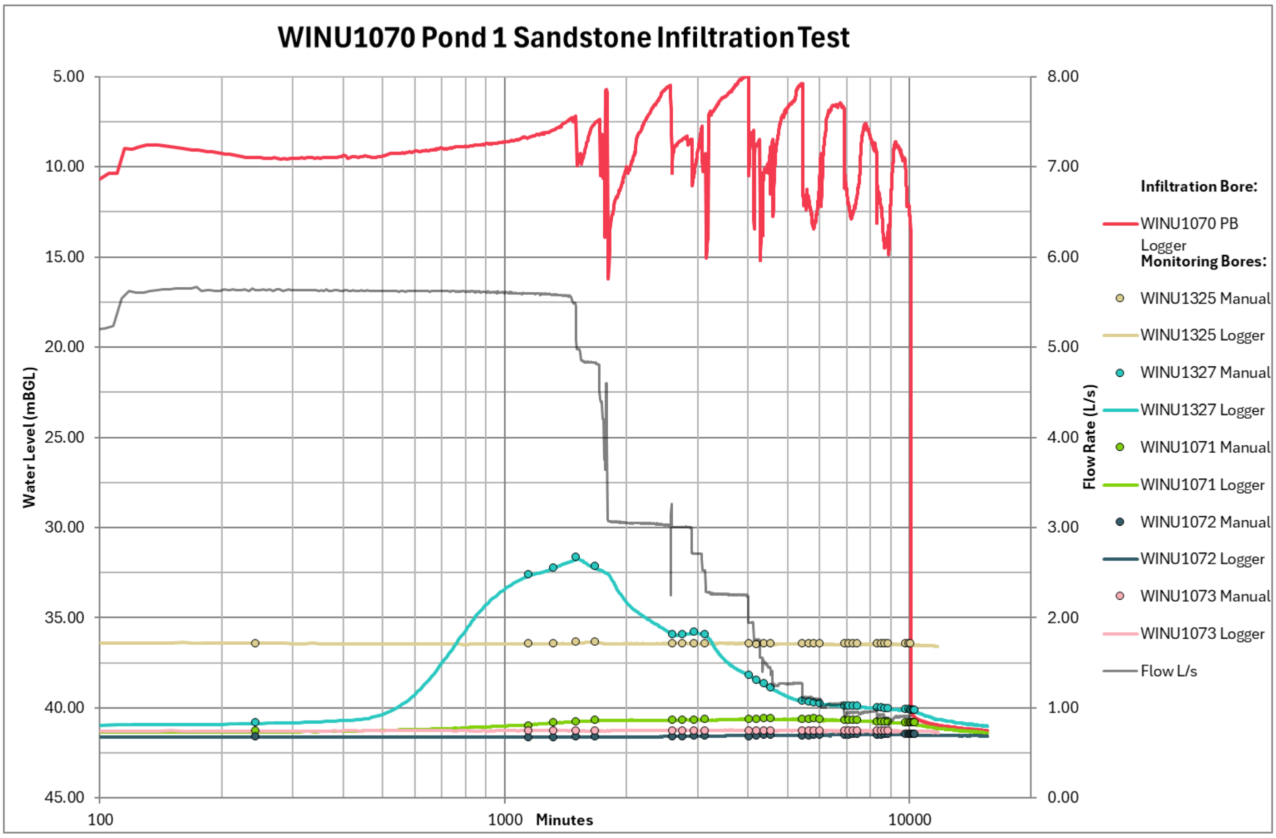

Figure 4-10: Pond 1 Sandstone WINU1070 MB Infiltration Test

4.4.2 Pond 2, WINU1326 Injection Testing

WINU1326 intersected mudstone at 57 m and screened from 38 to 56 m within the sandstone aquifer. SWL was recorded at 39.01 mBGL, and a constant head of approximately 3 mBGL was applied creating an effective head pressure of 36 m for the duration of the test.

Flow rates decreased from 9 to 6 L/s over the duration of the test, the highest sustained flow rates of all the tests. The measured mounding results are summarised in Table 4-8, with the highest mounding in the partially penetrating bore WINU1318, the only test where mounding in a partial penetration bore was observed. Despite the highest infiltration rates of all the tests, the peak water level mound was the lowest indicating a potential for a high lateral conductivity zone in the base of the sandstone at Pond 2. This is further evidenced by the increased water level of the two distal monitoring bores showing an increased lateral mobilization of water in the sandstone.

The initial flow rates remained consistent at 8.75 L/s for the first 90.3 hours before decreasing and re-establishing a new constant flow rate of approximately 6.2 L/s. The other sandstone bore tests the flow rates trended toward 1 L/s or less indicating WINU1326 was more successful at developing and removing drilling muds. Therefore the decrease in flows can be interpreted as the initial filling of storage and saturation of the sandstone at a rate of approximately 2.5 L/s.

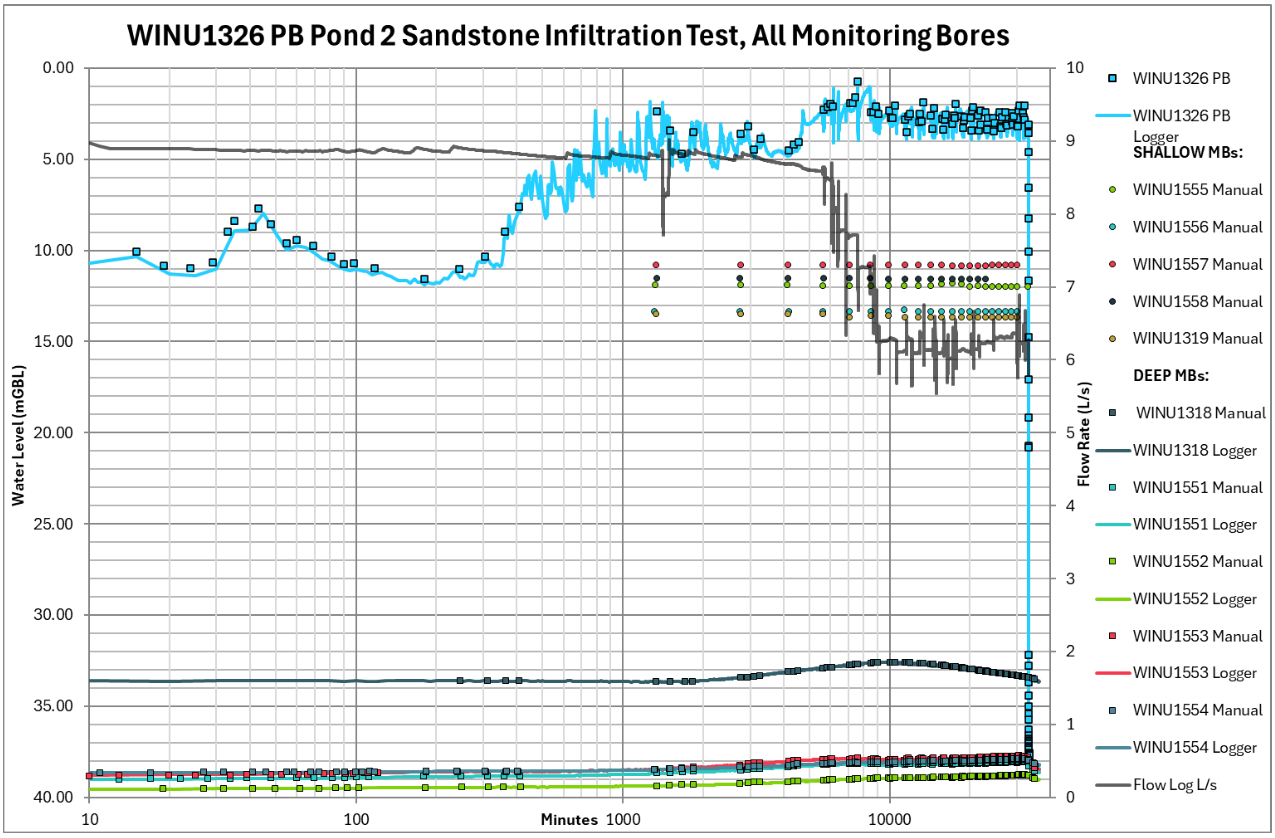

Figure 4-11: Pond 2 Sandstone test all monitoring bore water levels

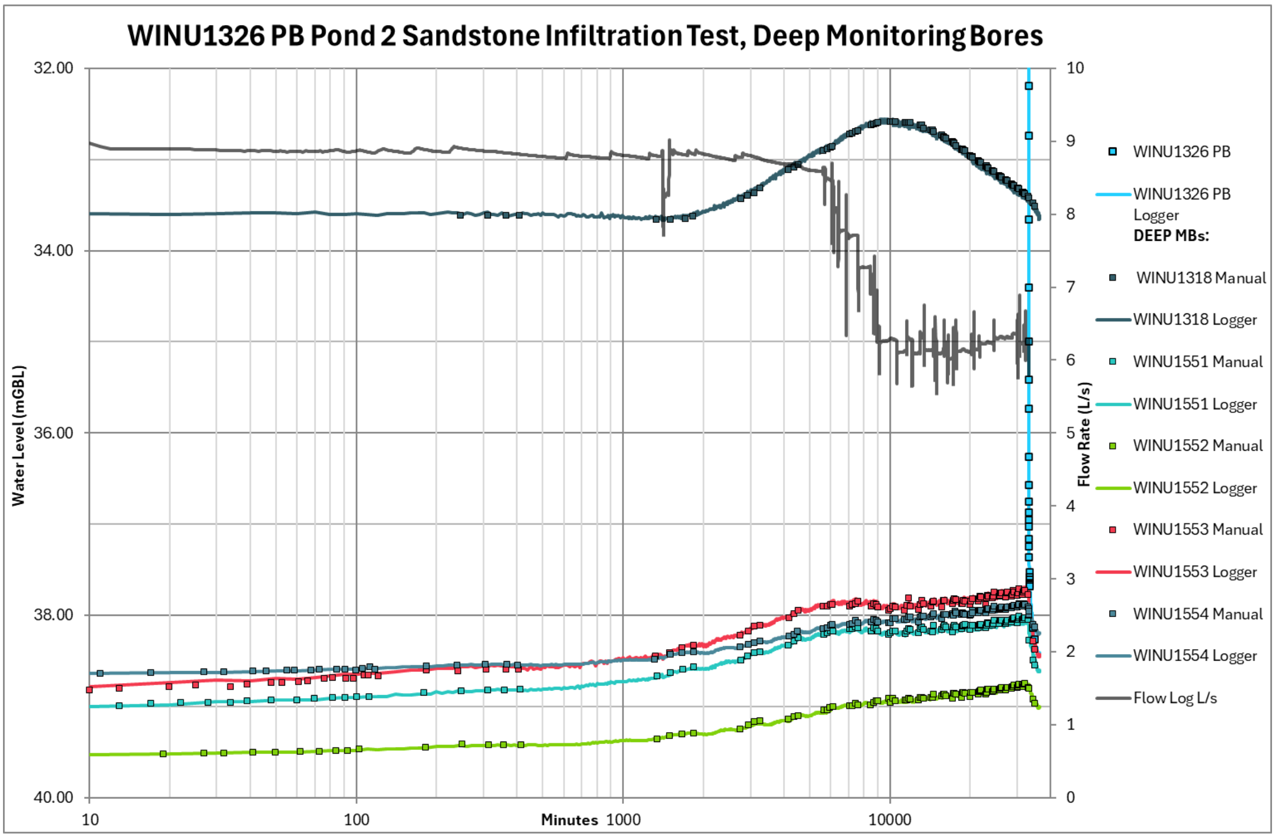

Figure 4-12: Pond 2 Sandstone test deep monitoring bore water levels

Table 4-8: Summary of pond 2 WINU1326 Sandstone test borehole observations, pumping duration 552 hrs (23 days)

Bore ID	Screened aquifer	Distance from injection bore (m)	Time of start WL rise (hrs)	Max WL rise (m)	Time to recover to SWL (hrs)
WINU1326 Injection bore	Sandstone	0	0	37.97	*N/A*
WINU1318	Partial Penetration Sandstone	5.6	1720	1.01	53
WINU1553	Sandstone	5.7	1501	0.70	*N/A*
WINU1551	Sandstone	12.0	690	0.65	*N/A*
WINU1554	Sandstone	38.7	1318	0.66	*N/A*
WINU1552	Sandstone	42.5	1230	0.59	*N/A*

5. Aquifer parameters

The results from these infiltration tests form the basis for calibrating the numerical modelling optimisation and have been used to update the conceptual model of the two key aquifers, each of which are summarised below.

5.1 Surficial Sands

Water level mounding results have been used to estimate the specific yield of the surficial sands by dividing the volume of water required to induce mounding in the aquifer by the volume of the mound as calculated from the graphs presented in Figure 5-1 and Figure 5-2 and assuming a symmetrical mound. The results are presented in Table 5-1 and other key findings below:

Table 5-1: Estimated specific yield of surficial sands

Test ID	HSU	Volume of aquifer mounding(m^3)	Volume of injected water (m^3)*	Specific yield (*Sy*)
Pond 1 Sump	Surficial sand	1,240	328	0.26
Pond 2 Sump	Surficial sand	3,859	1,102	0.28

**Calculated from factoring the total injected to achieve stable water levels in surficial sand bores, minus the volume leaking to the sandstone aquifer*

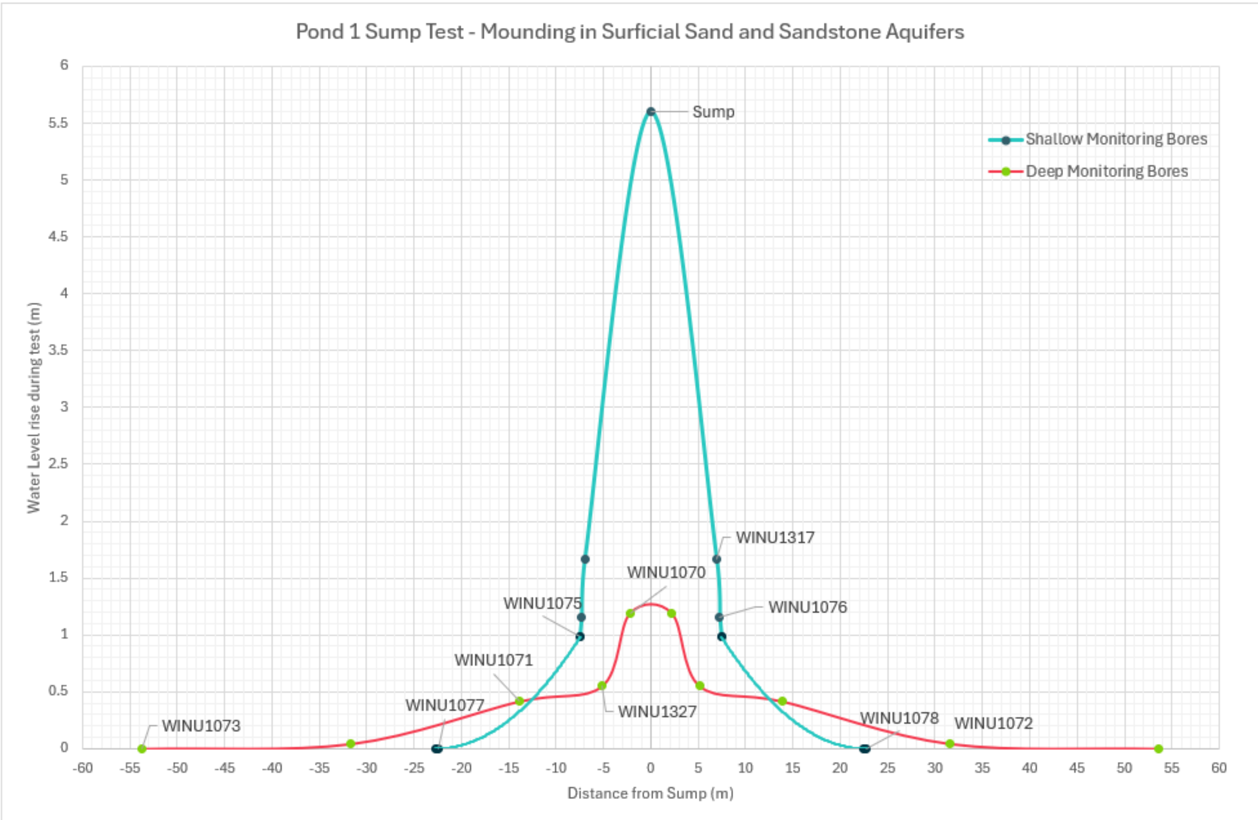

Figure 5-1: Pond 1 Sump test mounding results - note results have been mirrored around the sump

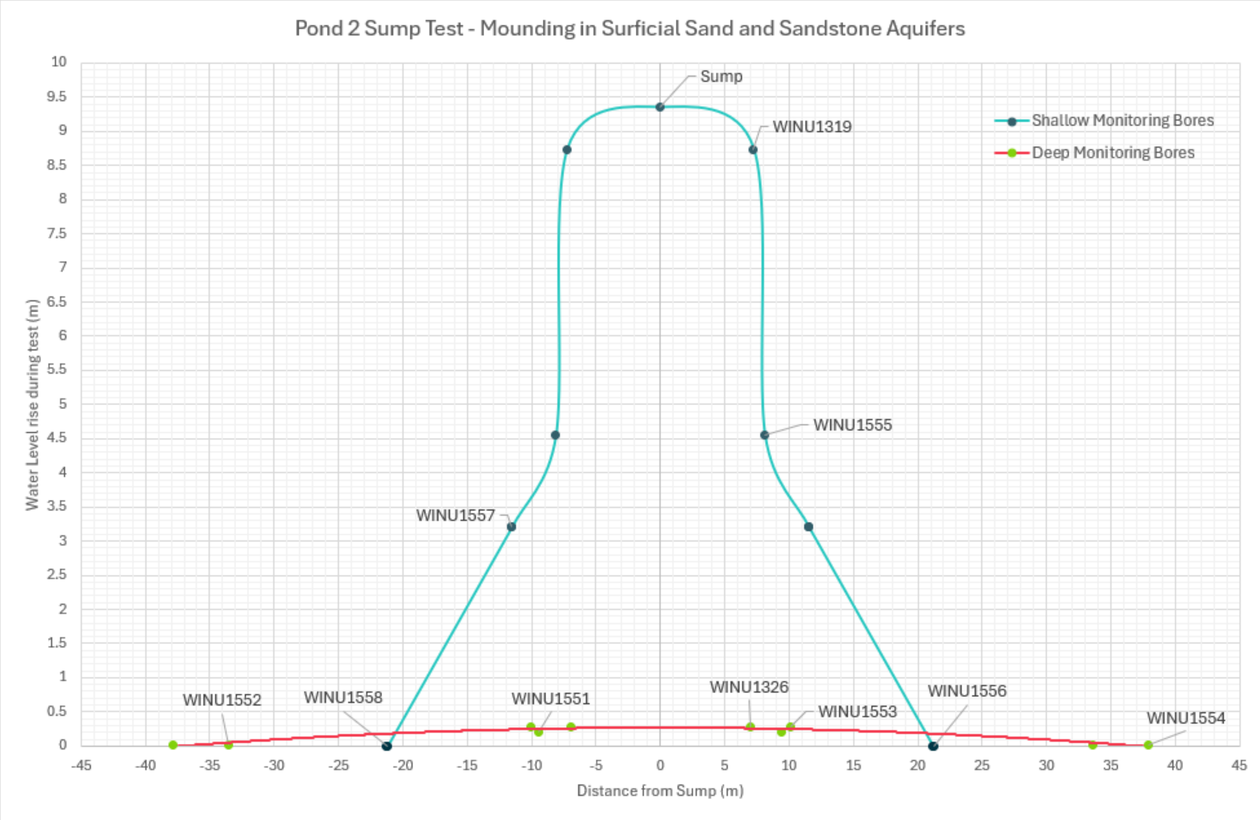

Figure 5-2: Pond 2 Sump test mounding results - note results have been mirrored around the sump

- Aquifer thickness impacts the amount of mounding. More lateral mounding observed at Pond 2 where aquifer thickness is on average 9.4 m compared to Pond 1's 5.6 m thickness, and mounding is more constrained horizontally.
- Increased saturation of the sands allowing for greater capillary action to draw water through the aquifer resulting in the infiltration rate increasing over the duration of the test.
- Hydraulic conductivity (saturated) of the surficial sand estimated from particle size distribution (PSD) analysis (Infiltration Pond Study, Advisian 2023): 1.20 to 9.35 m/d, 4.9 m/d average.
- Diurnal fluctuations in the flow rate to the sump show the impact of evaporation from the sump to be in the order of 0.06 to 0.14 L/s for a surface area.
- Algae began to grow in the base of the sumps from day 5 and on the surface of the water at the edges and corners where the water flow was minimal but had disappeared over time by day 16. If algal growth in infiltration ponds is persistent it has the potential to block pore space and reduce infiltration rates over time.
- Leakage from the surficial sands to the sandstone aquifer means the planned MAR bore locations need to be installed as far as practicable from the infiltration ponds to reduce the demand on the sandstone storage from both infiltration sources.

5.2 Competent Sandstone

Vertical leakage through the silcrete and competent sandstone aquiclude has been observed and relevant where weathering is prominent, therefore this HSU is better represented as a leaky aquitard.

Time taken for drainage and subsequent water level rise to be observed in the deep monitoring bores was 16.8 days into the test at Pond 1 where competent sandstone is more prominent.

This is compared to 10.8 days at pond 2 where there is less competent sandstone and vertical hydraulic conductivity of the sandstone is higher relative to competent sandstone.

Specific yield values are estimated to be 0.11 to 0.12, Table 5-2. Saturation in the competent sandstone is typically low, less than 3.7 m thick.

5.3 Sandstone

The volume of infiltrated water required to induce peak water level mounding presented in Figure 5-3 have been used to calculate the specific yield for sandstone from the four tests. The results in Table 5-2 show a difference in the available storage of the two sandstone lithologies with storage in the competent sandstone approximately 2.5 times less than sandstone.

The calculated storage values are likely to be high due to testing in discreet high conductivity zones at the base of the aquifer and are not expected to be representative of the bulk sandstone properties.

Table 5-2: Specific yield calculations for sandstone and competent sandstone

Pond Location	Test bore	Screened aquifer	Mound volume (m^3)	Volume of injected water (m^3)	Specific yield (*Sy*)
Pond 1	WINU1070	Sandstone	1,901	511	0.27
	WINU1325	***Partially Penetrating Competent Sandstone***	*3,892*	*480*	*0.12*
	WINU1327	***Competent Sandstone***	*3,442*	*377*	*0.11*
Pond 2	WINU1326	Sandstone	13,333	3,735	0.28

Volumes calculated from peak water level rise

Other relevant observations:

- The sandstone chips are more weathered and oxidised at the water table.
- Sandstone saturation at Pond 1 is up to 3.66 m thick with water level at 213.85 m AHD.
- Sandstone saturation at Pond 2 saturated water table is up to 12 m thick with water level at 211.15 m AHD.
- Bulk specific yield values range from 0.20 to 0.28.
- Heterogeneity in the sandstone is likely to result in some MAR bores being in reality more effective with higher infiltration rates than others

- Due to issues with developing the infiltration test bores, the MAR bores should be installed with a drilling method without the use of drilling muds
- Over time the sandstone aquifer will be impacted by injecting water with suspended and dissolved solids, blocking pore spaces and reducing well efficiency. The MAR bore efficiency should be tested periodically and periodic bore treatment and cleaning techniques should be used as required

To model infiltration and mounding in the sandstone aquifer a high homogenous hydraulic conductivity has to be applied. In reality the sandstone is heterogenous and high conductivities occur in discreet zones at the base of the sandstone HSU. The mudstone HSU underlying the sandstone aquifer remains conceptual as a basal aquiclude and no flow boundary.

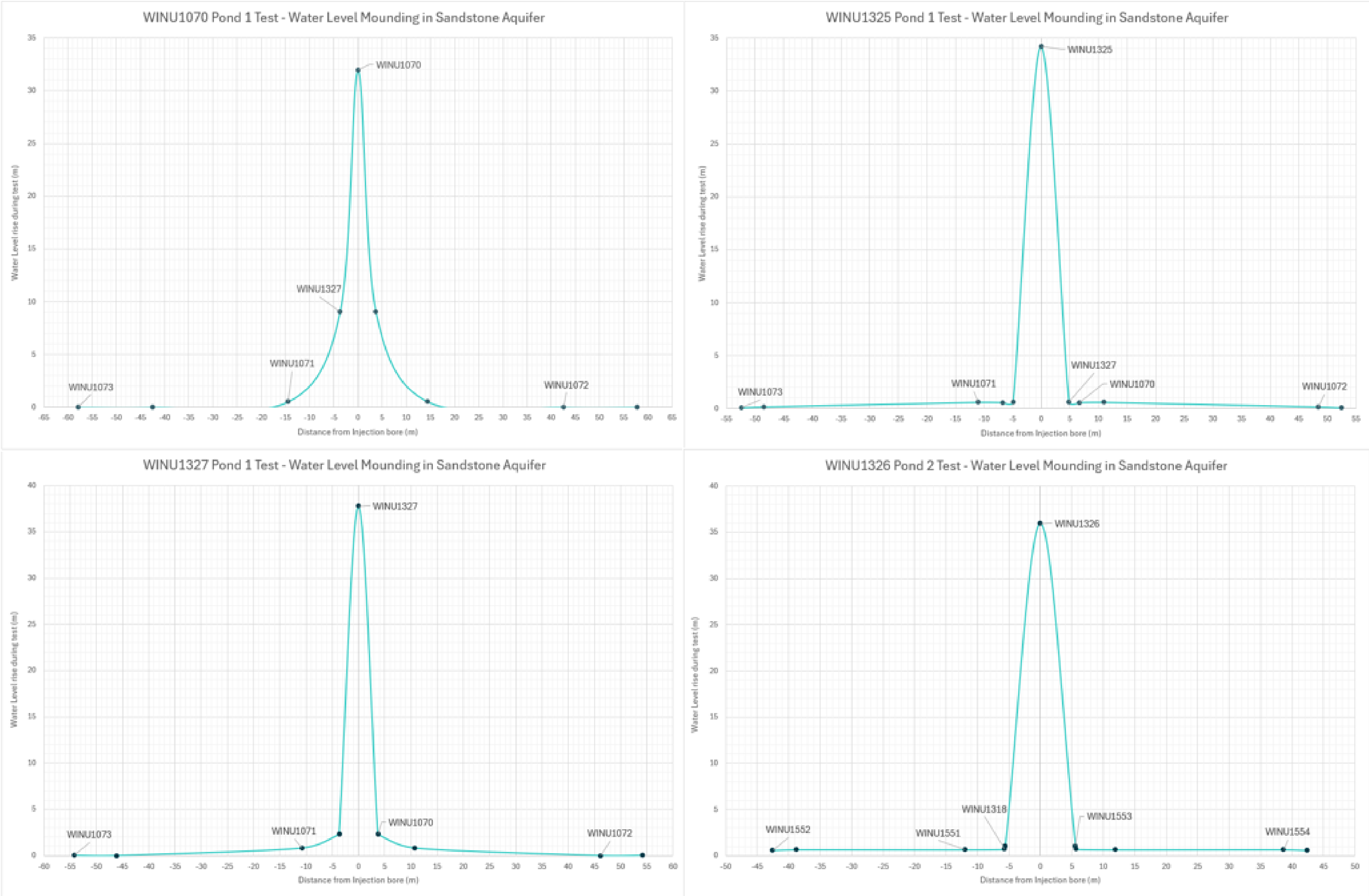

Figure 5-3: Water Level mounding results from Sandstone Aquifer tests - note observation bore results have been mirrored around the injection bore

6. Excess Water Disposal Modelling

6.1 Conceptualisation

Hydrogeological conceptualisation relevant to this study represents a minor refinement of the conceptual model presented in the updated H3 report for Winu (Worley, 2025b). The focus here is on unconfined sand and sandstone aquifer overlying the Permian mudstone which in H3 report is considered a single hydrostratigraphical unit (HSU).

The aquifer system considered in this study consists of aeolian sand cover overlying silcrete cemented material sitting at the top of the sandstone aquifer. The sandstone aquifer is considered to be formed of a more compact upper and more permeable lower part.

The silcrete layer has been previously assessed with very low permeability, practically separating the two aquifer units, however the recent testing established its function as leaky aquitard, allowing for hydraulic connection between surficial sands and deeper lying sandstone aquifer.

The aquifer and aquitard thicknesses are as follows:

- Surficial sands – up to 10 m
- Silcrete aquitard – 10 to 20 m
- Sandstone aquifer – up to 20 m

Some saturation is present at the base of the sandstone aquifer under natural conditions. Its thickness varies between 3 to 12 m in the study area (ie depth to groundwater) and groundwater flow direction is largely NNW, towards the Indian ocean.

Recharge to the groundwater system occurs episodically during cyclone events. It is assumed that the groundwater system is replenished largely through lateral inflow from the south, where outcrops receiving recharge are present. Diffuse recharge in sand-covered areas is hampered by large evaporation rates which prevent rainfall from reaching the deep-seated water table.

Groundwater leaves the area via lateral outflow towards NNW, while during Winu operation groundwater will be extracted for dewatering purposes. The average (P50) outputs through dewatering are estimated to be 105 L/s (3.3 GL/a) over the life of mine. Mining will require disposing of 0.74 GL/a (P50) up to 1.47 GL/a of extracted water through MAR or infiltration ponds, both situated upgradient from the mining pit (evaluated through this study).

There are no identified GDEs or other environmental receptors within the immediate vicinity of the study area.

6.2 Numerical Modelling

6.2.1 Objectives

The concept of infiltration ponds was previously examined by Advisian (2024), which was on two infiltration ponds (Pond 2 in a different location) and quarry concept – ie. pond dug into the base of the silcrete/ferricrete aquitard.

The objectives of the numerical modelling is to simulate excess water disposal through:

1. infiltration from two conceptual ponds, or
2. reinjection through managed aquifer recharge (MAR) into the sandstone aquifer, of annual excess water estimates over the life of mine.

This assessment also informs:

- indication of groundwater mounding that may affect environmental receptors
- potential recirculation of infiltrated/reinjected water back into the mine and estimation of such inflow rates

6.2.2 Model Setup

6.2.2.1 Model Domain Discretisation

An updated numerical model, presented in this report, was developed in MODFLOW-USG, based on learnings from previous numerical modelling (Advisian, 2024; Worley, 2025b). The previous Advisian (2024) model (also built in MODFLOW-USG) assumed pond and quarry scenarios, which are now superceded.

Additional geophysical exploration work as well as hydrogeological drilling and testing has led to conceptual updates which are incorporated in the current version of the model.

The current model domain is subregional (ie. smaller than Advisian, 2024, model) with the numerical mesh refined in the study area centred around the conceptual infiltration ponds, MAR borefield and the mining pit. The model domain covers 555 km^2 and is represented by 38,050 active cells (elements) spread over five model layers.

The model domain and its Voronoi discretisation mesh is shown in Figure 6-1. Mesh refinement to capture the detail of surplus management setup as well testing instrumentation is also presented in Figure 6-2 and Figure 6-3, respectively.

Refinement is required to improve the accuracy of simulated results, especially so for calibration of infiltration testing, to be able to represent distance between the tested bore or sump and their observation which are only several metres or several tens of metres away. Refinement in this part of the model mesh is therefore on a metre scale.

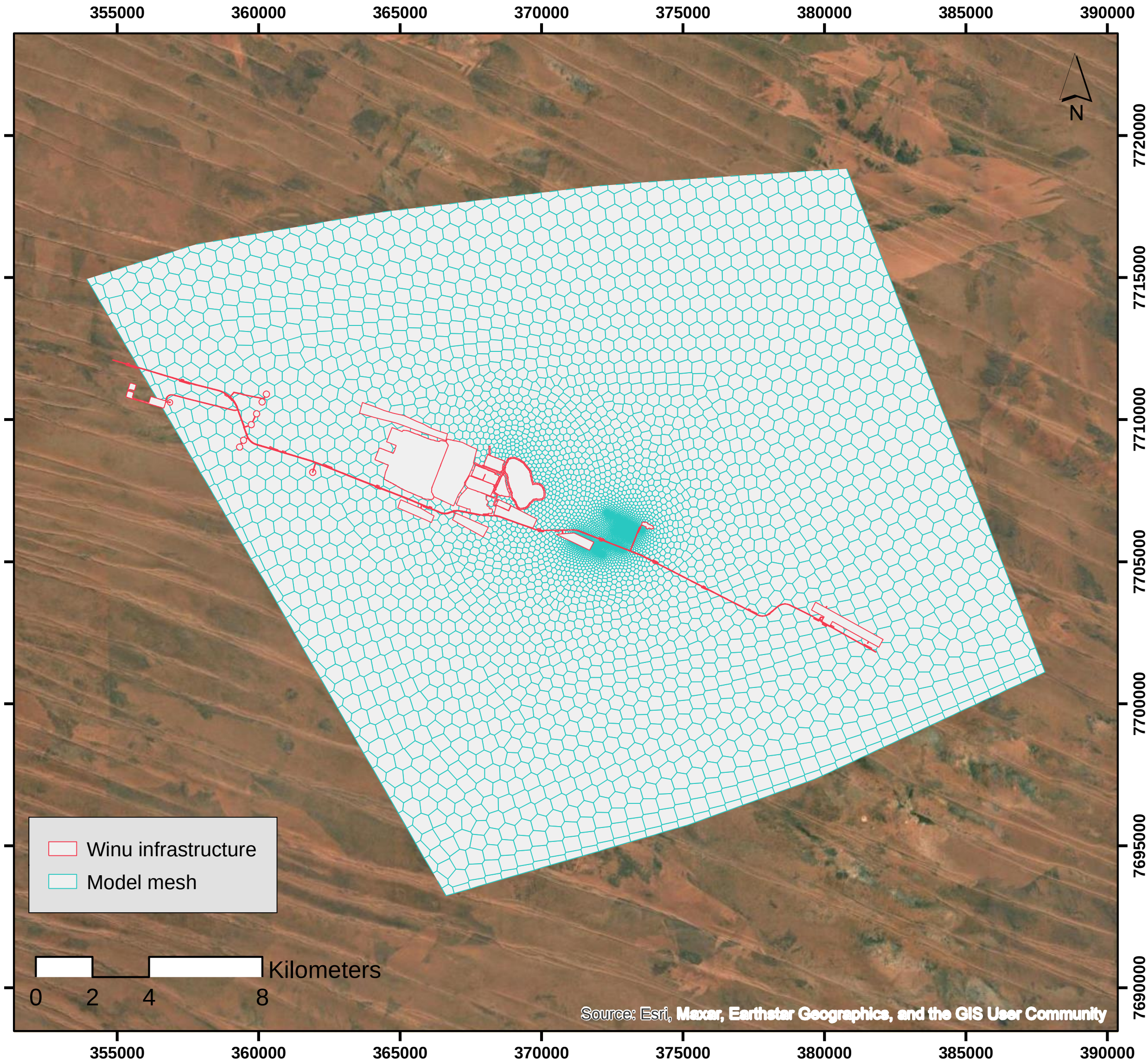

Figure 6-1 Numerical model mesh

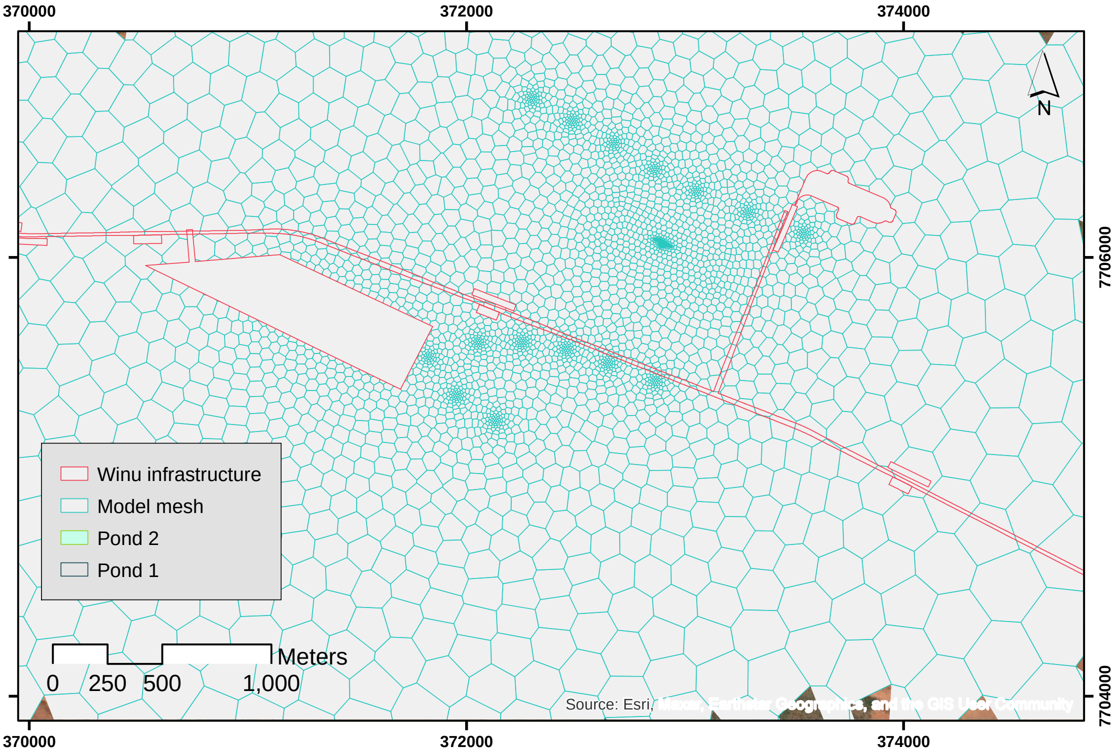

Figure 6-2 Numerical mesh – zoomed to study area (note refined locations of MAR bores)

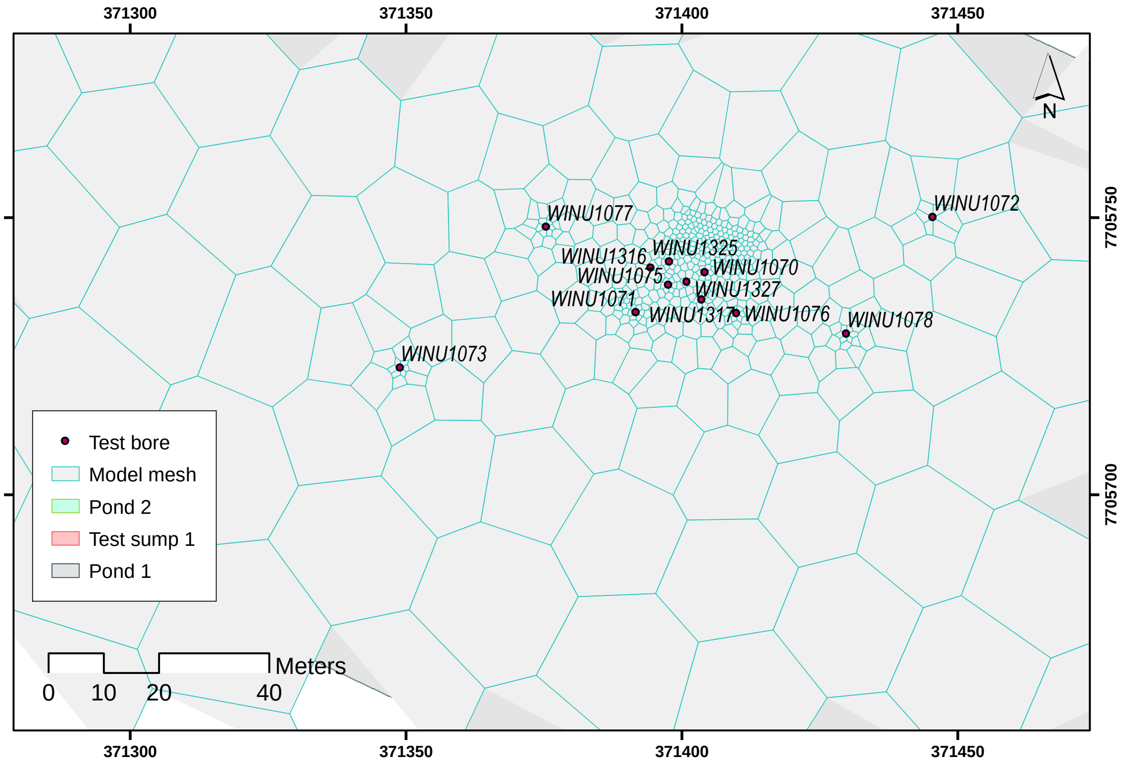

Figure 6-3 Numerical mesh – zoomed to test scale

6.2.2.2 Model Layers

This model consists of five layers:

- Layer 1 (ponds and test sumps). Top of this layer is set to the existing ground surface. Base of this layer is set 1.5 m below the existing ground surface. Outside of pond and sump areas this layer assumes the parameterisation of the surficial sand cover
- Layer 2 (surficial sand cover). The base of this layer is the inferred top of the silcrete layer, reinterpreted from recent geophysical profiling and hydrogeological drilling. Outside of the study area this is extrapolated and subject to future adjustment
- Layer 3 (Silcrete aquitard / competent sandstone)
- Layer 4 (Sandstone aquifer, competent part)
- Layer 5 (Sandstone aquifer, more permeable part)

6.2.2.3 Initial Groundwater Levels

Initial groundwater levels depict assumed groundwater flow directions and aquifer system saturation consistent with saturation present at the base of the sandstone aquifer. Groundwater levels in the study area are at 210 to 213 m AHD decreasing towards the northern domain boundary to 170 m AHD.

6.2.2.4 Infiltration Ponds and Test Sumps

Infiltration ponds (and sump infiltration tests) are simulated with aquifer properties and recharge (RCH) package. The ponds and sumps are represented with high K values, 1000 m/d) and Sy equal to 1.

Recharge rates applied during testing and simulated infiltration are converted from applied testing rates, and from annual excess water rates to match the respective sump and pond areas.

6.2.2.5 Mining Pit

The mining pit is modelled using the Drain (DRN) package, with head elevation consistent with the base of the sandstone layer. This ensures that if the groundwater mound developed at the infiltration pond, extends to the pit, then the water would spill (flow) into the pit. The DRN package also provides an estimate of inflow rates / volumes to the pit during excess disposal to either infiltration ponds or MAR. The mining pit dewatering setup is only active in predictive models (ie. not in the calibration model).

6.2.2.6 MAR Borefield

There are in total 15 MAR bore locations considered for this study. While they are conceptual, they were selected within existing heritage approved land and a nominal spacing of 200 m between each bore.

6.2.2.7 Initial Aquifer Parameters

While heterogeneity of aquifer system units is acknowledged, a zonal approach was followed in calibration with each layer of the model a uniform zone. Layer 1 is an exception since while predominantly representing surficial sand, the footprints of sumps and ponds in that layer have high K, Sy=1 properties.

The initial aquifer parameters were applied as follows:

Table 6-1 Initial aquifer parameter values

Aquifer system unit, layer	Kh (m/d)	Kv(m/d)	Ss (1/m)	Sy
Surficial sand, layers 1 and 2	10	10	$1x10^{-5}$	0.25
Silcrete/ferricrete aquitard, layer 3	0.004	0.004	$1x10^{-5}$	0.01
Sandstone (competent) aquifer, layer 4	0.02	0.02	$1x10^{-5}$	0.1
Sandstone aquifer (permeable), layer 5	1	10	$1x10^{-5}$	0.1
Void in sumps, ponds	1000	1000		1

6.2.2.8 Boundary Conditions

Regional groundwater throughflow (through sandstone aquifer) is implemented using boundary conditions on northern and southern boundaries, to mimic groundwater flow towards NNW. General head boundary is applied in the south at an elevation of 231 to 235 m AHD, while the northern boundary is at elevation of 170 m AHD, representing a flow gradient of approximately vertical drop of 1.7 m per 1 km distance.

6.2.3 Model Calibration to Infiltration Testing Results

6.2.3.1 Approach

Infiltration testing described in Section 4 forms the basis of observation data for model calibration. The calibration focus was to reflect the observed responses in monitoring bores by the model to applied infiltration/injection rates throughout the field tests.

Injection was applied to production bores which were drilled using mud and completed in the largely unsaturated section of the aquifer system. The bores could not be effectively developed using conventional means, therefore their infiltration capacity is not considered representative of their full potential. Responses in monitoring rather than production bores are used for understanding of aquifer's functional behaviour and model calibration.

The injection bores are represented using the WEL package and infiltration testing sumps are simulated using the recharge (RCH) package.

The sequence of infiltration and injection testing has been simulated. The calibration model has 24 stress periods, of which the first represents the steady state. Model parameterisation (K values only) was subsequently optimised using the PEST tools to improve the match between observed and modelled values.

6.2.3.2 Results

The calibration process led to some deviations from the initial values, most notably to adjustment of vertical K values. These were expected due to the hydraulic connectivity between the shallow and deep units observed during infiltration and injection testing.

The response of the most distant bores during testing was minimal, suggesting the vertical pathway which was confirmed by observing draw-up signals in deep (sandstone bores).

The extent of agreement between the observed and modelled values are shown in Figure 6-5 to Figure 6-8.

Several observations can be highlighted:

- Both, the deep and shallow bore responses to testing at Pond 1 site are well matched
- Modelled responses in injected bores are due to their inadequate development status and water level representing the cell which that bore occurs within
- Response in monitoring bores at Pond 2 site are consistently over-predicted by about two metres
- Trends and responses to aquifer stresses are well matched. An exception is the modelled response in WINU1552, that has not been confirmed by observation data
- The statistical measure of calibration performance expressed as normalised root mean square (RMS) is 6.7%, with residual mean of -1.31 m. The latter means that on average the model overpredicts the results by 1.3 m (explained by consistent difference in Pond 2 area observation bores). Bulk values of aquifer properties are used, and further improvement in the calibration match could be achieved if the model domain was split between zones representing Pond 1 and 2. Despite this minor difference the current match is considered sufficient (considering the lumped property approach) and meeting the Australian Groundwater Guideline recommendations.

The optimised aquifer parameter values are presented in Table 6-2:

Table 6-2 Calibrated aquifer parameters (updated parameters highlighted in red)

Aquifer system unit, layer	Kh (m/d)	Kv(m/d)	Ss (1/m)	Sy
Surficial sand, layers 1 and 2	**9.5**	**30**	$1x10^{-5}$	0.25
Silcrete/ferricrete aquitard, layer 3	**0.002**	**0.005**	$1x10^{-5}$	0.01
Sandstone (competent) aquifer, layer 4	**0.99**	**2**	$1x10^{-5}$	0.1
Sandstone aquifer (permeable), layer 5	**23.7**	**10**	$1x10^{-5}$	0.1

The Kv values do not conform to the typically applied pattern where Kv would be nominally considered as fraction of Kh value. More testing may be required to confirm or adjust these values, however limiting them to not exceed the value of Kh does not lead to a very different calibration run response.

The predictive models are set up with parameter values as presented in Table 6-2. The configuration of pre-injection water levels, expressed as depth to water over the study area is presented in Figure 6-4:

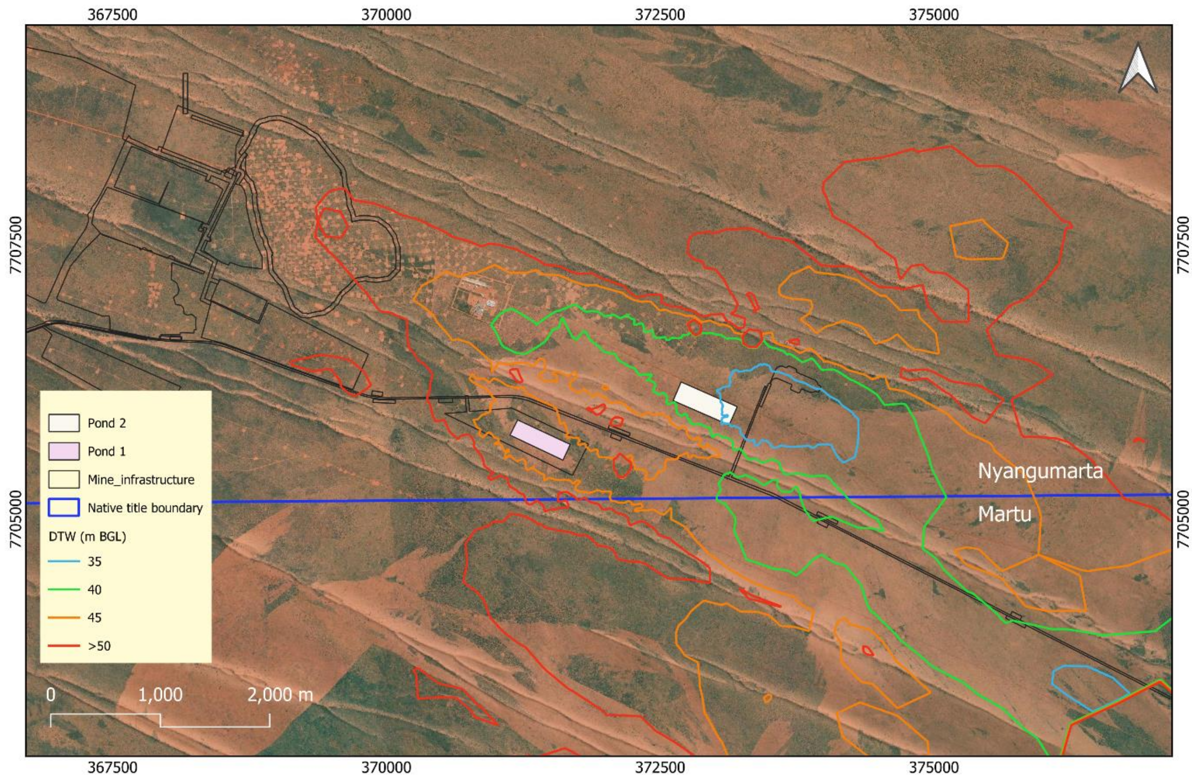

Figure 6-4 Pre-mining depth to water, derived from calibration model (not affected by pit dewatering)

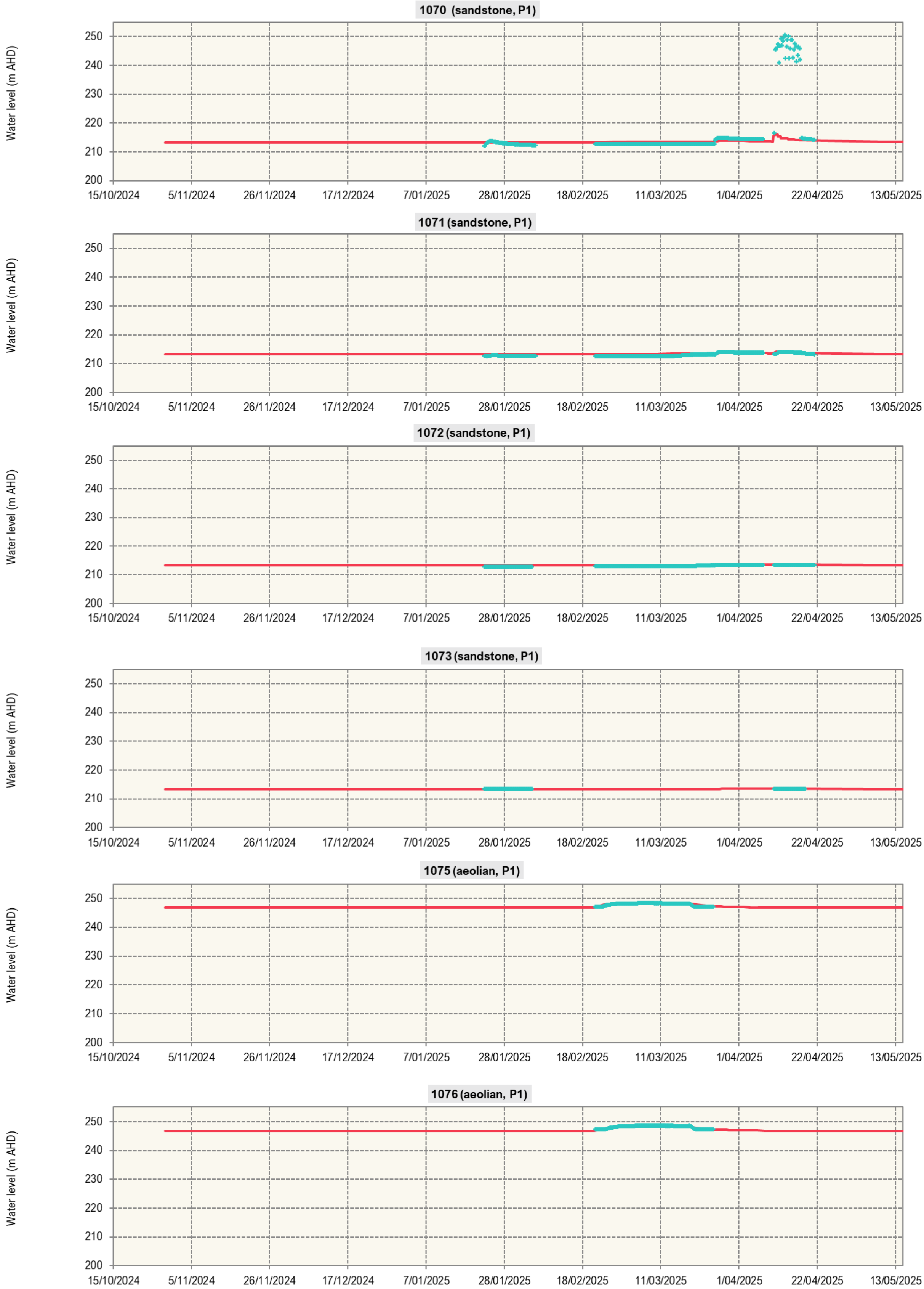

Figure 6-5 Observed and modelled responses from infiltration/injection testing – part 1

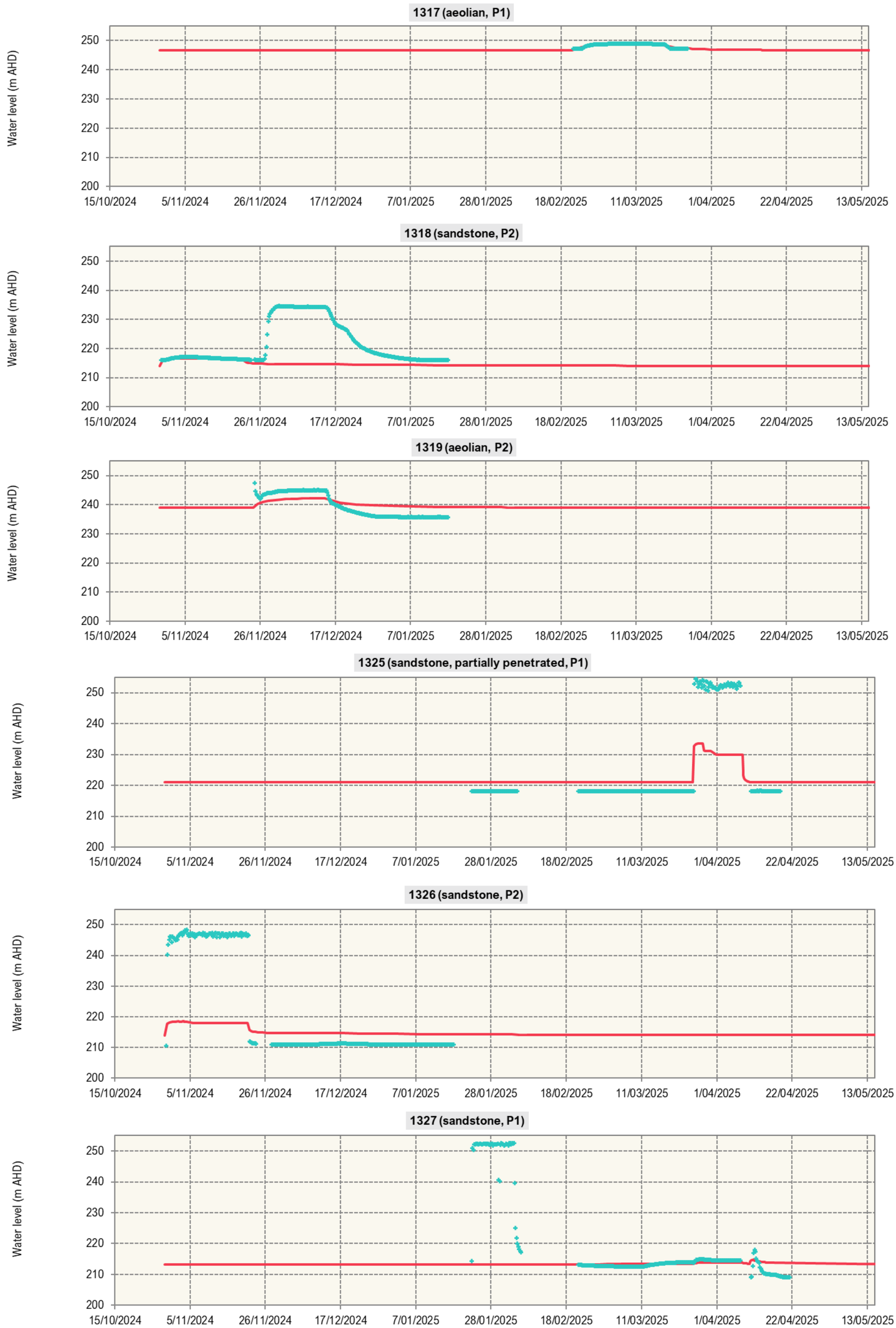

Figure 6-6 Observed and modelled responses from infiltration/injection testing – part 2

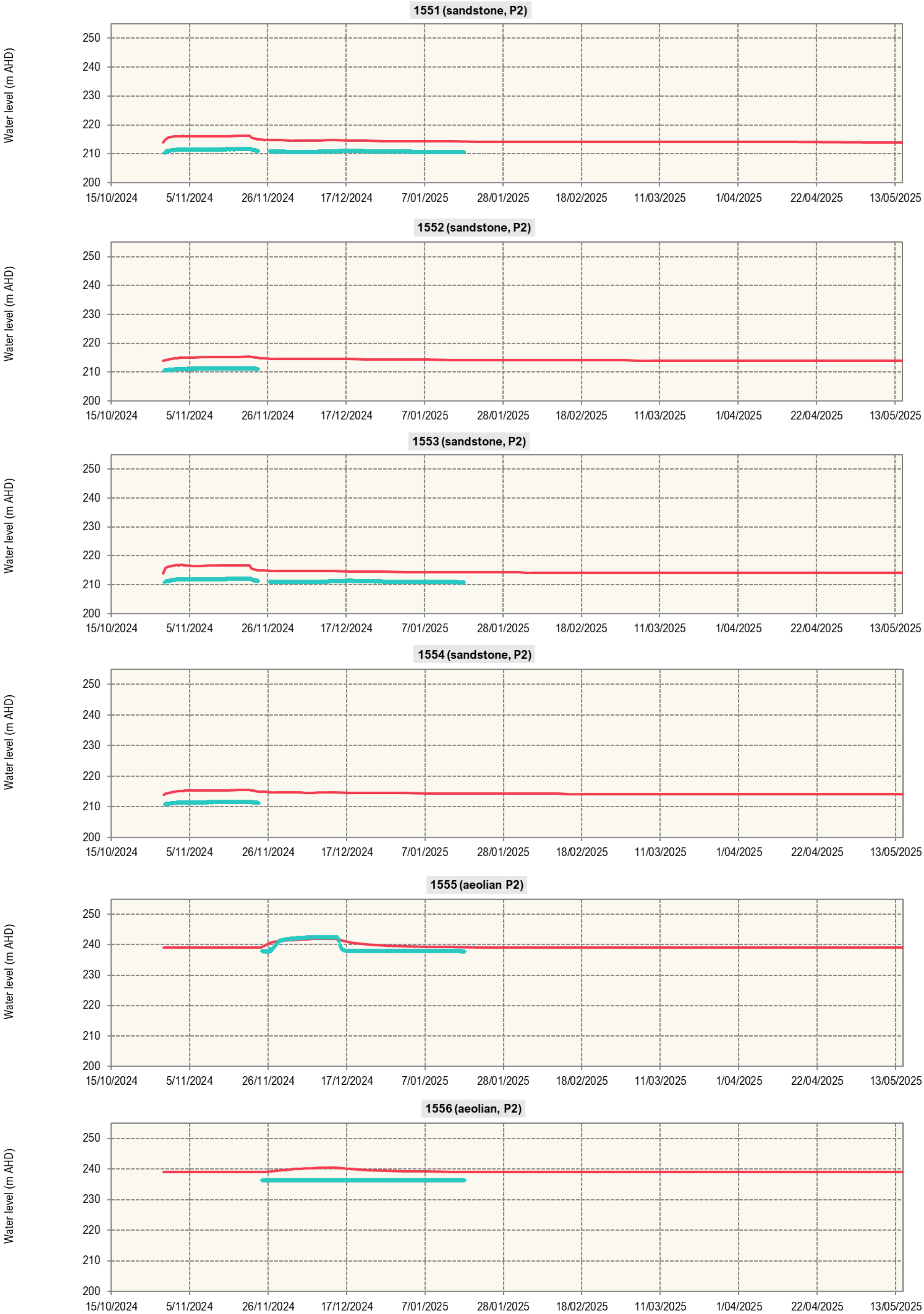

Figure 6-7 Observed and modelled responses from infiltration/injection testing – part 3

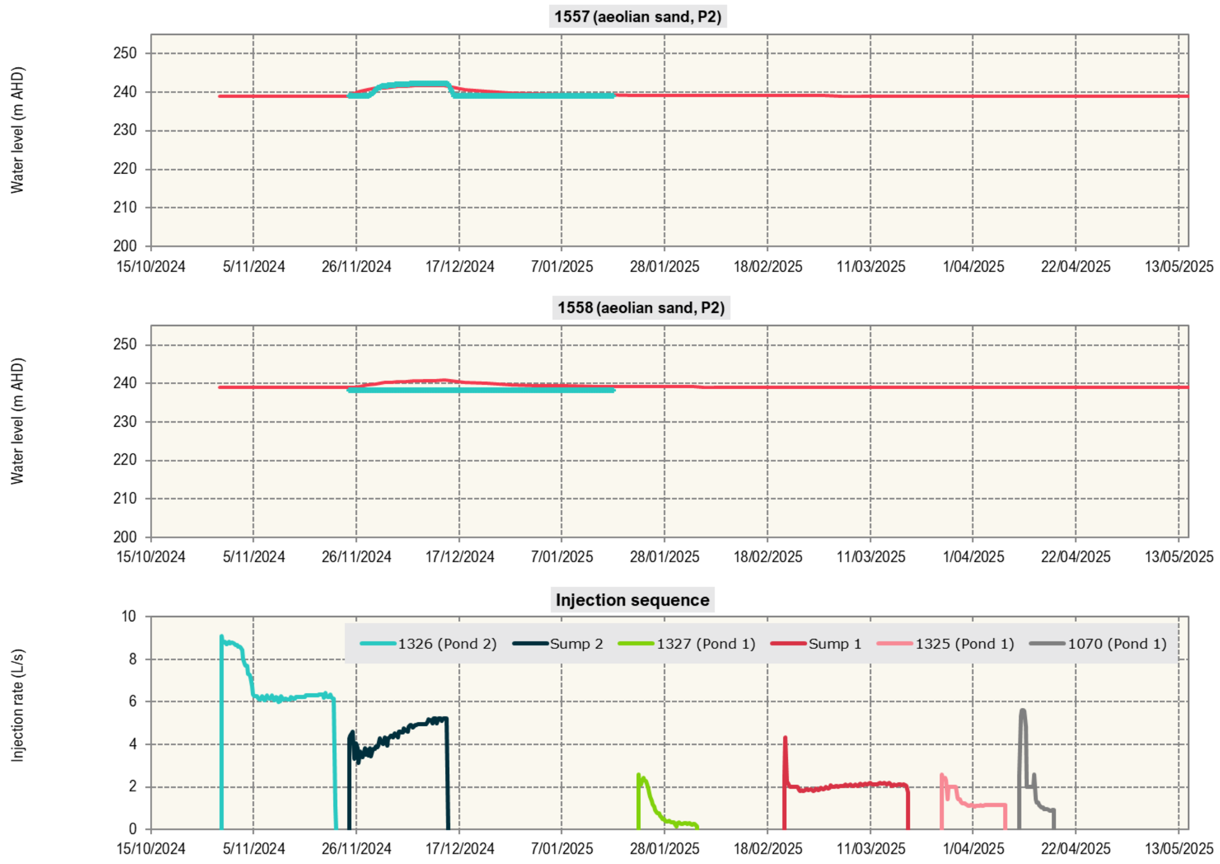

Figure 6-8 Observed and modelled responses from infiltration/injection testing – part 4

6.2.4 Predictive Simulations (Infiltration Capacity)

6.2.4.1 Setup

Predictive models are set up based on the calibration model, with one exception – pit dewatering effect is explicitly simulated during mining (not simulated in the calibration model). Predictive models consist of 34 stress periods (SP):

- SP 1, steady-state, with pit dewatering active
- SP2 to SP33, transient, each one-year duration with P90 infiltration/injection rates applied either to pond or MAR scenarios
- SP34, transient, one year duration, to simulate return to pre-injection/infiltration status

6.2.4.2 Infiltration Pond Option

The modelled areas of Ponds 1 and 2 are 84 and 103 hectares, respectively. The results indicate that surplus water managed through infiltration ponds will comply with the P90 surplus water demands:

- Two groundwater mounds will develop closely around the ponds within the surficial sand, but the majority of water volume is predicted to seep down to the sandstone aquifer.
- The mounds in the surficial sand in Year 9 of the mining operation (Figure 6-9), when the required infiltration volume is predicted to be the largest (4 GL/a), covers a small footprint.

- Mounding of the deeper sandstone aquifer will occur over a larger footprint, with some of the infiltrated water expected to flow back to the mining pit.
- In total, over the life of mine, the average back inflow into the pit from infiltration ponds is predicted to be 11 L/s or 23% of total infiltrated water.
- From peak infiltration in Year 9 the surplus volume will be gradually reduce which will also result in a smaller infiltration mound footprint over time. This is demonstrated with depth to water contours for Year 32, the last year of mining (Figure 6-10).

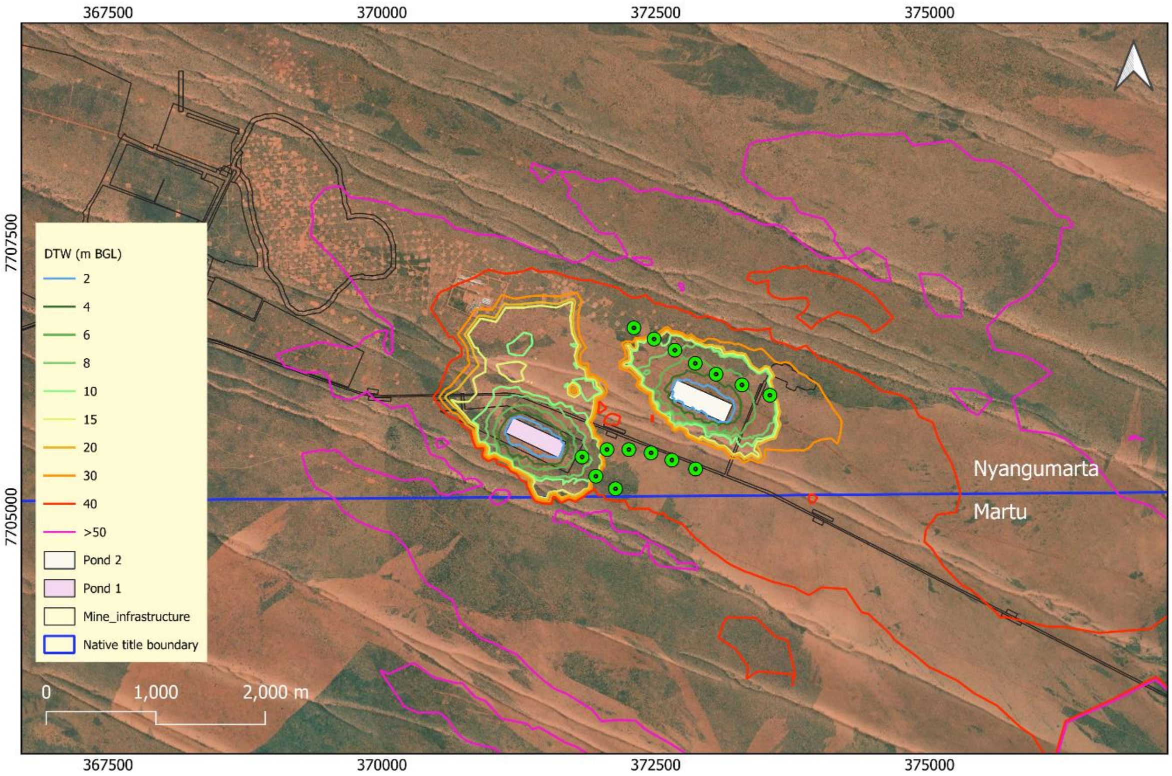

Figure 6-9 Modelled depth to water (m BGL) at Year 9 (Pond option)

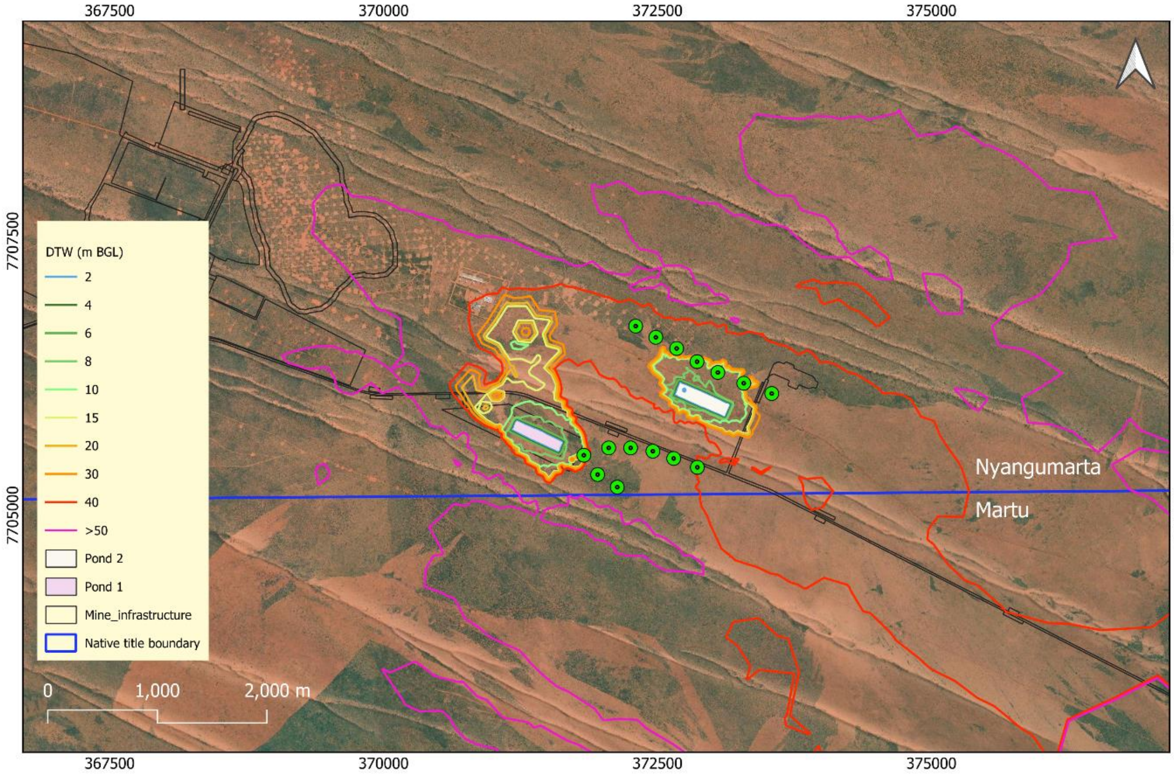

Figure 6-10 Modelled depth to water (m BGL) at Year 32 (Pond option, last year of mining)

6.2.4.3 MAR Option

MAR bores are all considered to inject surplus water into the sandstone aquifer (ie. no injection into the surficial sand will occur). The sandstone aquifer is assumed to be intercepted by the mining pit, from the very start of the predictive simulation period.

Predictive simulations of surplus volume injection through the MAR borefield consisting of 15 injection locations indicate that the borefield will be able to handle the P90 surplus water rates:

- For the MAR borefield to work the MAR bores will have to be capable of injecting 0.3 to 8.5 L/s each.
- The average injection rate per MAR bore over the life of mine for P90 case will have to be 3.1 L/s. WINU1326 was the only infiltration test bore with flows exceeding this rate.
- Groundwater mounding associated with injection is predicted to not reach the surficial sand even during the peak injection year (Year 9), with depth to water remaining well below the base of the surficial sand (Figure 6-11).
- During 32 years of mining the effect on groundwater levels will remain irrelevant to the surficial sand, which is predicted to remain practically unaffected by MAR injection and unsaturated. Water level at Year 32 will remain deep-seated as demonstrated in Figure 6-12.
- Over life of mine on average 15 L/s of injected water is predicted to be captured by the mining pit which is situated 2,200 to 2,500 m downgradient from the MAR borefields, representing approximately 31% of total infiltrating water.

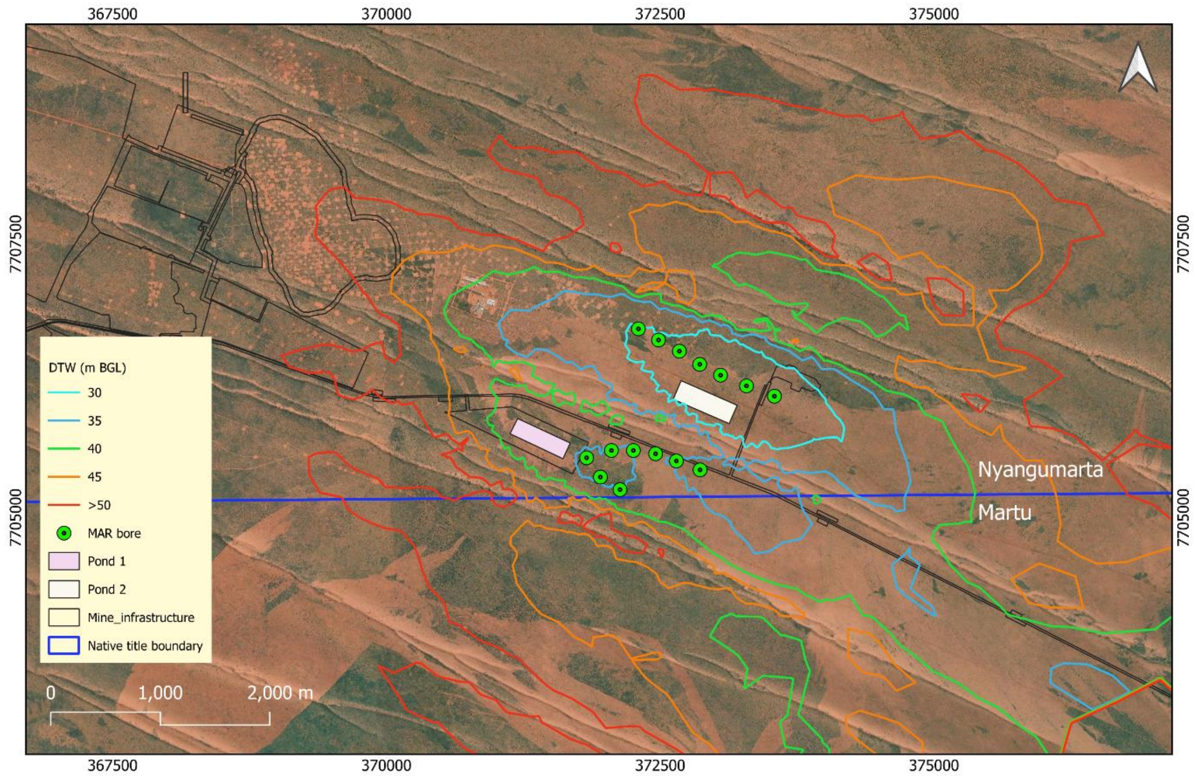

Figure 6-11 Modelled depth to water (m BGL) at Year 9 (MAR option)

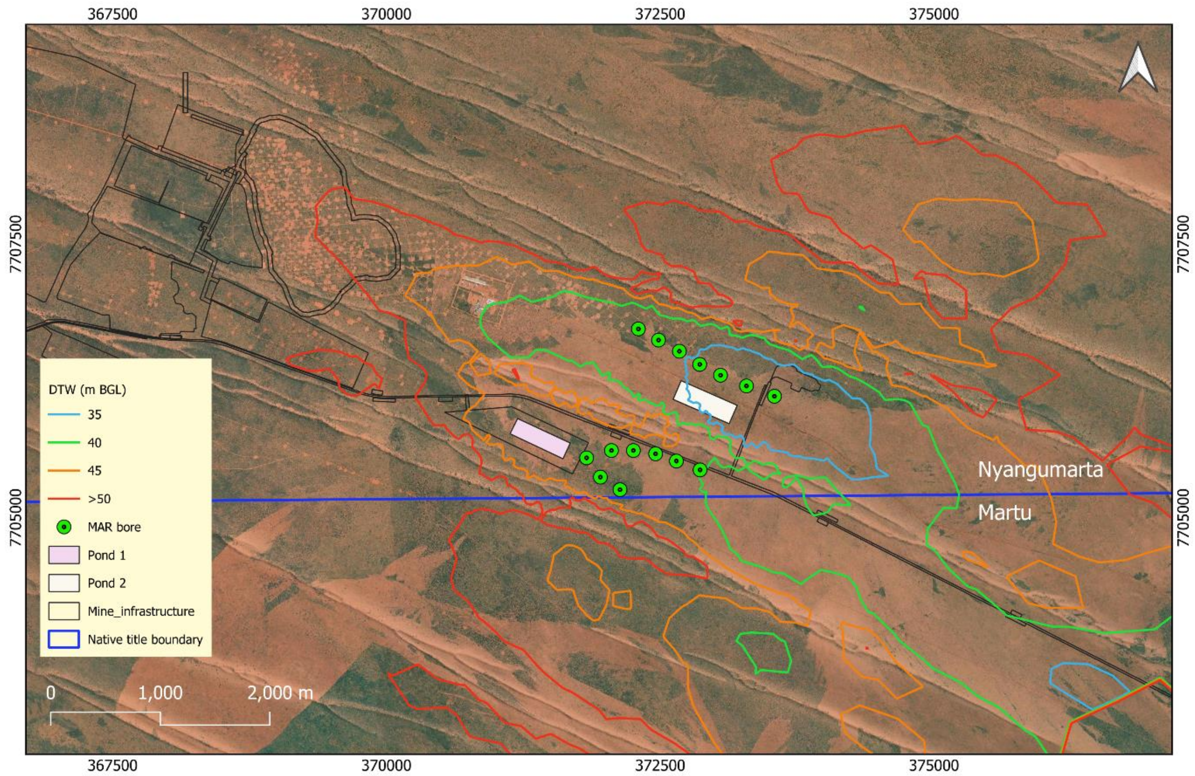

Figure 6-12 Modelled depth to water (m BGL) at Year 32 (Pond option, last year of mining)

6.2.5 Predictive Uncertainty Analysis (Infiltration Capacity)

Every model is a simplification of the actual aquifer system and is charged with various levels of uncertainty in its predictions. The sources of uncertainty including conceptual, parametric, observation error and others.

Uncertainty analysis in this case is employed through iterative ensemble smoother (PESTT-IES), based on generating an ensemble of similarly calibrated models parametric realisations. Calibration uncertainty in this case is directly propagated from calibrated into predictive realisations. All models are then evaluated stochastically, to arrive at percentile-based analysis in risk-based context, as proposed by Middlemis and Peeters (2018).

Table 6-3 Probabilistic context for uncertainty analysis

Percentile	Probability	Description
P10	>90%	It is **very likely** that the outcome is **larger** than this value
P10 to P33	67 to 90%	It is **likely** that the outcome is **larger** than this value
P33 to P67	33 to 67%	It is **as likely as not** that the outcome is **larger** than this value
P67 to P90	10 to 33%	It is **unlikely** that the outcome is **larger** than this value
P90	<10%	It is **very unlikely** that the outcome is **larger** than this value

The parameters varied in the probabilistic ensemble include hydraulic conductivity (horizontal and vertical) and specific yield. The histograms of parameter values used in the probabilistic runs ae shown in Appendix C.

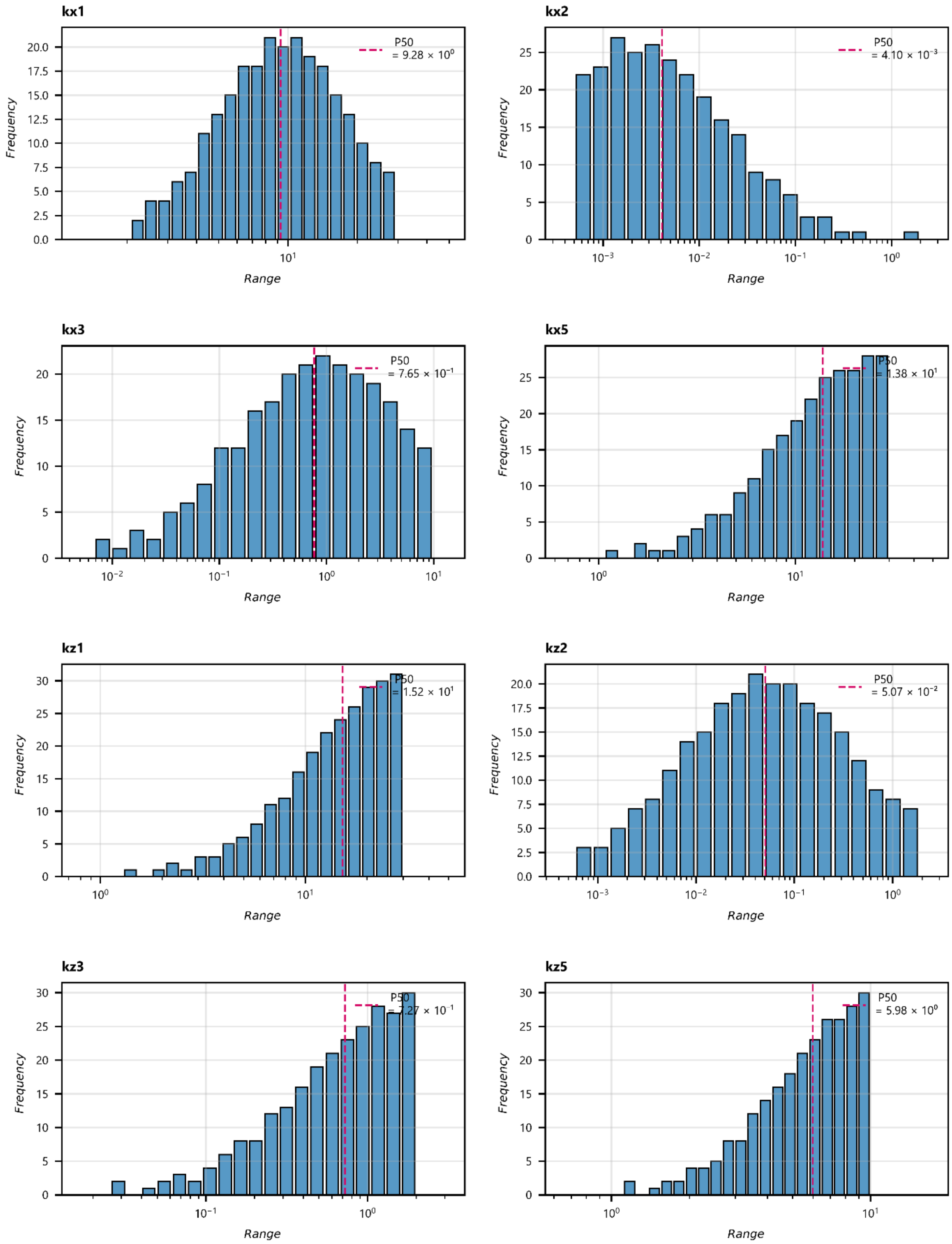

Figure 6-13 Parameter histograms for UA realisations (hydraulic conductivity)

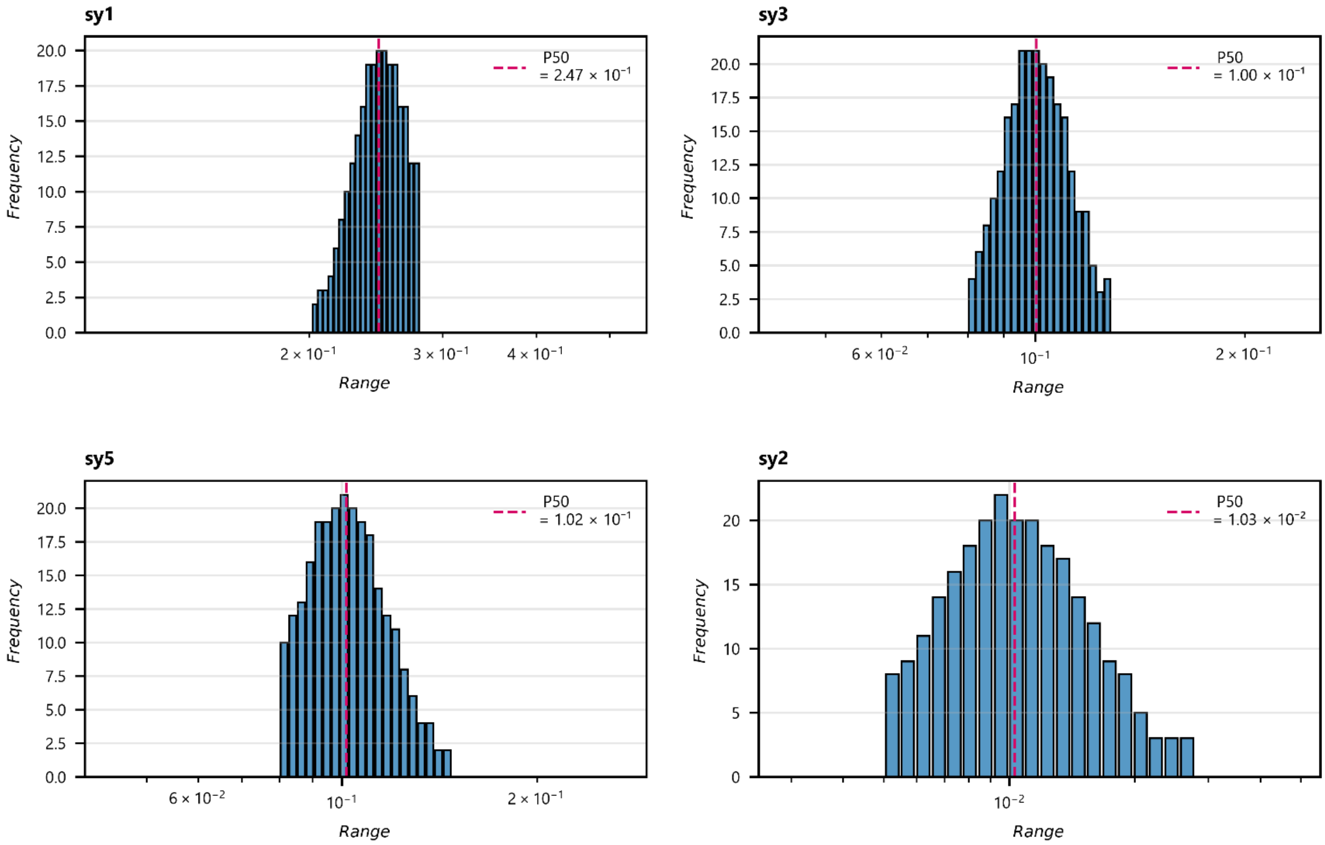

Figure 6-14 Parameter histograms for UA realisations (specific storage)

All realisations successfully converged and comply with calibration criteria for the majority of realisations.

The uncertainty analysis confirms the results of the predictive simulations in that:

- It is very unlikely that mounding affects surficial sands beyond the footprint of infiltration ponds, nominally 100 m away during peak times
- It is very unlikely that mounding affects surficial sands at a distance of more than 200 m from the infiltration ponds
- It is very unlikely that there would be some effect on surficial sands from the MAR option during the operational or recovery periods. During the peak year (Year 9), it is likely that depth to water will be more than 6 m BGL around the centre bores of MAR line along the Pond 2, and more than 15 m BGL around the MAR line along the Pond 1.

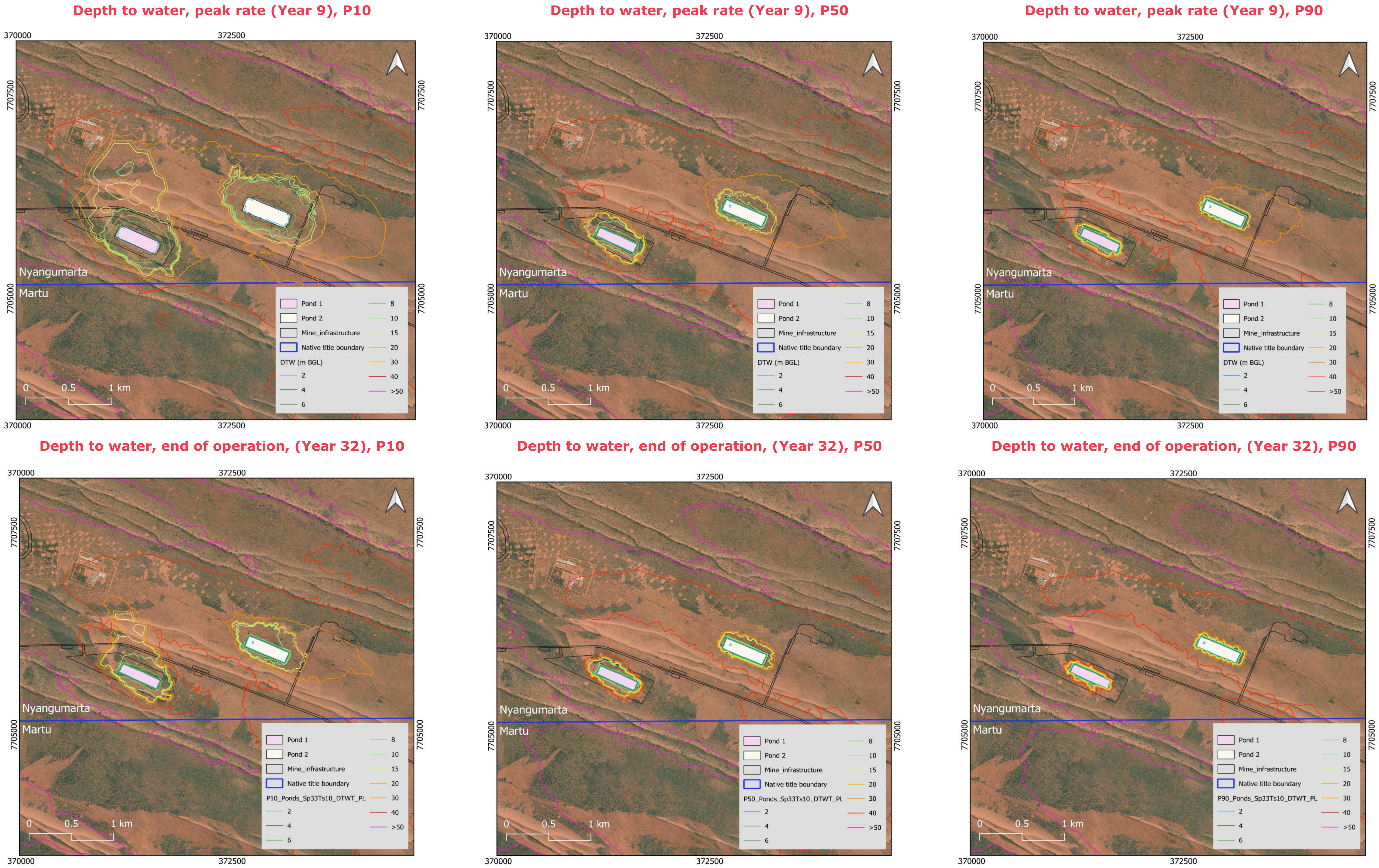

Figure 6-15 Predictive uncertainty analysis, Pond option - estimated depth to water (DTW) at P10, P50 and P90 levels

Depth to water, peak rate (Year 9), P10

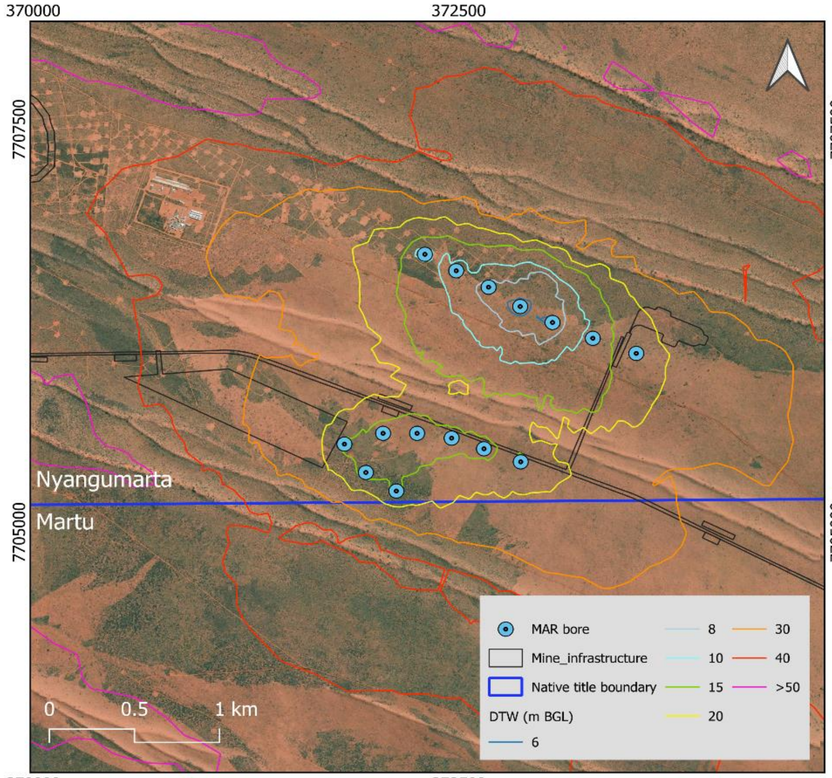

Depth to water, peak rate (Year 9), P50

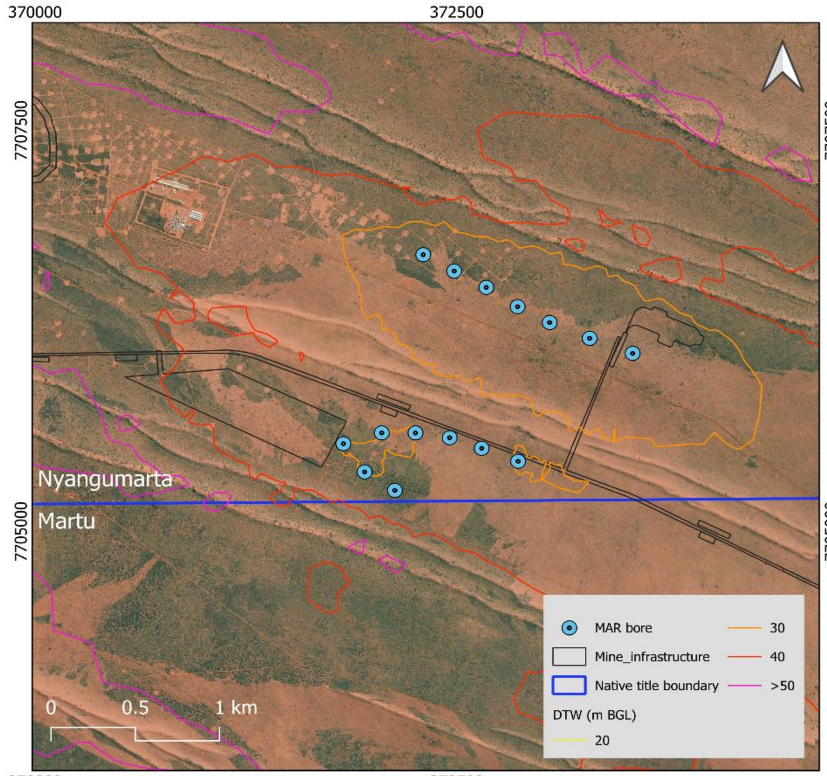

Depth to water, peak rate (Year 9), P90

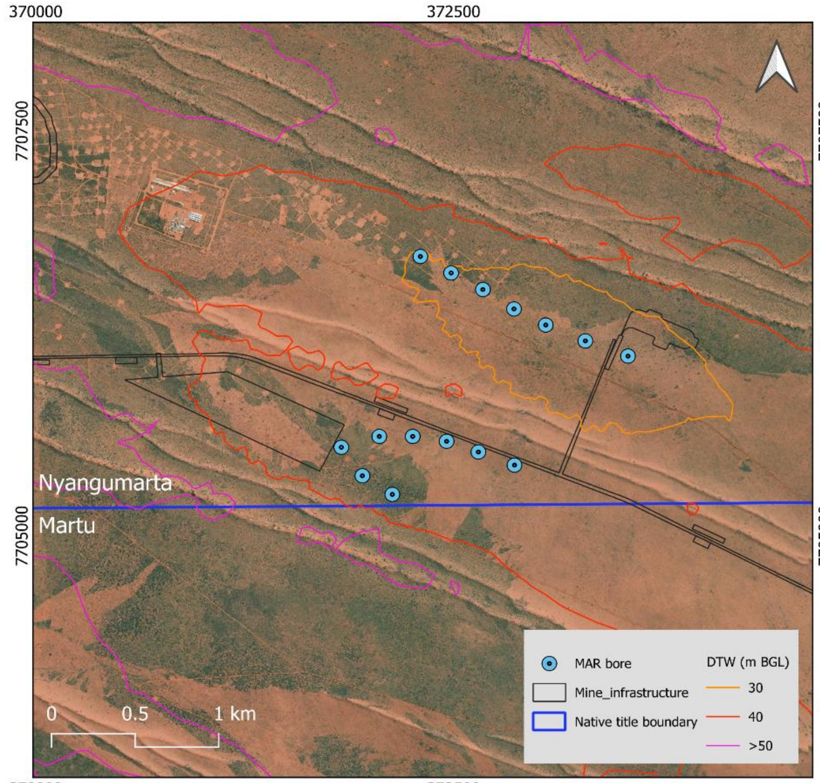

Depth to water, end of operation, (Year 32), P10

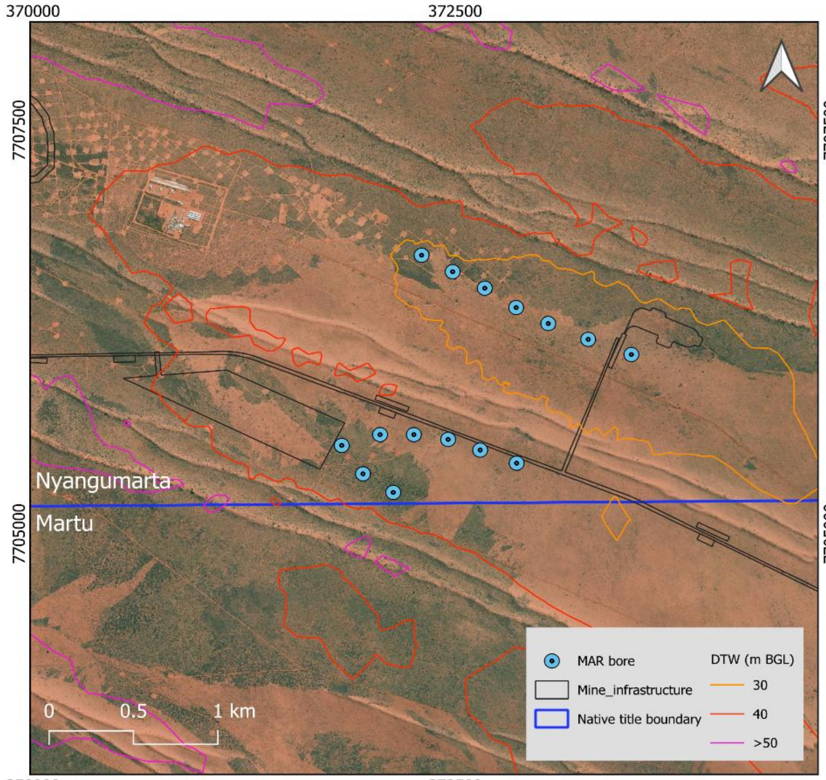

Depth to water, end of operation, (Year 32), P50

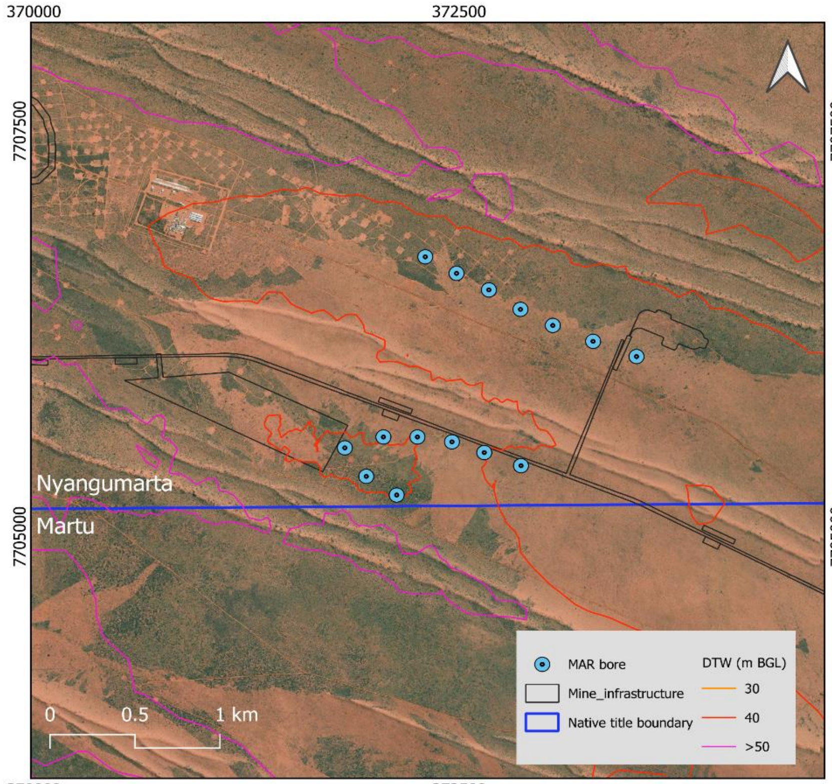

Depth to water, end of operation, (Year 32), P90

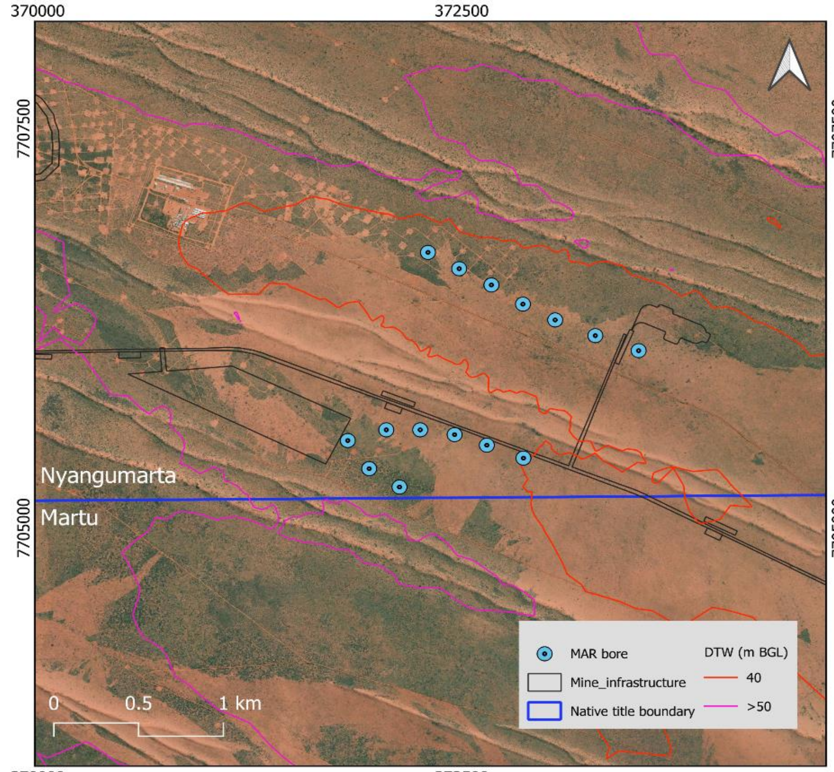

Figure 6-16 Predictive uncertainty analysis, MAR option - estimated depth to water (DTW) at P10, P50 and P90 levels

6.2.6 Solute Transport Modelling

6.2.6.1 Setup

The groundwater flow model that simulates the infiltration/injection capacity option was adapted, with solute transport modules, to simulate the plume migration, associated with surplus water from either the ponds or MAR bores within the sandstone aquifer, and its partial capture by the mining pit. The following updates to the groundwater flow model were applied to develop the solute transport simulation:

- Two cases are considered: infiltration ponds (Pond option) and injection through MAR bores into the sandstone aquifer (MAR option)
- The recharge (RCH) package was used to represent infiltration (and input concentration) into the pond conceptualised in the surficial sand cover.
- Concentration of the infiltrated water (through RCH package) was specified to be 3,740 mg/L. This value is based on pumping test data in close proximity to the proposed pit at WINU0917 (November 2023). The input concentration can be, in reality, different and can vary in time in response to dewatering, drawing water of different qualities.
- Concentration from the GHB inflow boundary representing the contribution from regional throughflow was specified to be 290 mg/L.
- Initial concentration of the aquifer system is specified to be 290 mg/L based on groundwater sampling of WIDI0020.
- The longitudinal, transverse, and vertical transverse dispersivity values were specified to be 200, 20, and 2 m, respectively. The longitudinal dispersivity is representative of approximately 5% of plume length, with order of magnitude lower values for transverse components of dispersivity tensor.
- The MAR option assumes injection of water of the same quality, ie. with concentration of 3,740 mg/L.
- Following the operational period of infiltration or injection of 32 years, the model simulated the migration of the plume originated from surplus water over a period of 100 years. At the end of operational period infiltration/injection rates were set at zero.

Key considerations associated with solute transport modelling are:

- Surficial sand cover, relevant for the pond option, is understood to not host groundwater under natural conditions. In theory, there may be limited groundwater available after infrequent occurrences of cyclonic-related rainfall. That minor volume or its part may be evaporated, however the more likely scenario is that leaks to the underlying sandstone aquifer. The existing drilling data confirm that surficial sands are unsaturated.
- Surficial sands represent a relatively homogeneous material (fine sand) composed of relatively inert quartz grains. There is no available evidence of significant clayey materials. It is therefore assumed that sand reactivity is minor, possibly limited to minor occurrence of ferric hydro-oxides that may be present in some locations. In any case, our solute transport simulations are limited to TDS (salinity), for which reactive transport considerations are not necessary.
- The underlying layer of silcrete/ferricrete was previously thought to practically form a no flow boundary for further vertical migration of solutes, however recent testing for this project has confirmed connectivity between the surficial sand and the deeper sandstone aquifer.

- The sinks for solutes in the current model are the mining pit and outflow through the northern GHB boundary. Where water is almost at surface (Pond option), evaporation may also be present, however this is currently not modelled.
- Release of water into the pond(s) is similar to flood conditions resulting in quick saturation of underlying surficial sands (due to their relatively high permeability and effective porosity). Any unsaturated flow effects are not considered as these would be of a very short duration.
- The leaky silcrete layer facilitates further vertical transfer of surplus water into the sandstone aquifer. A progressively growing mound of groundwater will develop due to incidences of infiltration events, in the sandstone aquifer. The mound will grow radially from the pond with a segment of it being captured by the mining pit.
- Reactivity of sandstone aquifer matrix is considered to be minor with respect to overall dissolved solids. Due to the presence of water in the sandstone aquifer with TDS approximately an order of magnitude lower than discharge, mixing processes, are important.
- Surplus water introduced through the ponds into the sand/silcrete/sandstone pathway will be captured by the open pit at concentrations determined by mixing with ambient groundwater.

6.2.6.2 Surplus Plume Evolution

The key aspects of the predicted plume evolution during the 32 years of operation followed by simulated 100 years of mound dissipation and plume redistribution can be outlined as follows:

Pond option:

- The main plume will develop in the sandstone aquifer due to the largely vertical flow from the Pond option (through unsaturated surficial sand and silcrete); and due to injection into this aquifer through the MAR option
- The plume will develop a circular shape, which during peak infiltration year (Year 9), is predicted to have a radius of about 3 km, extending to the north and west of the infiltration ponds (Figure 6-17).
- This shape and footprint are predicted to be similar up until the end of the operational period (Year 32)
- Following the cessation of infiltration the plume will start to move towards north but also maintaining the capture pattern at the mining pit.
- The plume concentrations in its centre will remain high. Vertical recharge in this model is considered negligible, however in reality cyclonic events may represent intermittent opportunities for recharge reaching the sandstone aquifer and providing further dilution.
- The plume is predicted to experience slow dissipation, migration towards north, and redistribution, partly delayed by the capturing effect of the mining pit.

MAR option:

- Surplus plume developed through MAR injection is predicted to have slightly different shape but similar footprint
- The plume behaviour is predicted to be similar, but with comparatively faster dissipation, and redistribution, especially during the post-operational period. This is attributed to the direct injection into the sandstone, without delaying effects present with the more complex pathway (and longer residence times) associated with the Pond option.

Surplus plume, peak infiltration rate (Year 9 of operation)

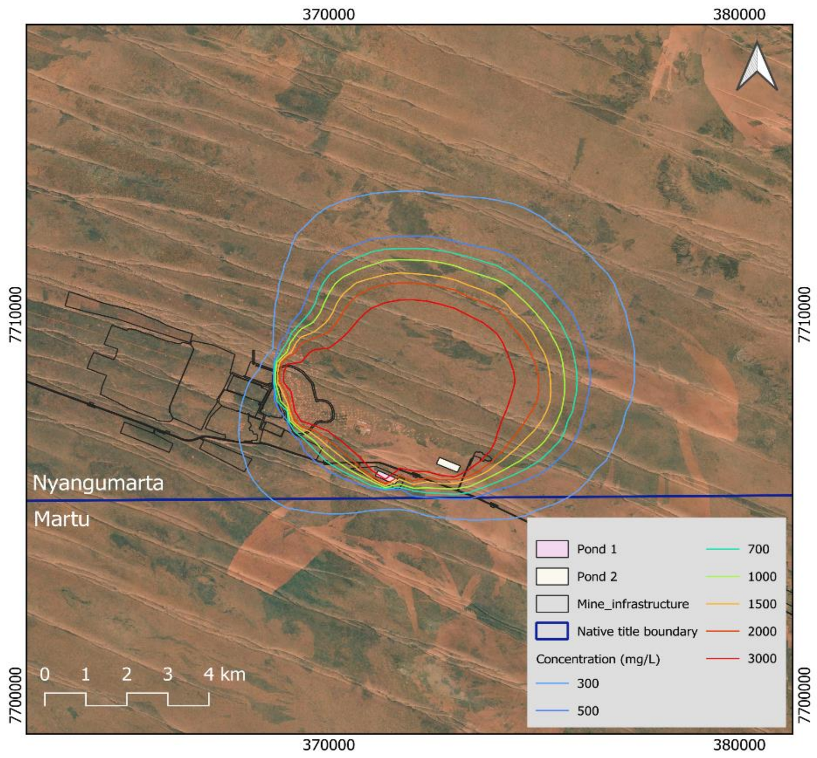

Surplus plume, end of infiltration (Year 32 of operation)

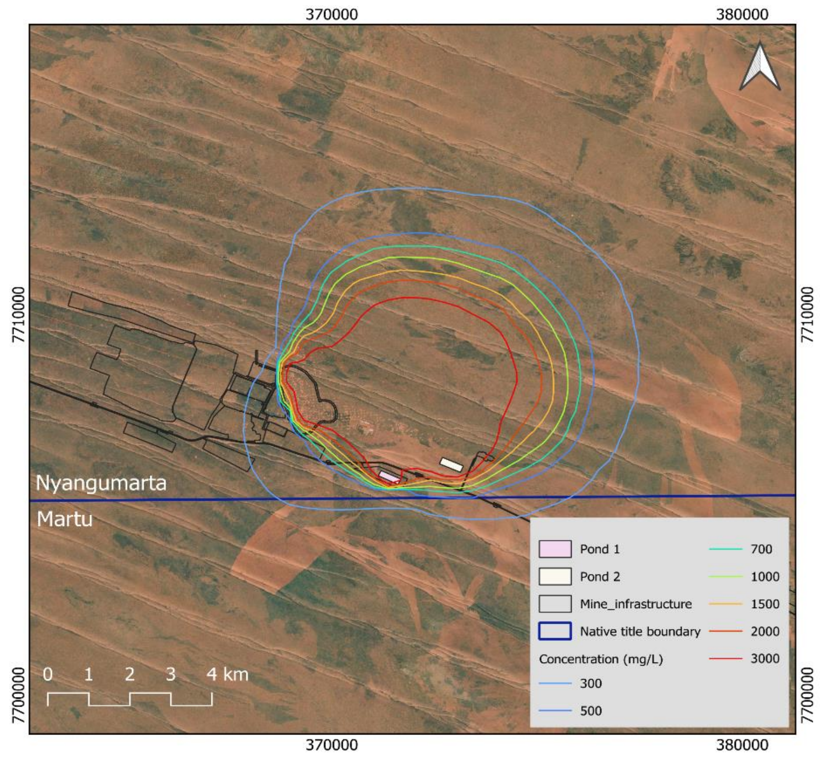

Surplus plume, Year 10 after infiltration ceases

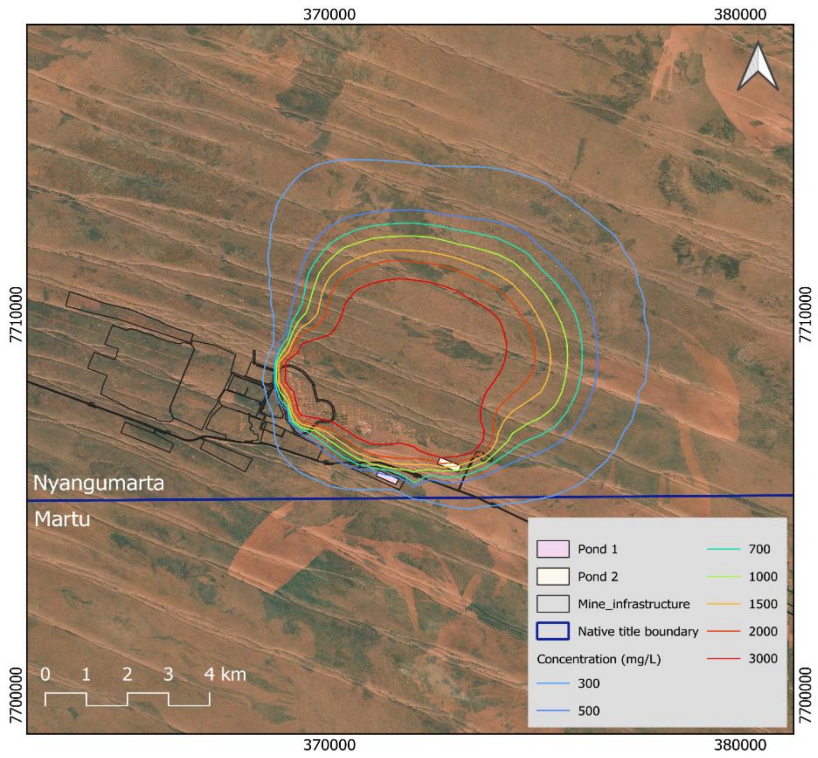

Surplus plume, Year 20 after infiltration ceases

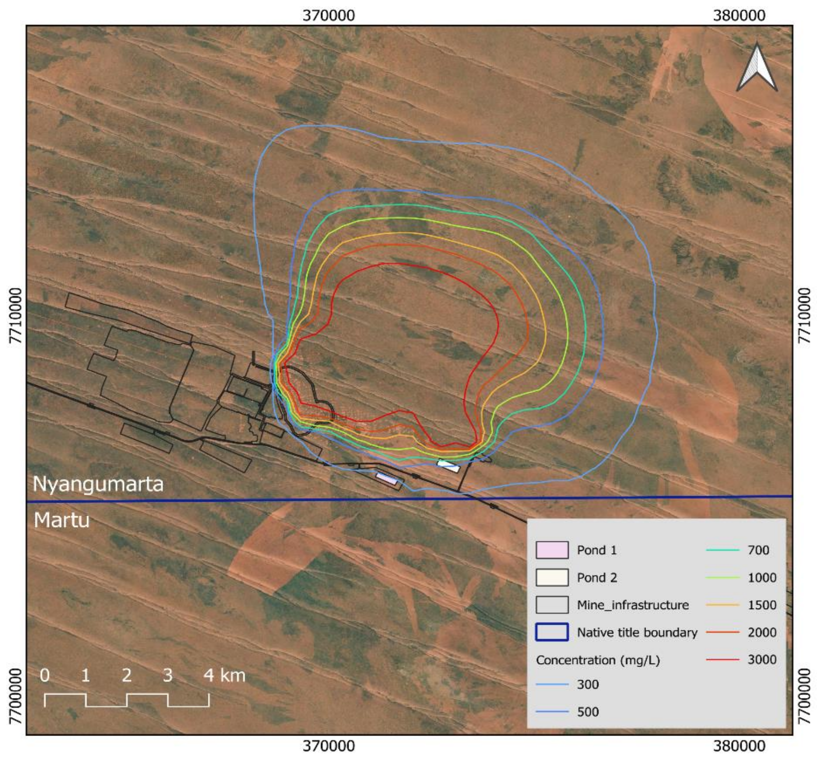

Surplus plume, Year 50 after infiltration ceases

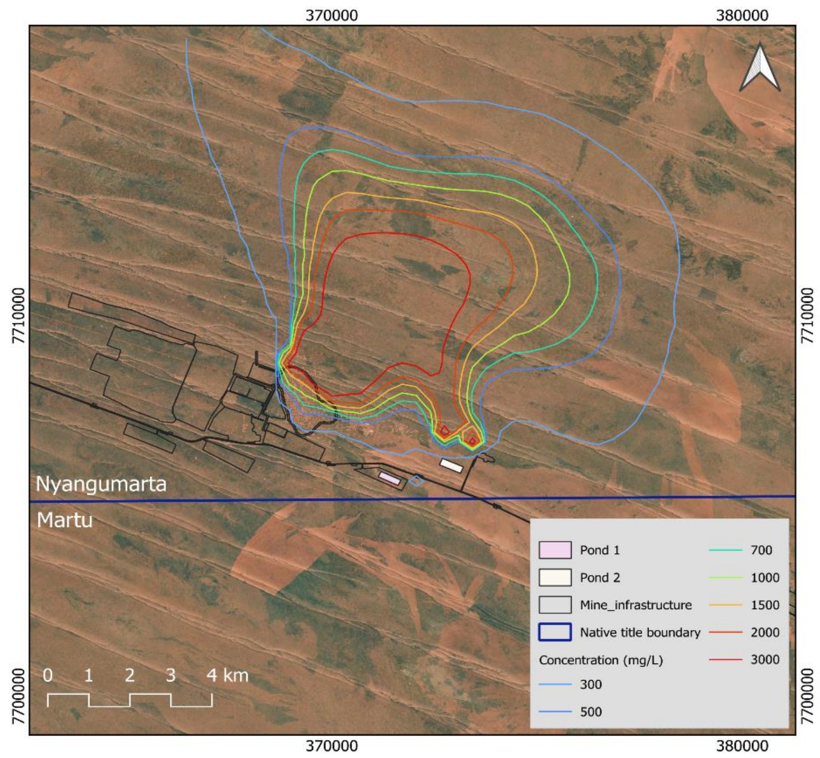

Surplus plume, Year 100 after infiltration ceases

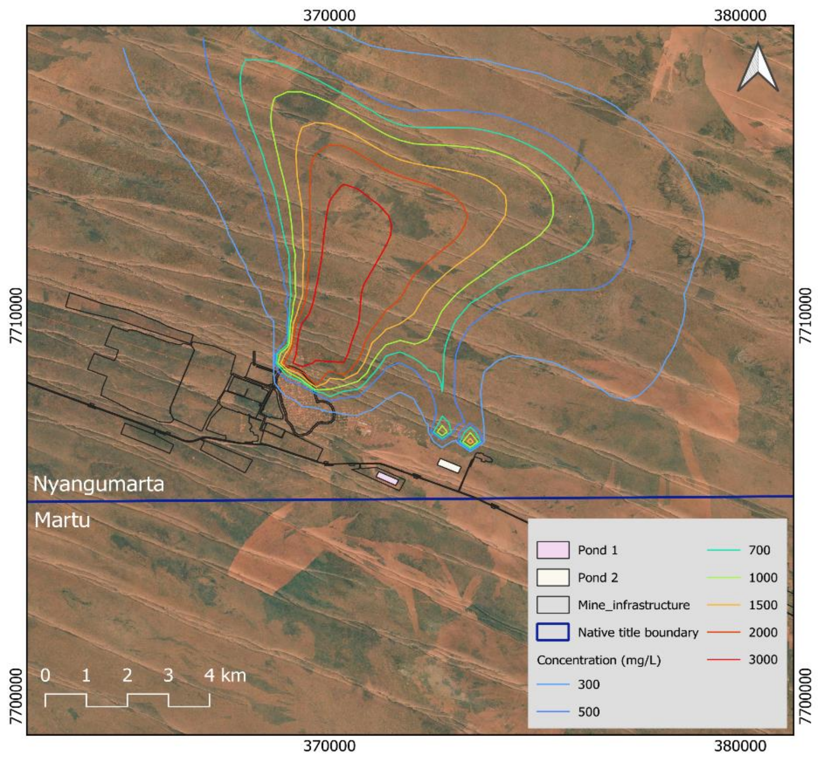

Figure 6-17 Predicted surplus plume concentrations in sandstone aquifer, Pond option

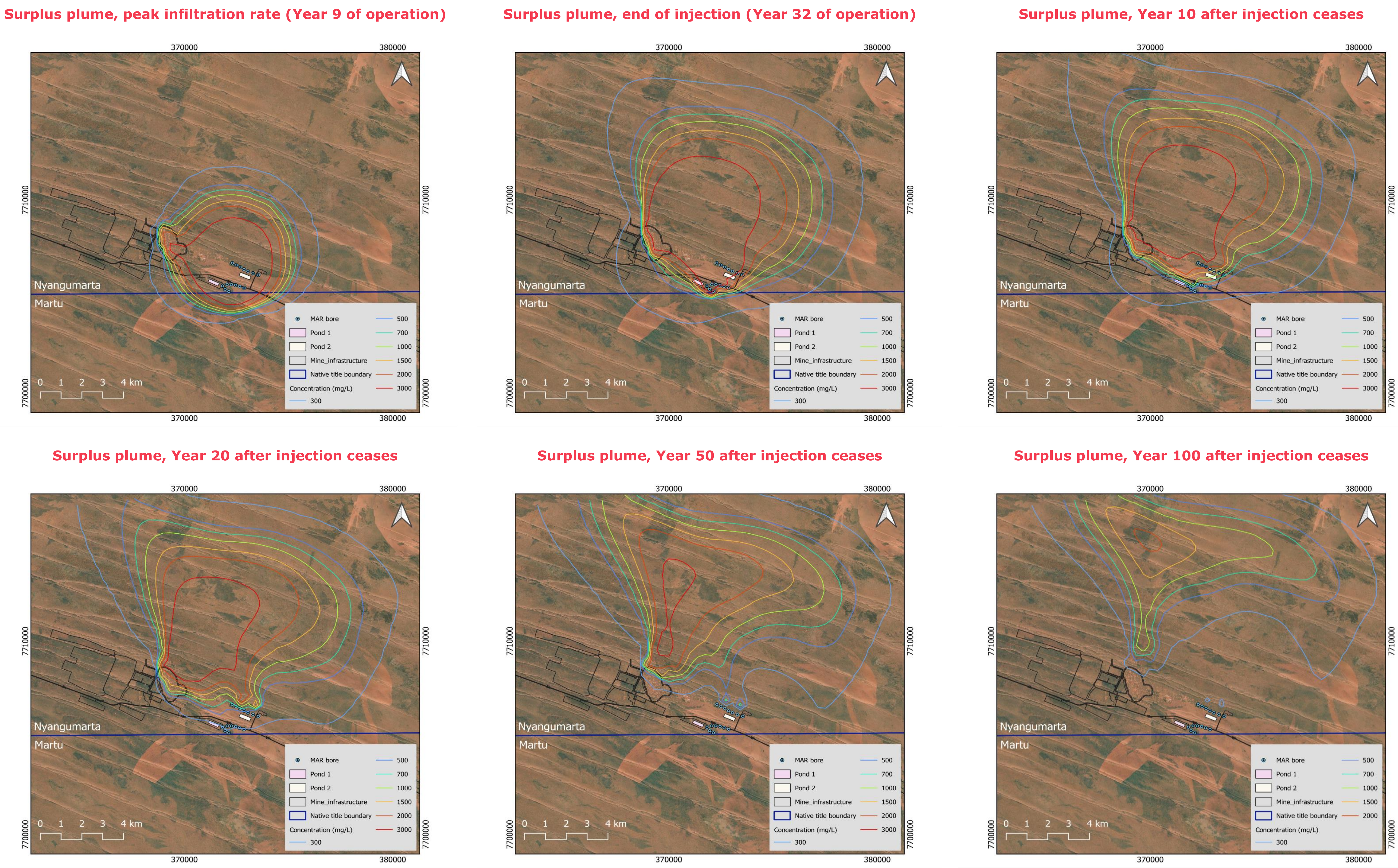

Figure 6-18 Predicted surplus plume concentrations in sandstone aquifer, MAR option

6.2.7 Summary of Results

6.2.7.1 Comparison of Options

Infiltration testing and numerical modelling indicate the viability of both nominal options for surplus water management. There are some relatively minor differences related to groundwater mounding effects, recycling of water back into the mining pit, and demands on footprint which affect site logistics and heritage and environmental values.

The MAR option is considered to have fewer undesirable impact on all counts, however the Pond option is still considered viable, not discounting its importance as providing contingency and buffer for potential peak surplus water management demands, also allowing for regular maintenance of the MAR system.

The differences in pit inflows are:

- MAR option, average return of 15 L/s (31% of injected volume)
- Ponds option, average return of 11 L/s (23% of infiltrated volume)

6.2.7.2 Recommended Option

Although both Options, MAR and pond infiltration are technically feasible based on the modelling results, certain site-specific constraints and the uncertainty surrounding the distribution and continuity of competent sandstone may limit the effectiveness of either option as a stand-alone solution.

Given these limitations, a combined approach is recommended at this stage of the study. This would involve directing preferential flow to the MAR bores, with any excess or overflow being diverted to the infiltration ponds. This hybrid strategy increases system resilience and optimises water recharge under variable site conditions. This option is illustrated in Figure 6-19.

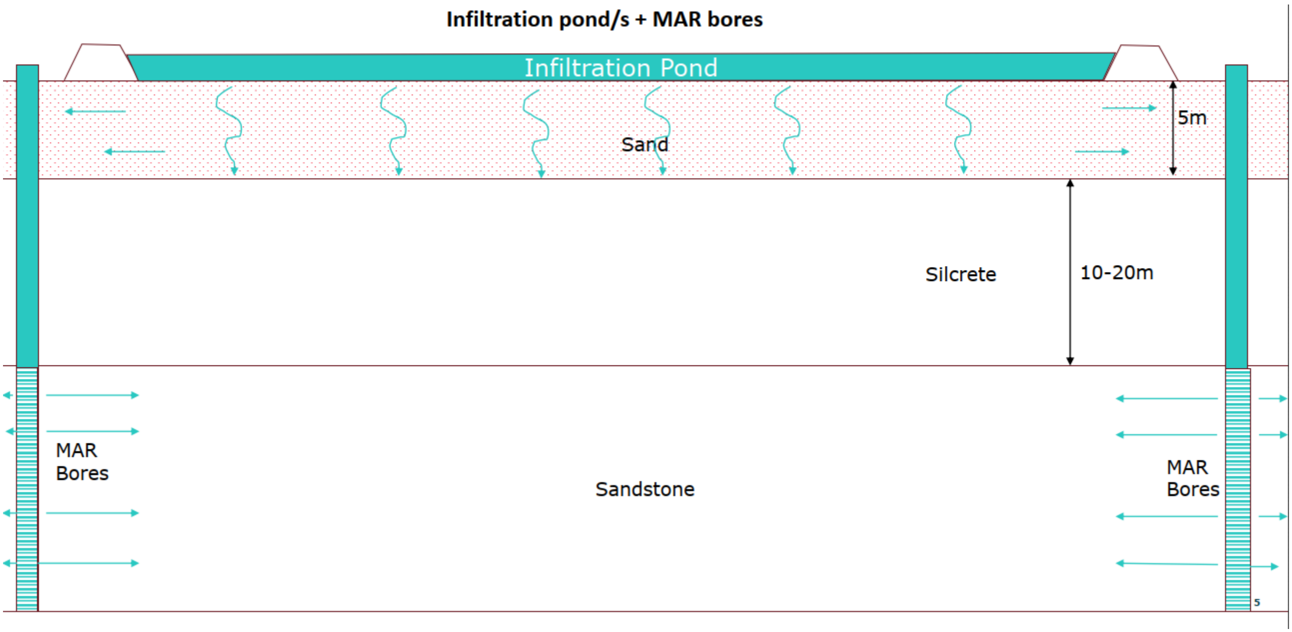

Figure 6-19 Schematic of the recommended surplus water management setup

The MAR bores shall be drilled and installed into the partially saturated sandstone aquifer, the base of which is approximately 40 to 50 m below ground across the two pond locations. The preferred location of the MAR bores is to the eastern side of the infiltration ponds to increase the distance from and to reduce the amount of recirculation towards the mine pit. A nominal spacing of 200 m between each bore is to be applied to distribute surplus water using the saturation of the sandstone aquifer, and to accommodate logistical and regulatory constraints.

MAR bore locations (in two lines) are best arranged in (1) a chevron pattern pointing towards the Pond 1 , and (2) in line along Pond 2, to reduce the number of and to minimise the mounding effect of MAR bores near the ponds.

6.2.7.3 Impact Assessment

The results of numerical modelling support an assessment of the potential risks posed by the Pond and MAR management options, on mining operations and environmental and heritage values at Winu.

A comparison of impacts suggests that the MAR option has negligible potential impact on environmental and heritage values at Winu:

- The Pond option presents a small potential risk of occasional prolonged periods with occurrences of near surface groundwater and establishment of associated groundwater dependent ecosystems (GDEs), or if connectivity between sands and the sandstone aquifer is partly compromised.
- The MAR option injects the water into the sandstone layer. It does not result in groundwater mounding within the surficial sand layer (above the silcrete aquitard), and therefore does not present a risk of establishment of groundwater dependent vegetation at the surface,
- The estimated ground disturbance area for the Pond option is also considered greater than for the MAR option.
- The MAR option is likely to produce slightly higher rates of groundwater inflow to the mine pit. However, the estimated inflow rates to the mine pit attributable to injection are manageable and should not impact on mining operations.
- Both the Pond and MAR options can be constructed without directly impacting on the dunes.
- Since the Pond option may result in the formation of a temporary surface water body appropriate flora and fauna management measures will be required, during operations.
- At mine closure the infiltration pond(s) can be backfilled and rehabilitated to natural surface.

6.2.7.4 Uncertainties Associated with Predictive Simulations

Model predictions are based on field testing of two sites within the footprints of the likely pond locations. The area where effects on the groundwater system are assessed is however larger and cannot be covered by field investigation.

The model thus necessarily assumes that model conceptualisation and parameterisation remains as established from testing and extrapolated, including the properties of the tested sites, over the larger area of the mounding footprint, for either Pond or MAR option.

If the actual conditions do not conform with this conceptual understanding, the likely effects of injection/ponding will be different. The relatively high permeability of sandstone unit and the hydraulic connectivity through silcrete, indicated by recent testing described in this document, must be similar to what is presented in this model for the predictions to reflect the actual future conditions.

7. Conclusions and Recommendations

7.1 Conclusions

A PFS-level surplus water management study, evaluating pond infiltration and MAR injection options was completed based on field investigations and numerical modelling. The focus of the study is to examine the viability of options to manage P90 assessed surplus water, which represents in total 47.3 GL over 32 years of mining.

Proposed surplus mine infrastructure is situated 2 to 2.5 km southeast of the future open mine pit and took into consideration sensitive environmental and heritage areas.

RTC exploration data, geophysical and hydrogeological investigations establish the presence of two aquifer system, that is only partly saturated. The shallow surficial sand cover is up to 10 m thick and separate from the deeper sandstone aquifer (on average 20 to 30 m thick) by a largely heterogeneous silcrete body (on average 10 to 15 m thick) which functions as a leaky aquitard. Depth to groundwater in the study area is 35 m BGL or more.

Two conceptual infiltration ponds, covering 84 and 103 hectares each, installed at the surface of the surficial sand cover, and the MAR borefield nominally consisting of 15 locations into the sandstone aquifer have been evaluated through the use of numerical model developed in MODFLOW-USG and calibrated to observations from the infiltration and injection trial testing.

Both options are indicated by numerical modelling as viable and able to manage the surplus water requirements over the life of the Project, based on the several conceptual assumptions:

- Aquifer properties can be extrapolated from tested areas to larger areas which would represent future mounding footprints. This means that the heterogeneity effects that may be present especially in the sandstone aquifer would not significantly affect the bulk aquifer properties examined by testing and used in numerical modelling
- The MAR option assumes that each MAR location would be able to handle average inflow rates around 3 L/s but up to 8.5 L/s during peak times.
- The MAR option does not result in any mounding in the surficial sand
- The Pond option will result in raised water levels in the surficial sand around the perimeter of infiltration ponds. The Pond option also assumes that the silcrete aquitard is sufficiently leaky to allow seepage of water into the underlying sandstone aquifer, as indicated by infiltration trials.
- Numerical simulations predict that there will be a return of some surplus water into the open mining pit, most notably via the sandstone aquifer. These are estimated by modelling to be 11 to 15 L/s for the Pond and MAR options respectively. These rates are considered manageable by mining infrastructure.

While the MAR option does not represent a potential risk of presence of near surface groundwater, the Pond option may create small zones amenable to establishment of groundwater dependent ecosystems.

7.2 Recommendations

To further assess and confirm the feasibility of surplus water management system for mine dewater at the Project site, the following recommendations are made:

- Extend hydrogeological investigations to areas potentially affected by mounding from the MAR and Pond option to confirm the lithological units, their thicknesses, hydraulic properties (permeability and storativity), and the leaky nature of the silcrete aquitard. These need to extend downgradient from the surplus water management infrastructure towards the open pit and to the north, in the direction of groundwater flow.
- Use drilling techniques for installation of test and MAR bores that do not make use of muds. Factor in the need for periodic cleanup of MAR bores to maintain their injection capacity.
- Assess the water quality in the receiving sandstone aquifer, the likely water quality of the surplus/injected water and assess the risk of clogging due to precipitation e.g. of iron minerals.
- Update numerical modelling based on additional hydrogeological investigations to confirm the viability of both options and/or make adjustments where necessary.
- Assess the effect of infrequent, high intensity rainfall events on Pond option performance and additional risk of mounding.

8. List of References

Advisian, 2023: Winu Gold and Copper Project: Infiltration Pond Study. Technical report for RTC, Rev0, dated 28 September 2023

Advisian, 2024: Winu Excess Water Management: Solute Transport Modelling (Groundwater), Quarry and Pond Options. Technical Memorandum for RTC, Rev0, dated 15 February 2024

Knight Piésold, 2024: Pre-Feasibility Study Geotechnical Investigation Infiltration Ponds. Factual Report for RTC, Rev A: C0007-0300-C-REP-00045, dated 21 November 2024

Worley, 2025a: Rio Tinto Water Balance, Winu Copper Gold Project. Technical report for RTC, Rev0: REP-WB-039, dated 25 March 2025

Worley, 2025b: Rio Tinto Copper H3 Hydrogeological Assessment, Winu Project Area. Technical report for RTC, Rev1: REP-HG-032, dated 20 March 2025

Appendix A. Geophysical Investigation Outcomes

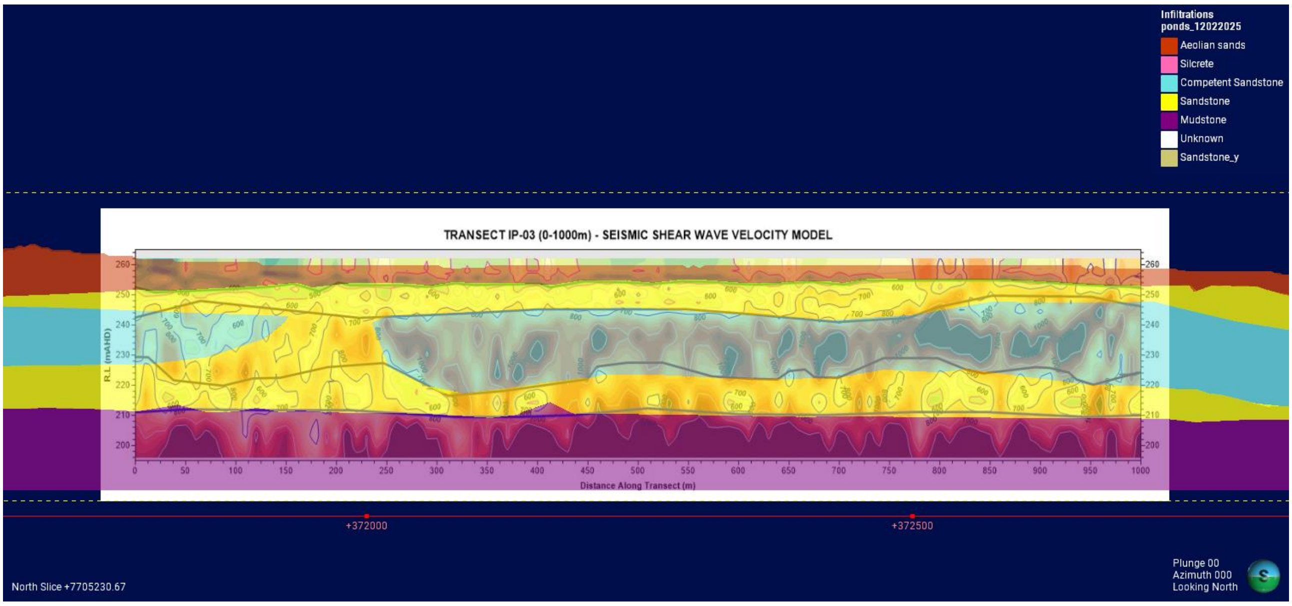
Infiltrations ponds_12022025
Aeolian sands
Silcrete
Competent Sandstone
Sandstone
Mudstone
Unknown
Sandstone_y
TRANSECT IP-03 (0-1000m) - SEISMIC SHEAR WAVE VELOCITY MODEL
R.L (mAHD)
Distance Along Transect (m)
+372000
+372500
North Slice +7705230.67
Plunge 00
Azimuth 000
Looking North

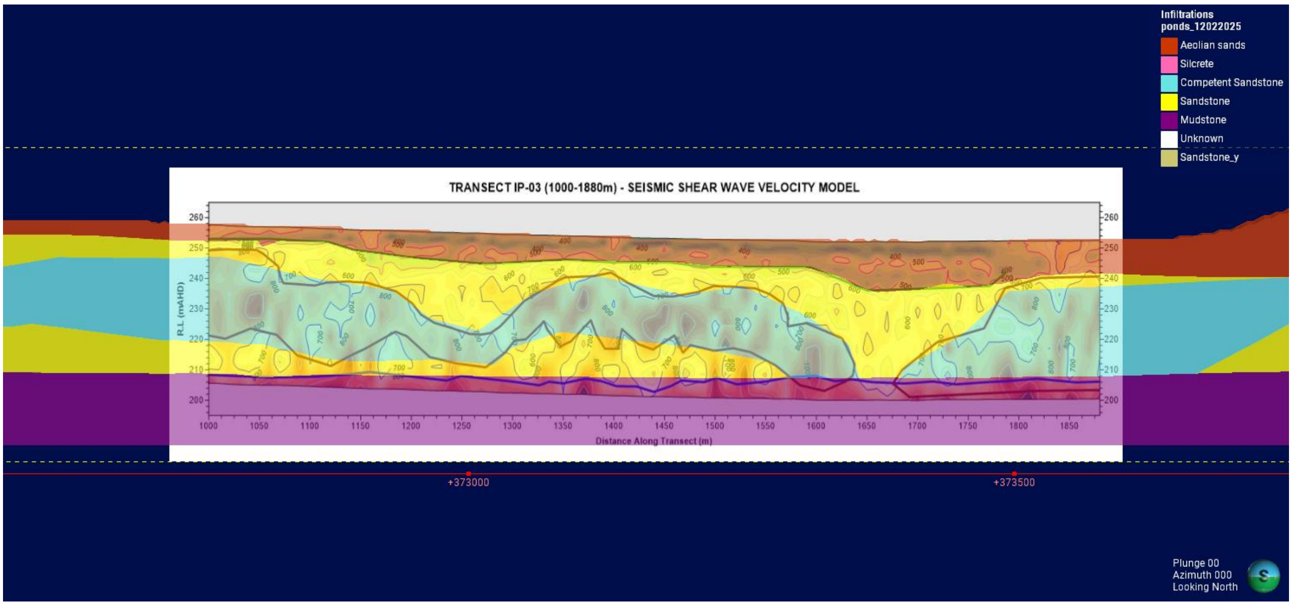
Infiltrations ponds_12022025
Aeolian sands
Silcrete
Competent Sandstone
Sandstone
Mudstone
Unknown
Sandstone_y
TRANSECT IP-03 (1000-1880m) - SEISMIC SHEAR WAVE VELOCITY MODEL
R.L (mAHD)
Distance Along Transect (m)
+373000
+373500
Plunge 00
Azimuth 000
Looking North

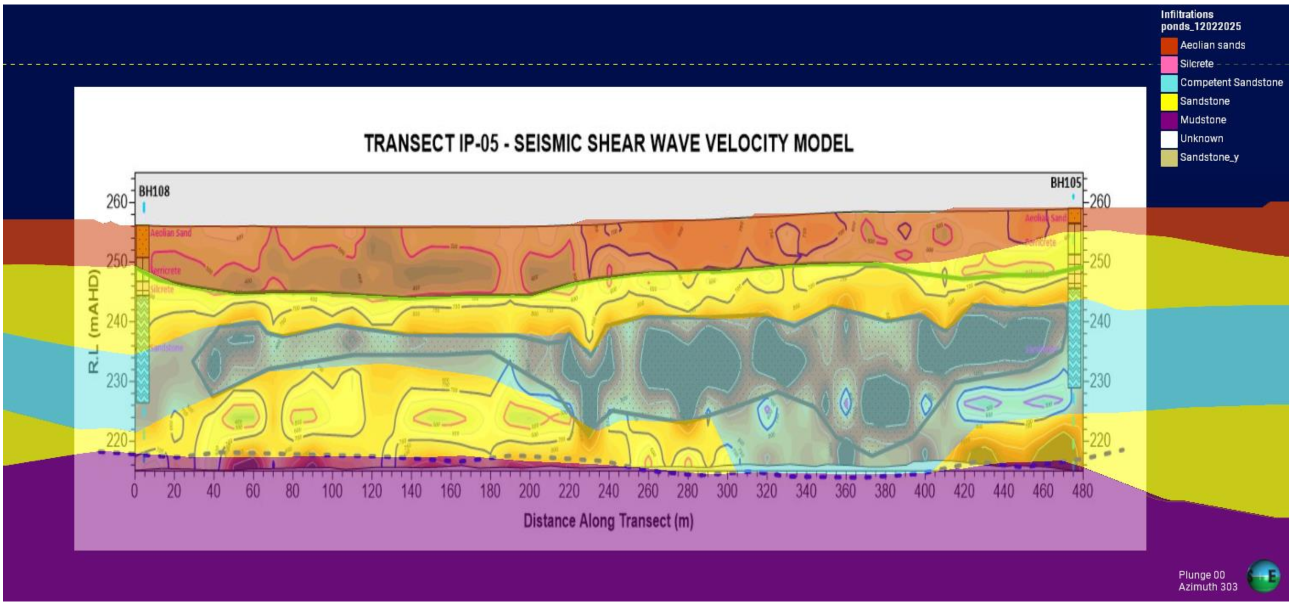

TRANSECT IP-05 - SEISMIC SHEAR WAVE VELOCITY MODEL
Infiltrations ponds_12022025
Aeolian sands
Silcrete
Competent Sandstone
Sandstone
Mudstone
Unknown
Sandstone_y
BH108
BH105
R.L (mAHD)
Distance Along Transect (m)
Plunge 00
Azimuth 303

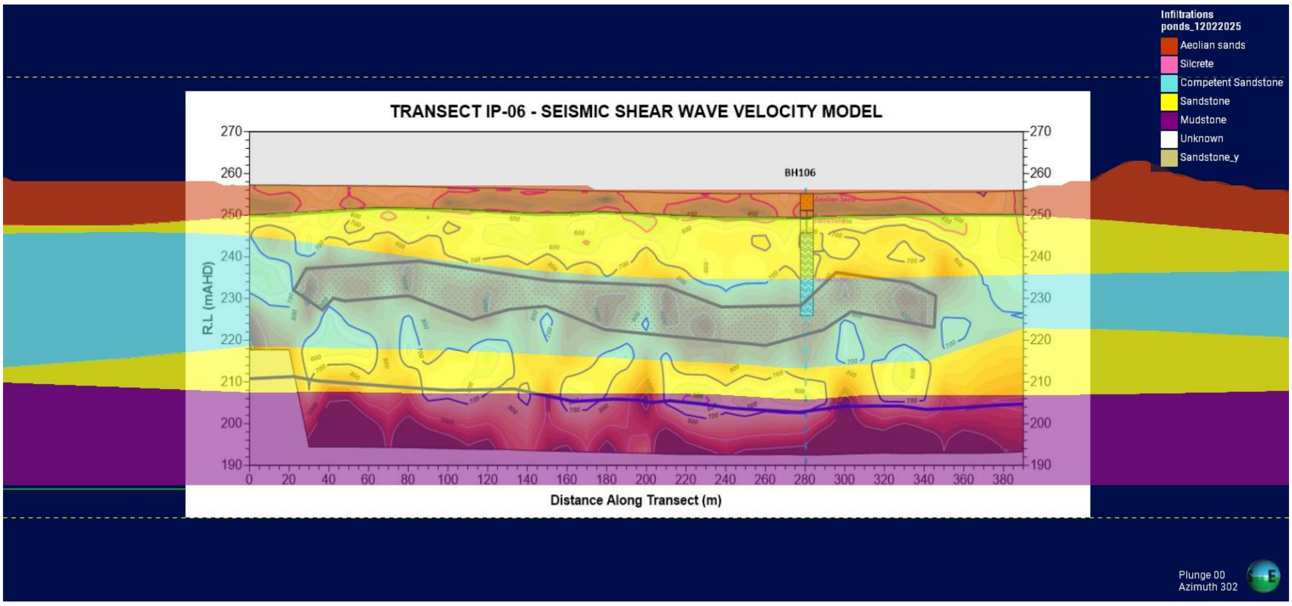

TRANSECT IP-06 - SEISMIC SHEAR WAVE VELOCITY MODEL
Infiltrations ponds_12022025
Aeolian sands
Silcrete
Competent Sandstone
Sandstone
Mudstone
Unknown
Sandstone_y
BH106
R.L (mAHD)
Distance Along Transect (m)
Plunge 00
Azimuth 302

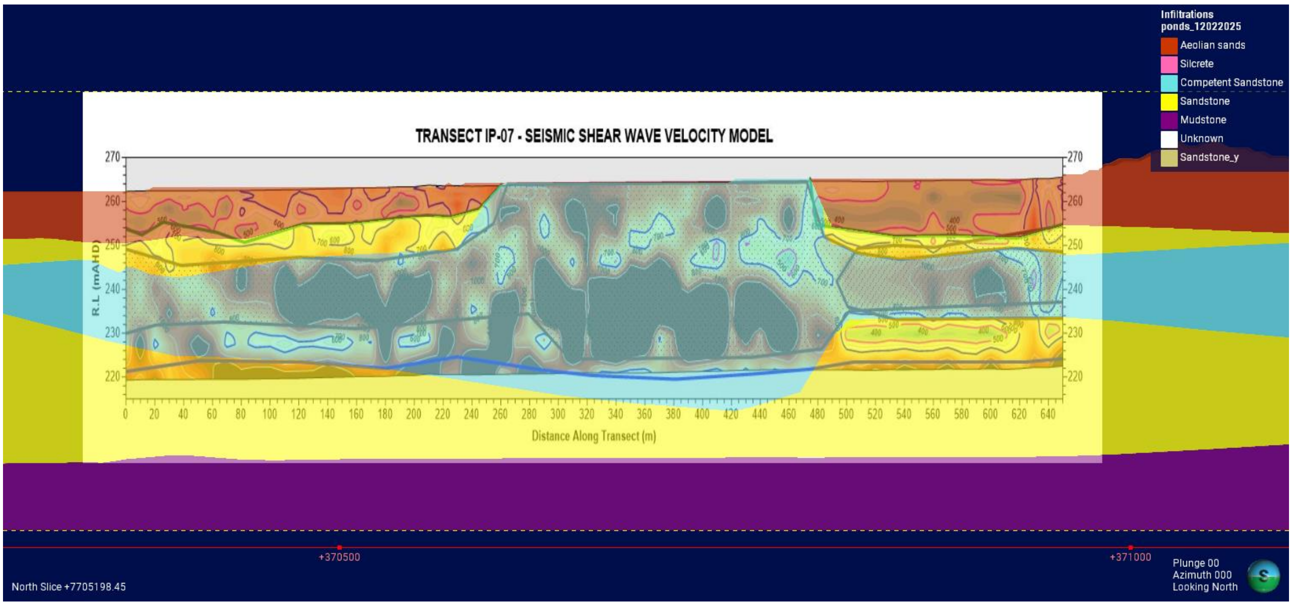

TRANSECT IP-07 - SEISMIC SHEAR WAVE VELOCITY MODEL
Infiltrations ponds_12022025
Aeolian sands
Silcrete
Competent Sandstone
Sandstone
Mudstone
Unknown
Sandstone_y
R.L (mAHD)
Distance Along Transect (m)
+370500
+371000
North Slice +7705198.45
Plunge 00
Azimuth 000
Looking North

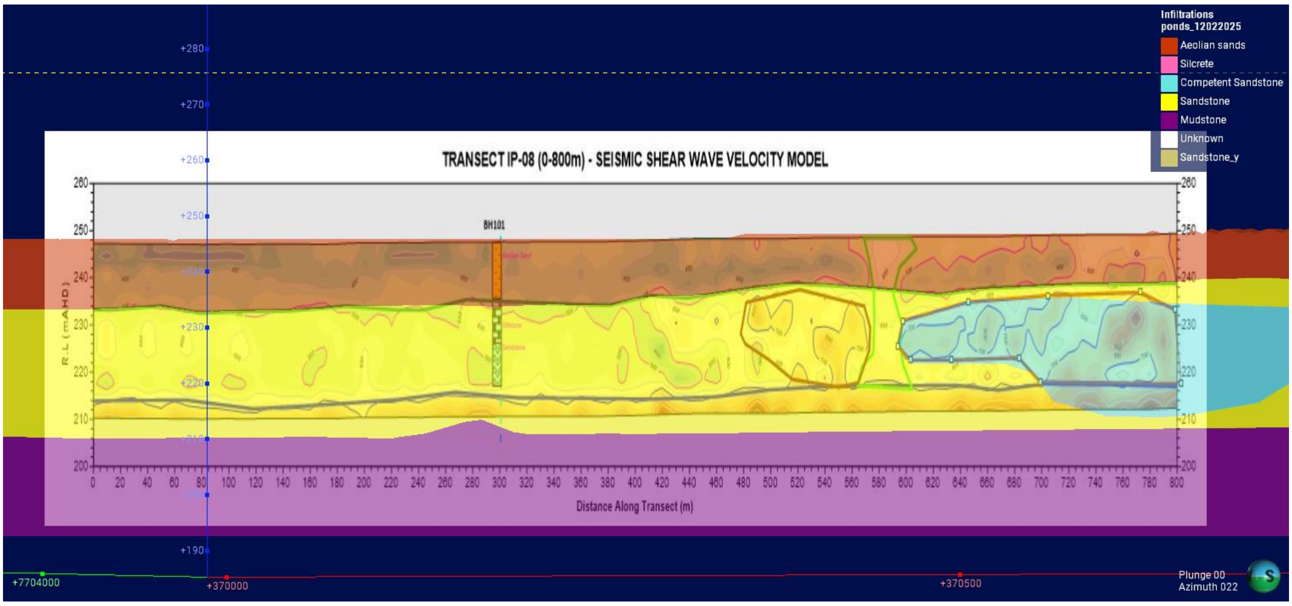

TRANSECT IP-08 (0-800m) - SEISMIC SHEAR WAVE VELOCITY MODEL
Infiltrations ponds_12022025
Aeolian sands
Silcrete
Competent Sandstone
Sandstone
Mudstone
Unknown
Sandstone_y
BH101
R.L (mAHD)
Distance Along Transect (m)
+7704000
+370000
+370500
Plunge 00
Azimuth 022

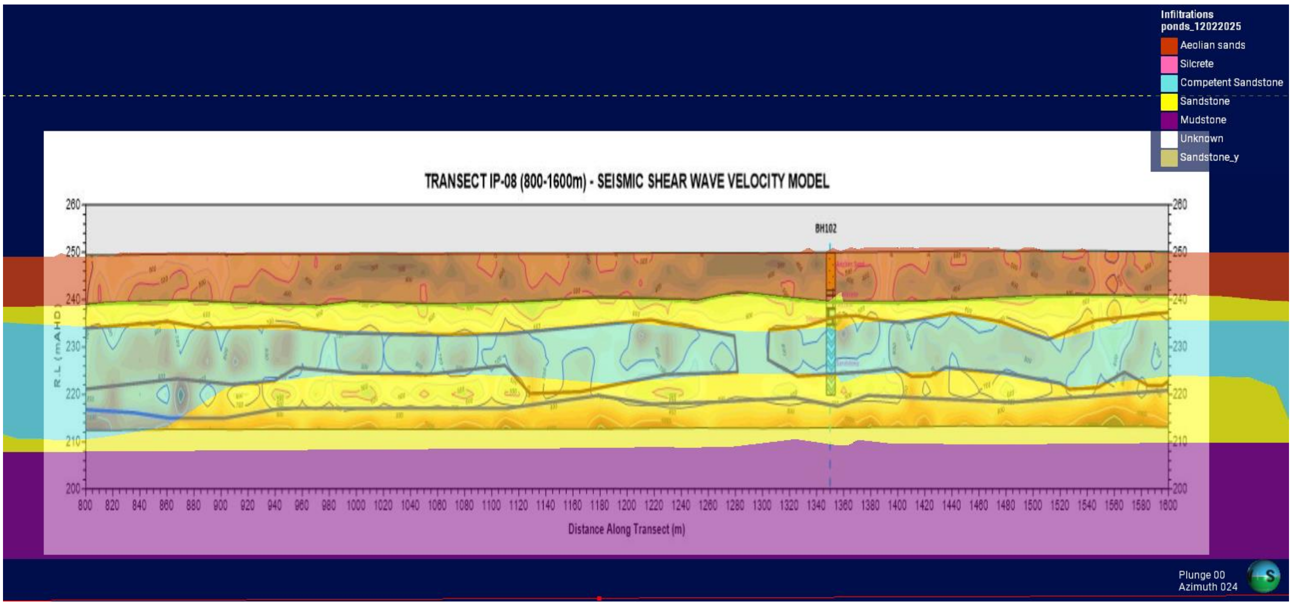
Infiltrations ponds_12022025
Aeolian sands
Silcrete
Competent Sandstone
Sandstone
Mudstone
Unknown
Sandstone_y
TRANSECT IP-08 (800-1600m) - SEISMIC SHEAR WAVE VELOCITY MODEL
BH102
R.L (mAHD)
Distance Along Transect (m)
Plunge 00
Azimuth 024

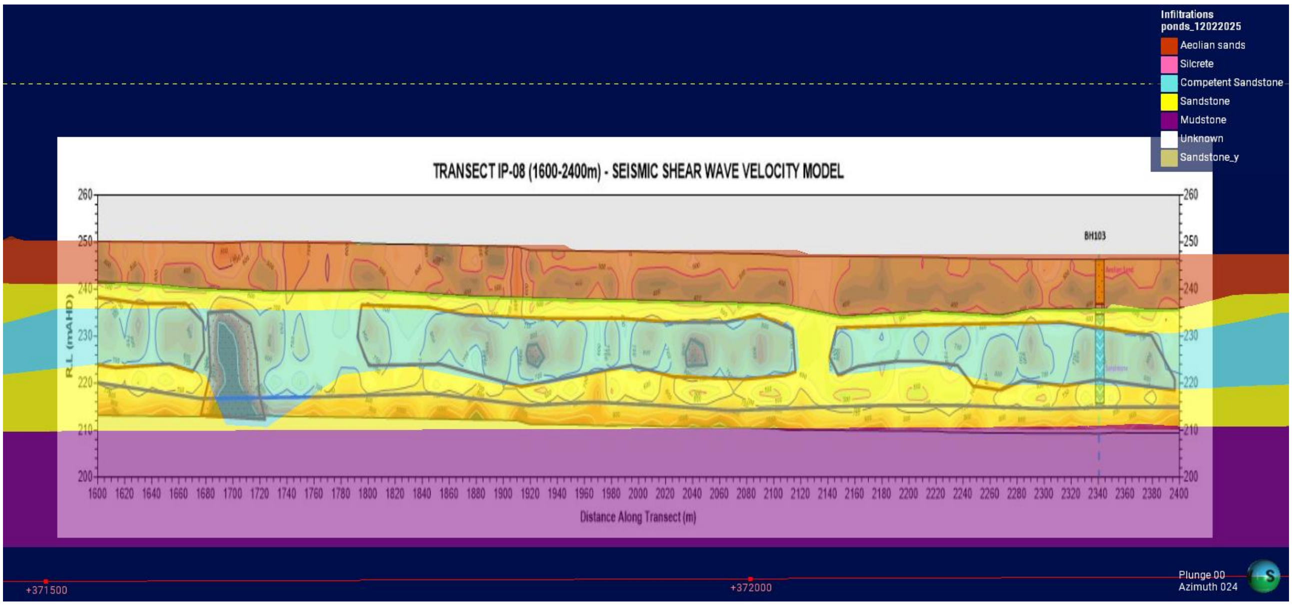
Infiltrations ponds_12022025
Aeolian sands
Silcrete
Competent Sandstone
Sandstone
Mudstone
Unknown
Sandstone_y
TRANSECT IP-08 (1600-2400m) - SEISMIC SHEAR WAVE VELOCITY MODEL
BH103
R.L (mAHD)
Distance Along Transect (m)
+371500
+372000
Plunge 00
Azimuth 024

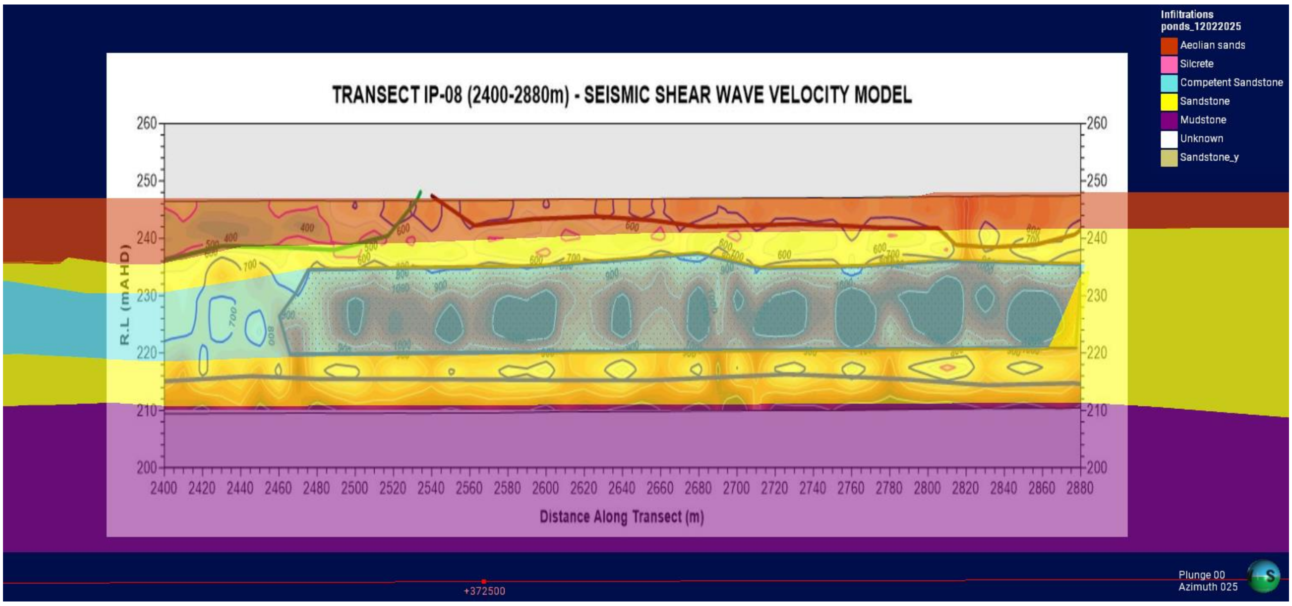
TRANSECT IP-08 (2400-2880m) - SEISMIC SHEAR WAVE VELOCITY MODEL
Infiltrations ponds_12022025
Aeolian sands
Silcrete
Competent Sandstone
Sandstone
Mudstone
Unknown
Sandstone_y
R.L (mAHD)
Distance Along Transect (m)
Plunge 00
Azimuth 025

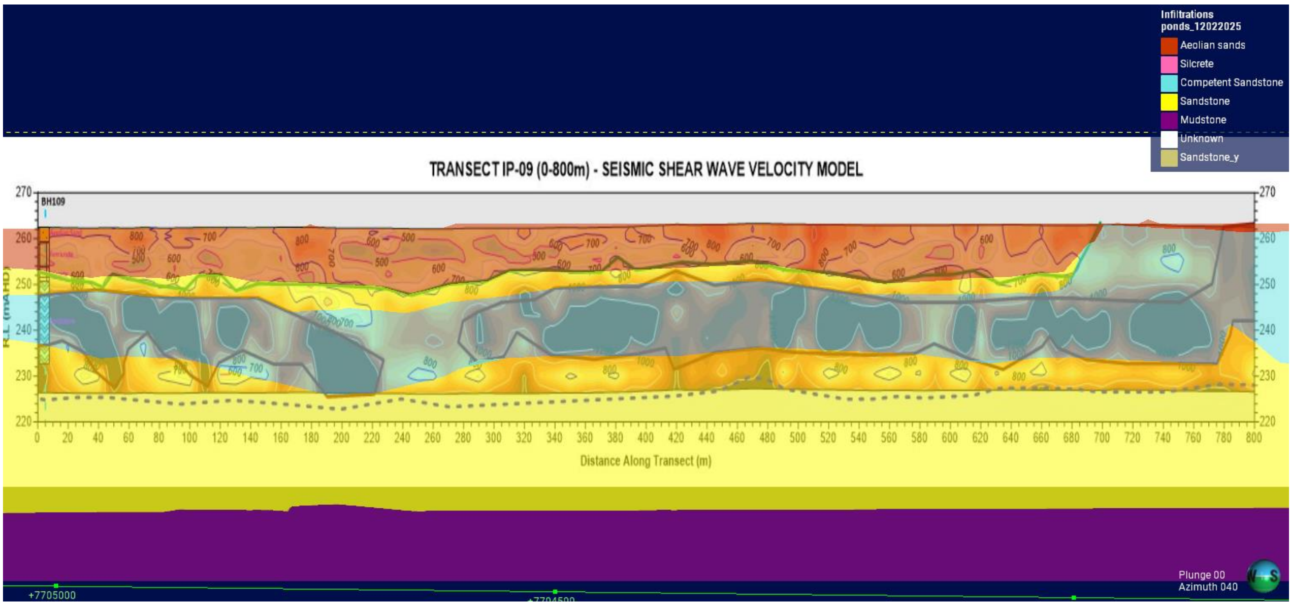
TRANSECT IP-09 (0-800m) - SEISMIC SHEAR WAVE VELOCITY MODEL
Infiltrations ponds_12022025
Aeolian sands
Silcrete
Competent Sandstone
Sandstone
Mudstone
Unknown
Sandstone_y
BH109
Distance Along Transect (m)
Plunge 00
Azimuth 040

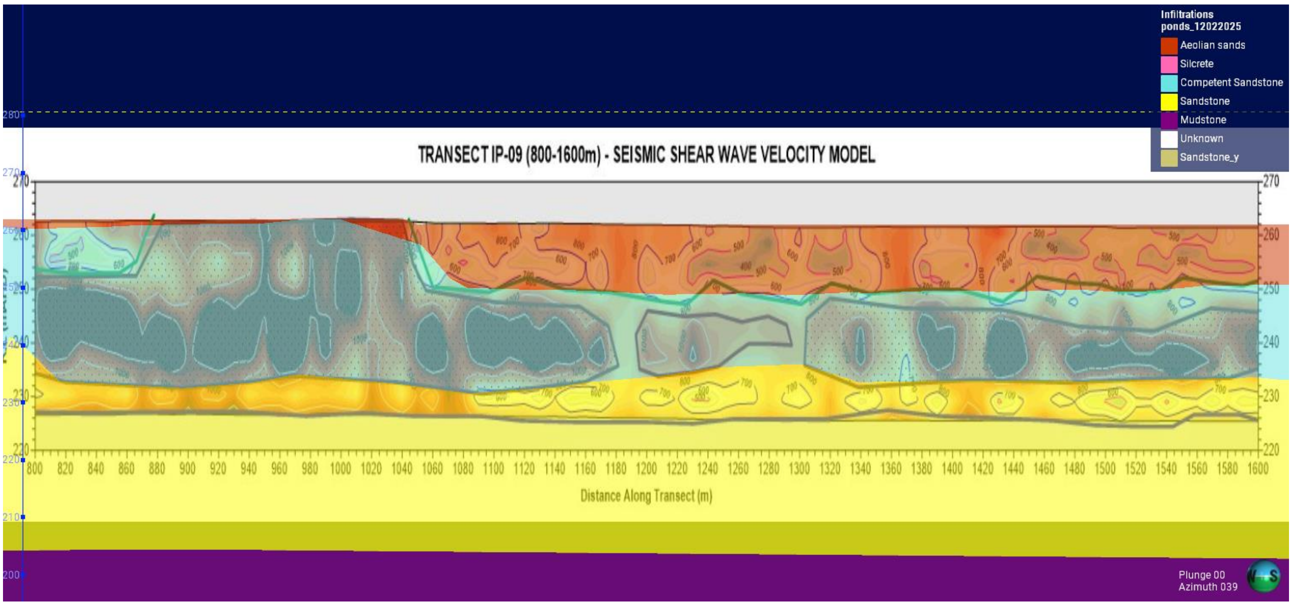
TRANSECT IP-09 (800-1600m) - SEISMIC SHEAR WAVE VELOCITY MODEL
Infiltrations ponds_12022025
Aeolian sands
Silcrete
Competent Sandstone
Sandstone
Mudstone
Unknown
Sandstone_y
Distance Along Transect (m)
Plunge 00
Azimuth 039

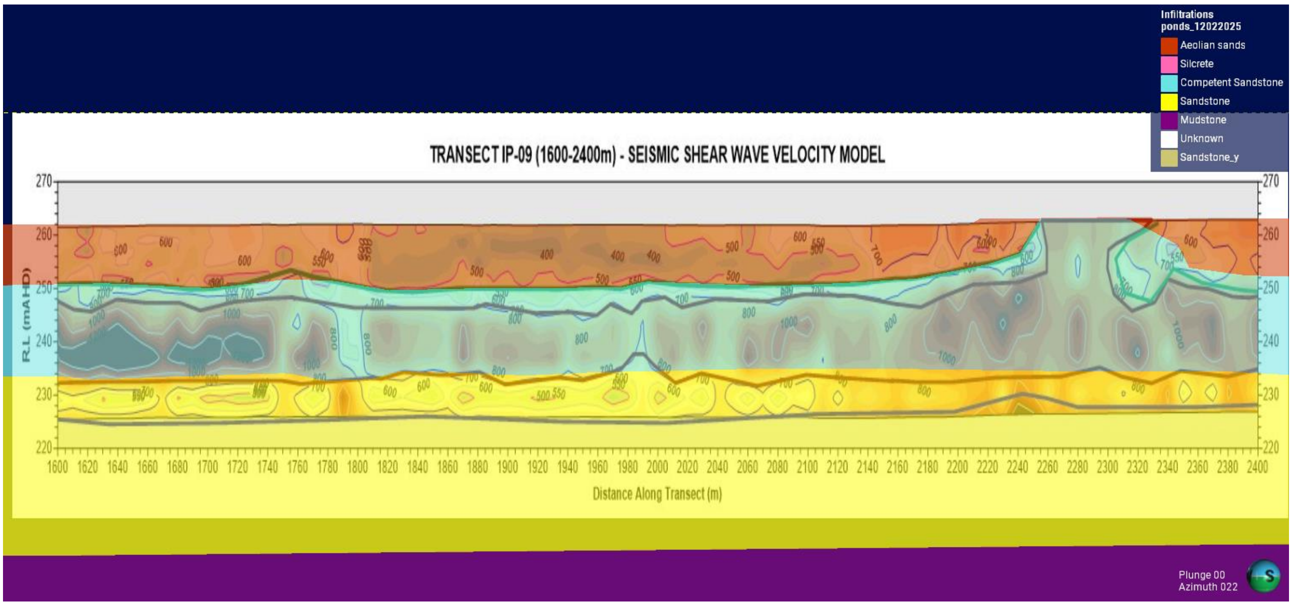
TRANSECT IP-09 (1600-2400m) - SEISMIC SHEAR WAVE VELOCITY MODEL
Infiltrations ponds_12022025
Aeolian sands
Silcrete
Competent Sandstone
Sandstone
Mudstone
Unknown
Sandstone_y
R.L (mAHD)
Distance Along Transect (m)
Plunge 00
Azimuth 022

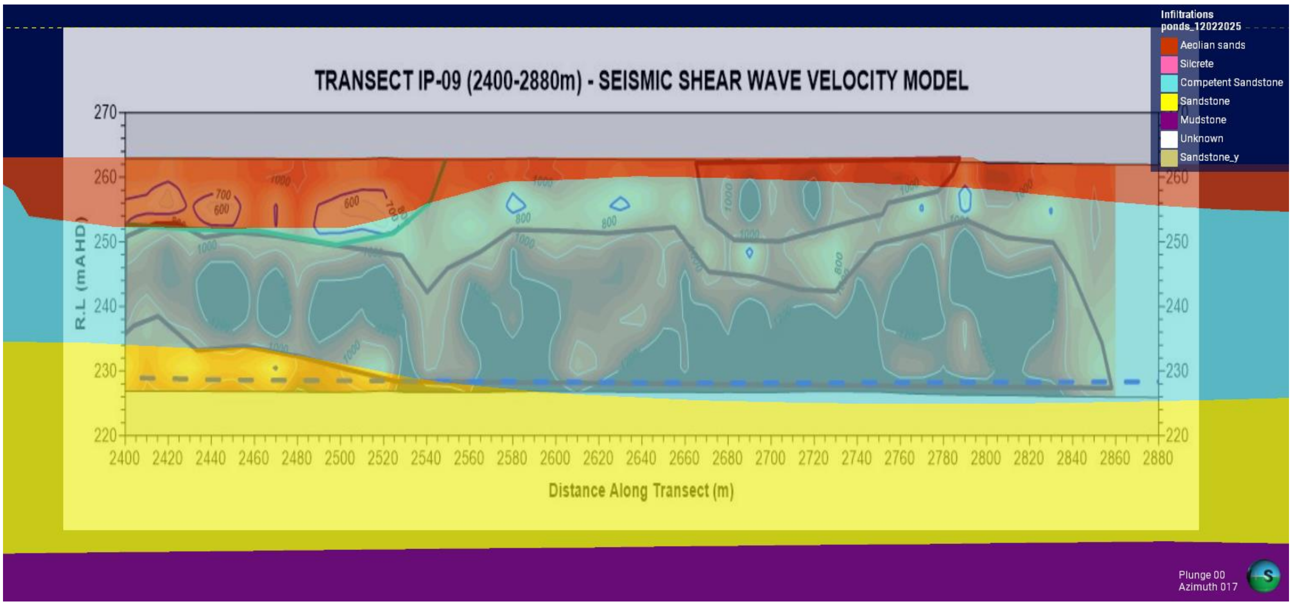

Infiltrations ponds_12022025
Aeolian sands
Silcrete
Competent Sandstone
Sandstone
Mudstone
Unknown
Sandstone_y
TRANSECT IP-09 (2400-2880m) - SEISMIC SHEAR WAVE VELOCITY MODEL
R.L (mAHD)
Distance Along Transect (m)
Plunge 00
Azimuth 017

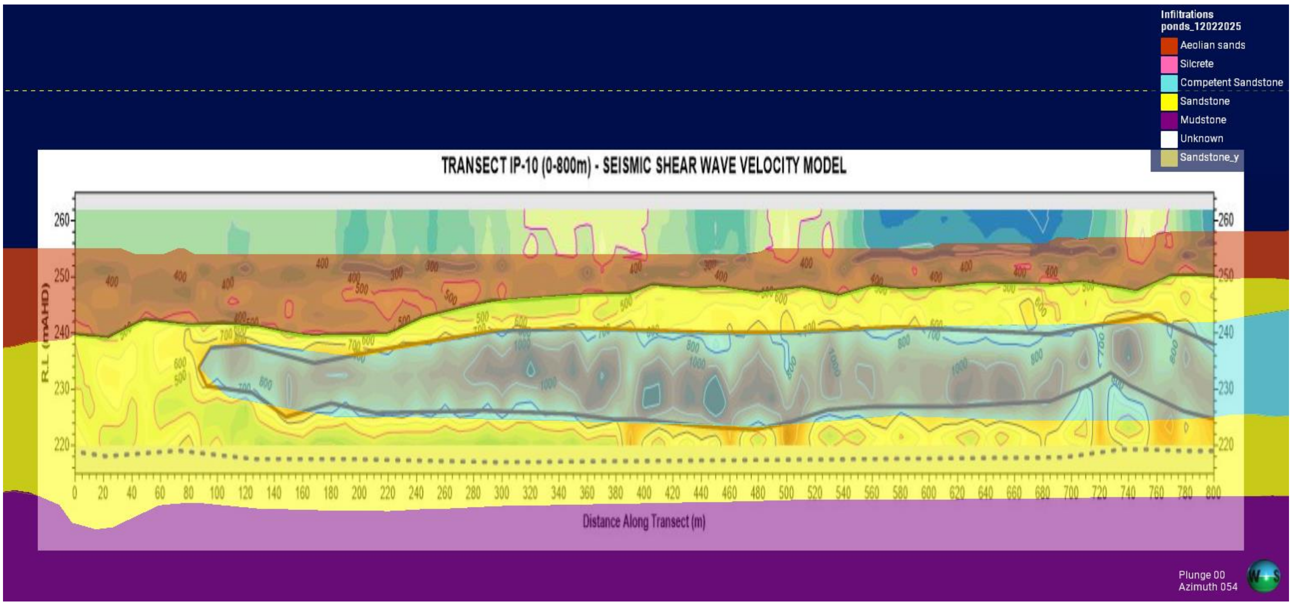

Infiltrations ponds_12022025
Aeolian sands
Silcrete
Competent Sandstone
Sandstone
Mudstone
Unknown
Sandstone_y
TRANSECT IP-10 (0-800m) - SEISMIC SHEAR WAVE VELOCITY MODEL
R.L (mAHD)
Distance Along Transect (m)
Plunge 00
Azimuth 054

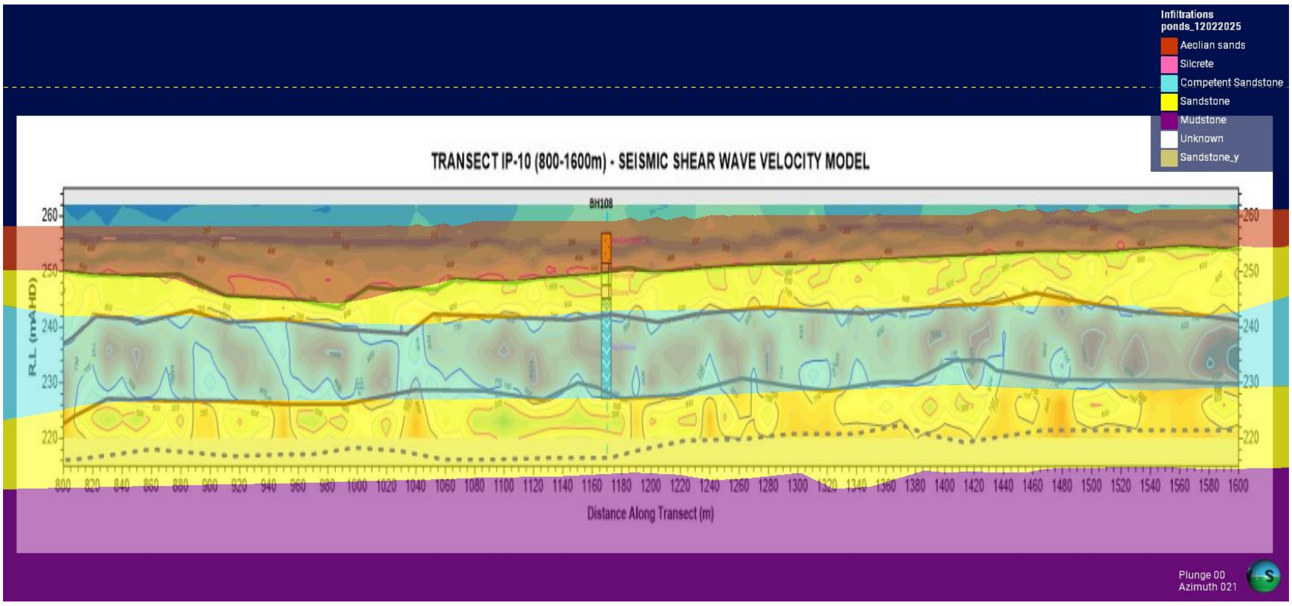
TRANSECT IP-10 (800-1600m) - SEISMIC SHEAR WAVE VELOCITY MODEL
Infiltrations ponds_12022025
Aeolian sands
Silcrete
Competent Sandstone
Sandstone
Mudstone
Unknown
Sandstone_y
BH108
R.L (mAHD)
Distance Along Transect (m)
Plunge 00
Azimuth 021

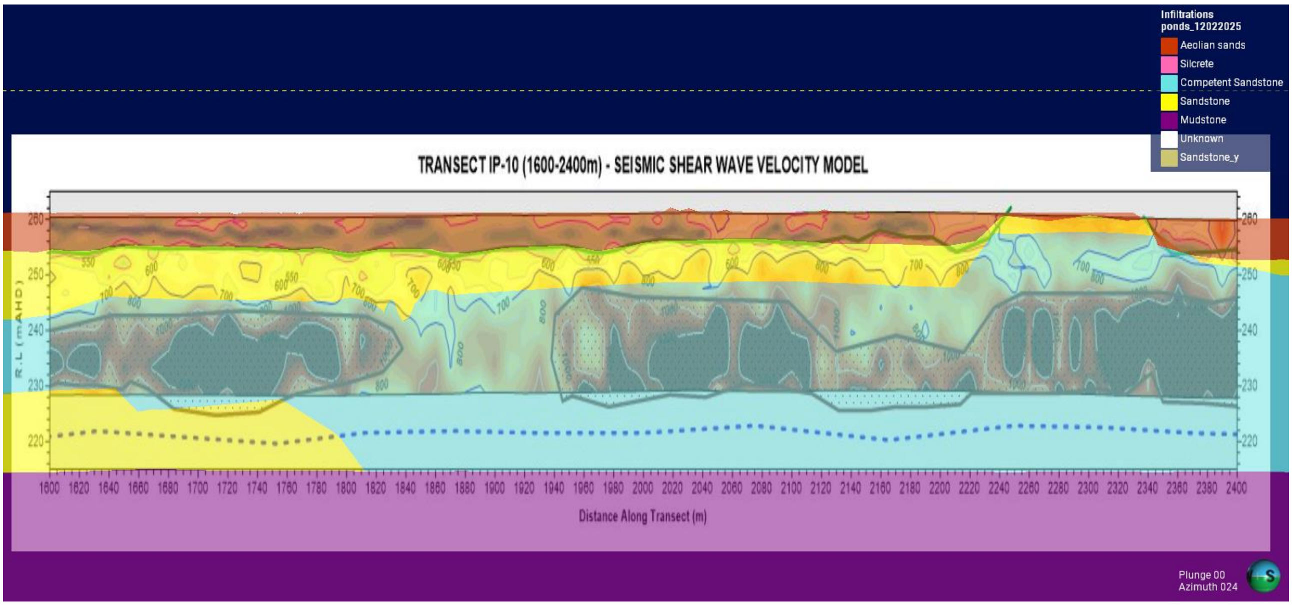
TRANSECT IP-10 (1600-2400m) - SEISMIC SHEAR WAVE VELOCITY MODEL
Infiltrations ponds_12022025
Aeolian sands
Silcrete
Competent Sandstone
Sandstone
Mudstone
Unknown
Sandstone_y
R.L (mAHD)
Distance Along Transect (m)
Plunge 00
Azimuth 024

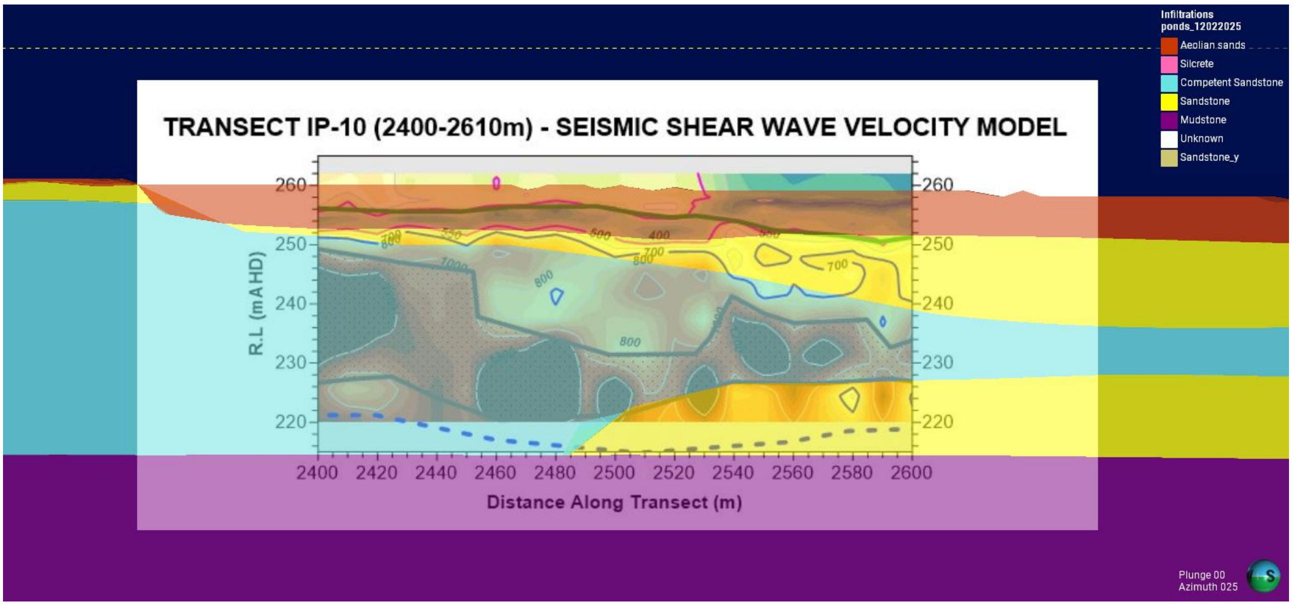

Infiltrations ponds_12022025
Aeolian sands
Silcrete
Competent Sandstone
Sandstone
Mudstone
Unknown
Sandstone_y
TRANSECT IP-10 (2400-2610m) - SEISMIC SHEAR WAVE VELOCITY MODEL
R.L (mAHD)
260
250
240
230
220
2400 2420 2440 2460 2480 2500 2520 2540 2560 2580 2600
Distance Along Transect (m)
Plunge 00
Azimuth 025

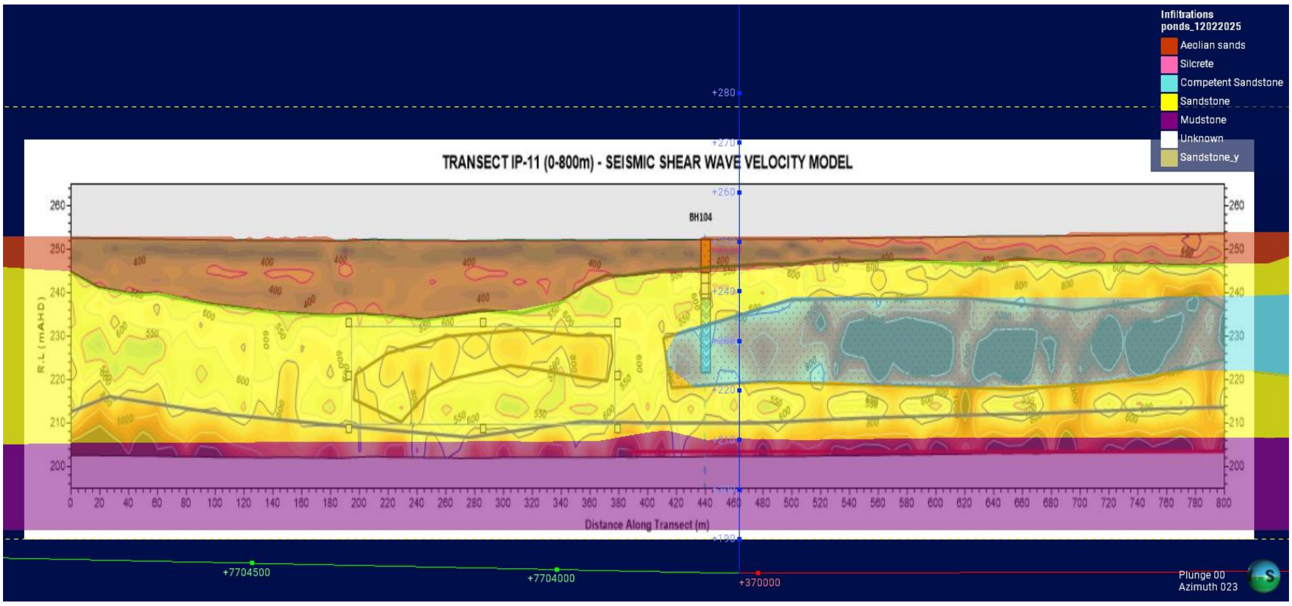

Infiltrations ponds_12022025
Aeolian sands
Silcrete
Competent Sandstone
Sandstone
Mudstone
Unknown
Sandstone_y
TRANSECT IP-11 (0-800m) - SEISMIC SHEAR WAVE VELOCITY MODEL
BH104
R.L (mAHD)
Distance Along Transect (m)
+7704500
+7704000
+370000
Plunge 00
Azimuth 023

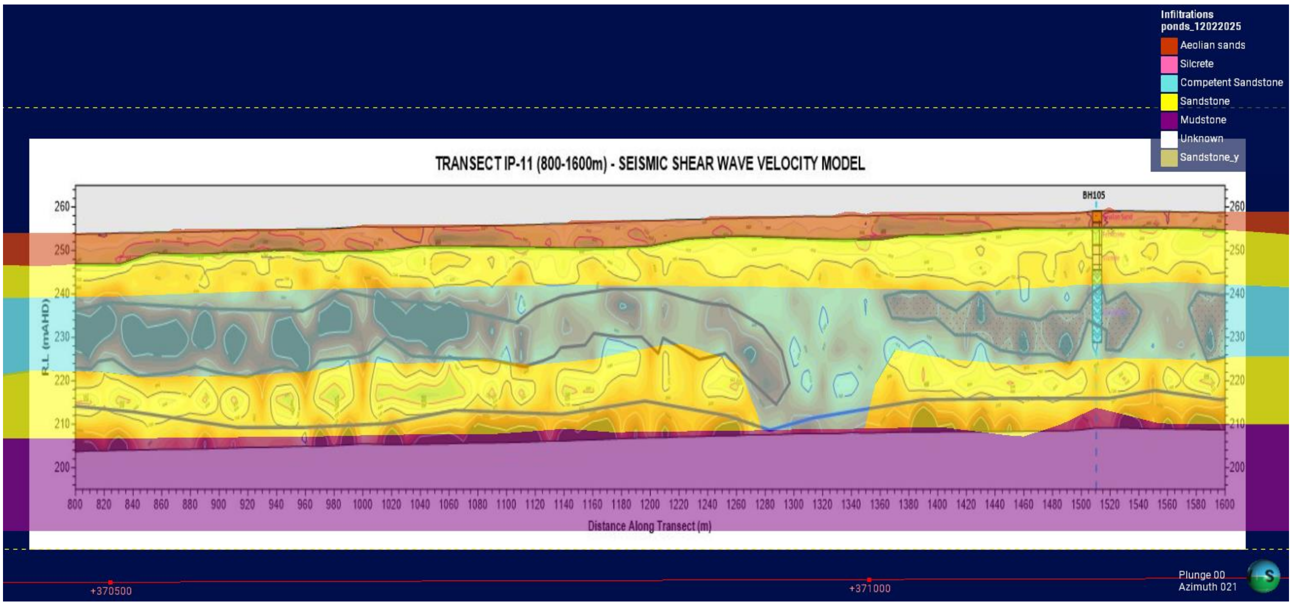
Infiltrations ponds_12022025
Aeolian sands
Silcrete
Competent Sandstone
Sandstone
Mudstone
Unknown
Sandstone_y
TRANSECT IP-11 (800-1600m) - SEISMIC SHEAR WAVE VELOCITY MODEL
BH105
R.L. (mAHD)
Distance Along Transect (m)
+370500
+371000
Plunge 00
Azimuth 021

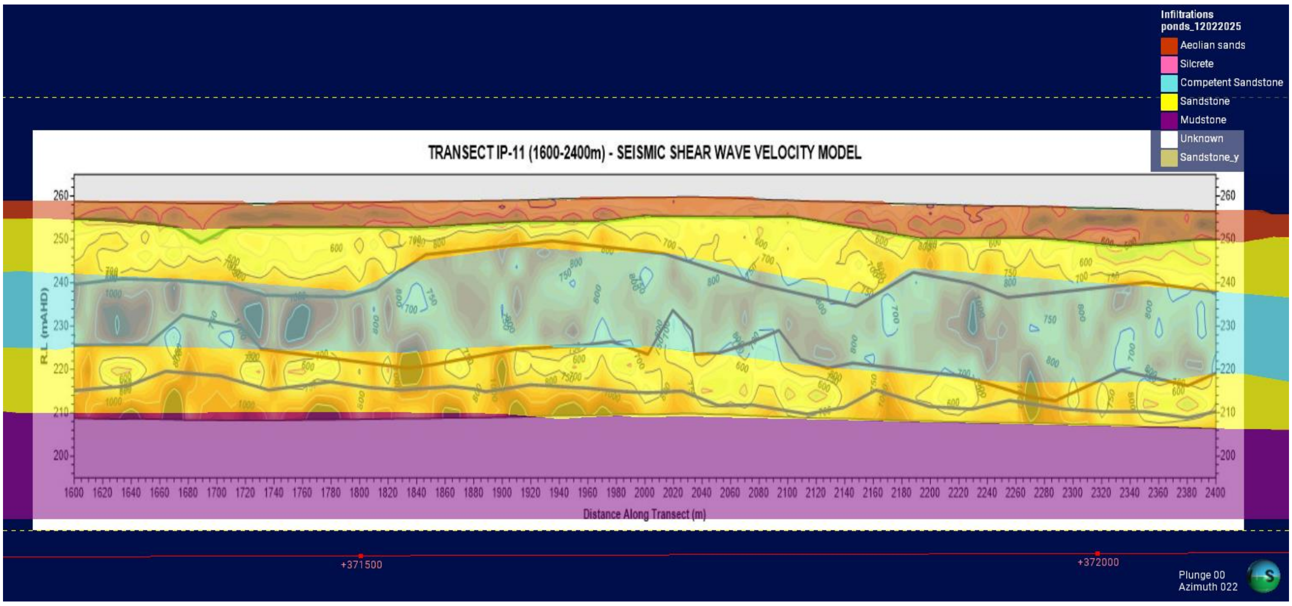
Infiltrations ponds_12022025
Aeolian sands
Silcrete
Competent Sandstone
Sandstone
Mudstone
Unknown
Sandstone_y
TRANSECT IP-11 (1600-2400m) - SEISMIC SHEAR WAVE VELOCITY MODEL
R.L. (mAHD)
Distance Along Transect (m)
+371500
+372000
Plunge 00
Azimuth 022

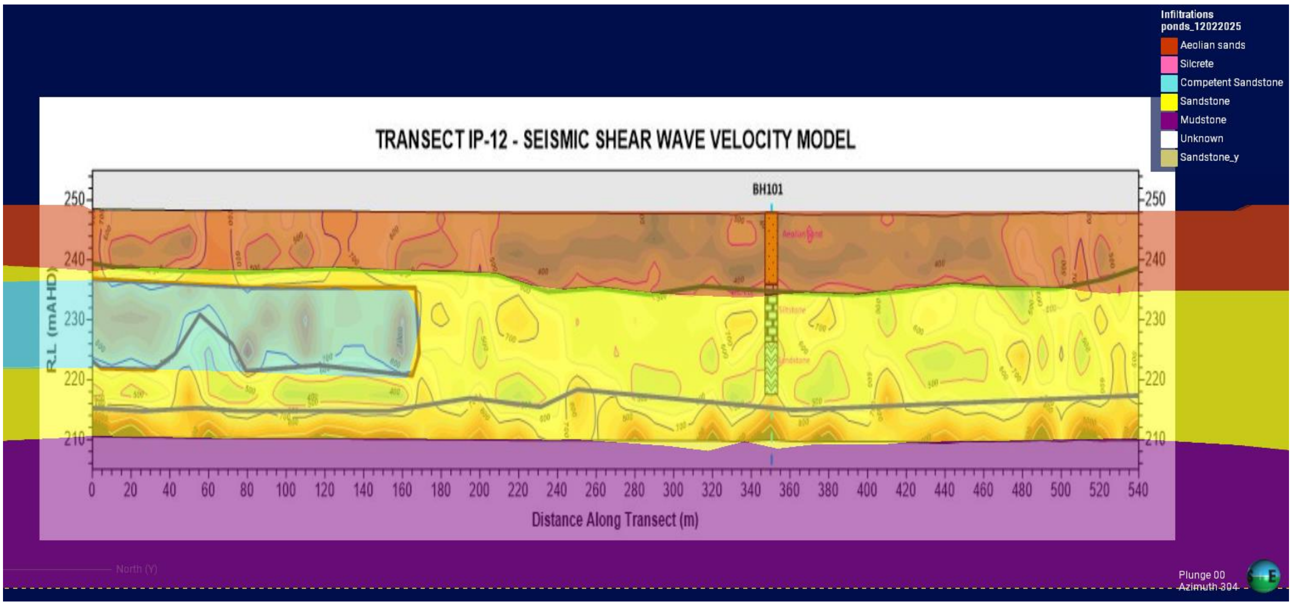
TRANSECT IP-12 - SEISMIC SHEAR WAVE VELOCITY MODEL
BH101
R.L (mAHD)
Distance Along Transect (m)
Infiltrations ponds_12022025
Aeolian sands
Silcrete
Competent Sandstone
Sandstone
Mudstone
Unknown
Sandstone_y
Plunge 00
Azimuth 304

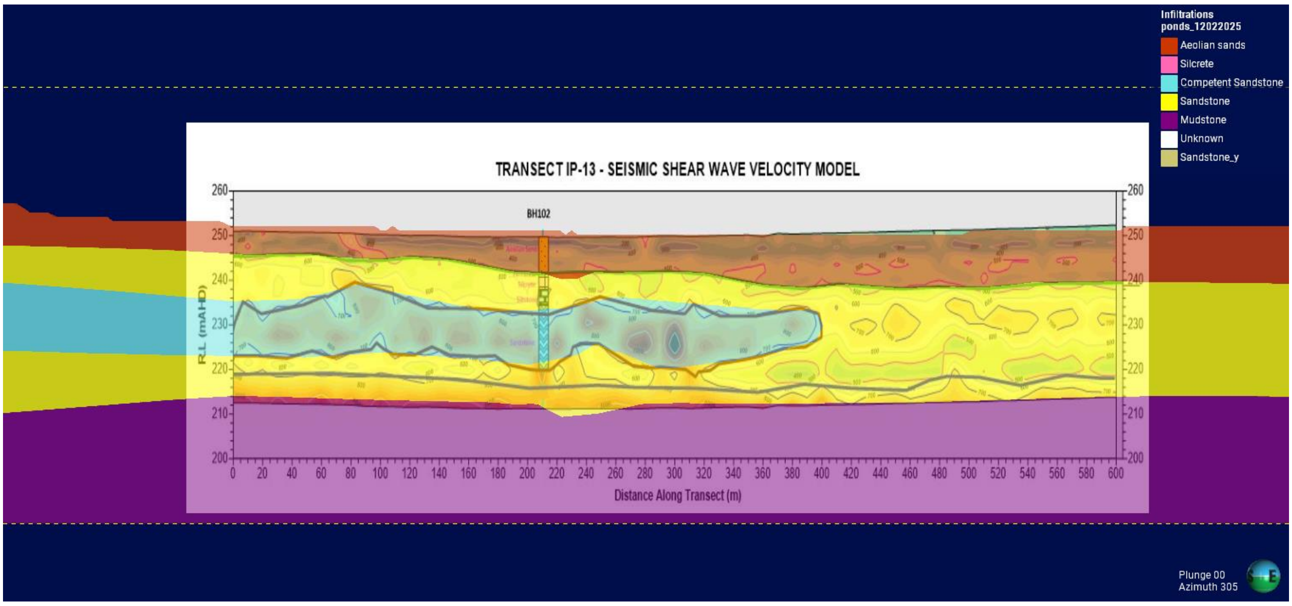
TRANSECT IP-13 - SEISMIC SHEAR WAVE VELOCITY MODEL
BH102
R.L (mAHD)
Distance Along Transect (m)
Infiltrations ponds_12022025
Aeolian sands
Silcrete
Competent Sandstone
Sandstone
Mudstone
Unknown
Sandstone_y
Plunge 00
Azimuth 305

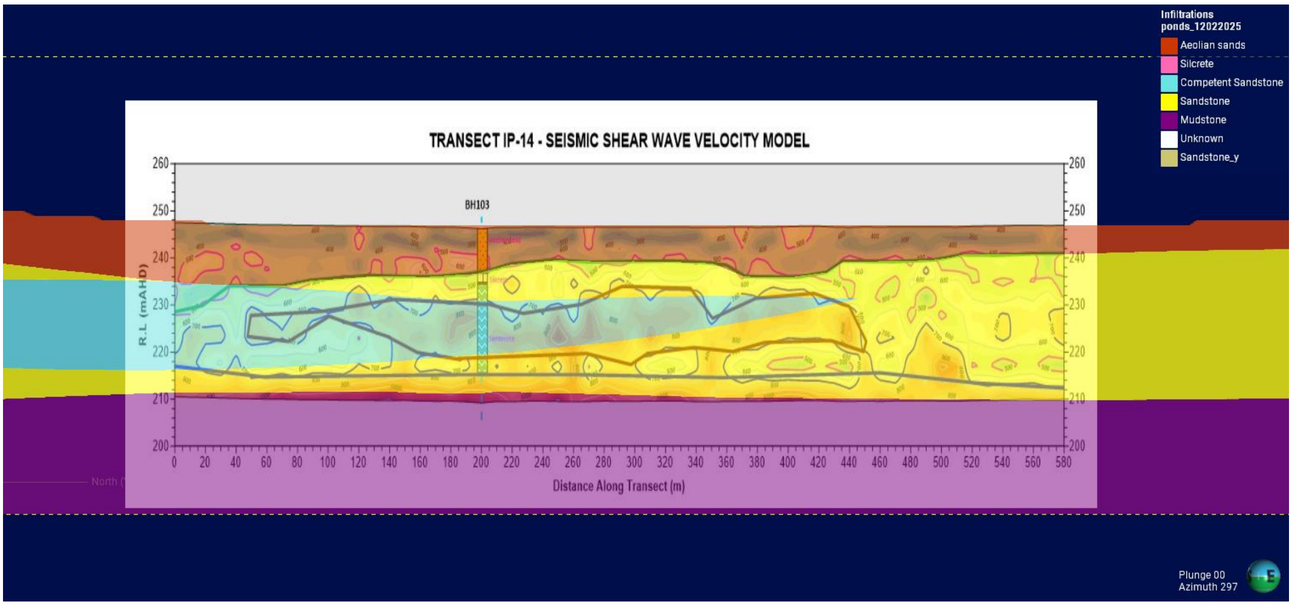
Infiltrations ponds_12022025
Aeolian sands
Silcrete
Competent Sandstone
Sandstone
Mudstone
Unknown
Sandstone_y
TRANSECT IP-14 - SEISMIC SHEAR WAVE VELOCITY MODEL
BH103
R.L (mAHD)
Distance Along Transect (m)
Plunge 00
Azimuth 297
E

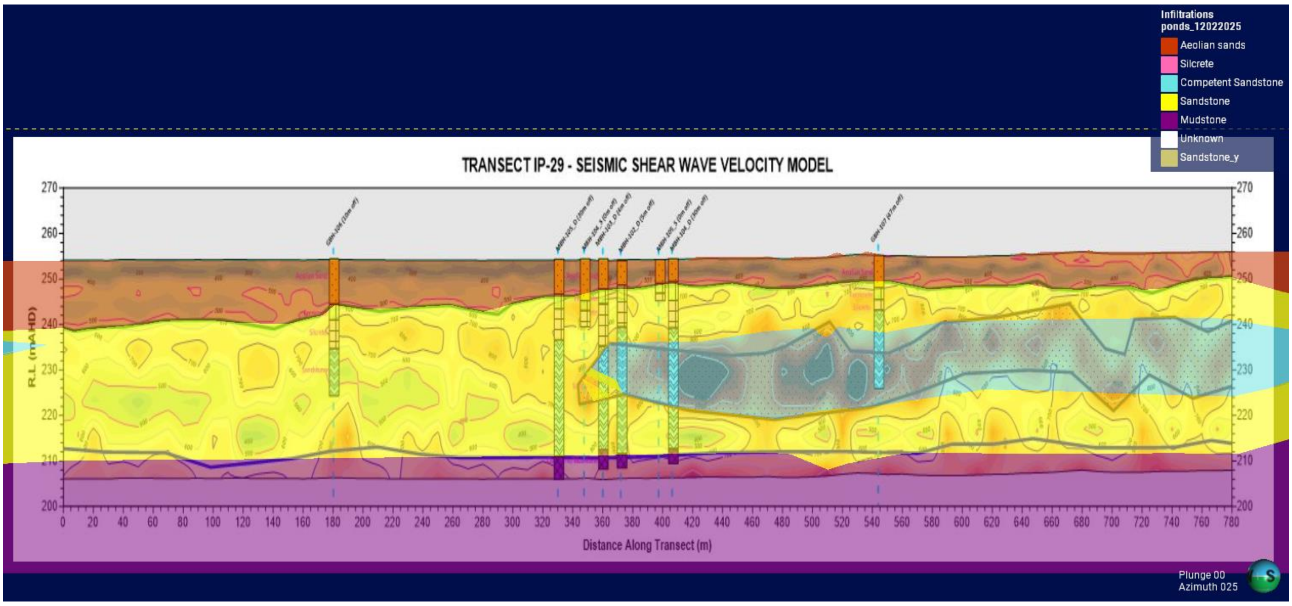
Infiltrations ponds_12022025
Aeolian sands
Silcrete
Competent Sandstone
Sandstone
Mudstone
Unknown
Sandstone_y
TRANSECT IP-29 - SEISMIC SHEAR WAVE VELOCITY MODEL
R.L (mAHD)
Distance Along Transect (m)
Plunge 00
Azimuth 025
S

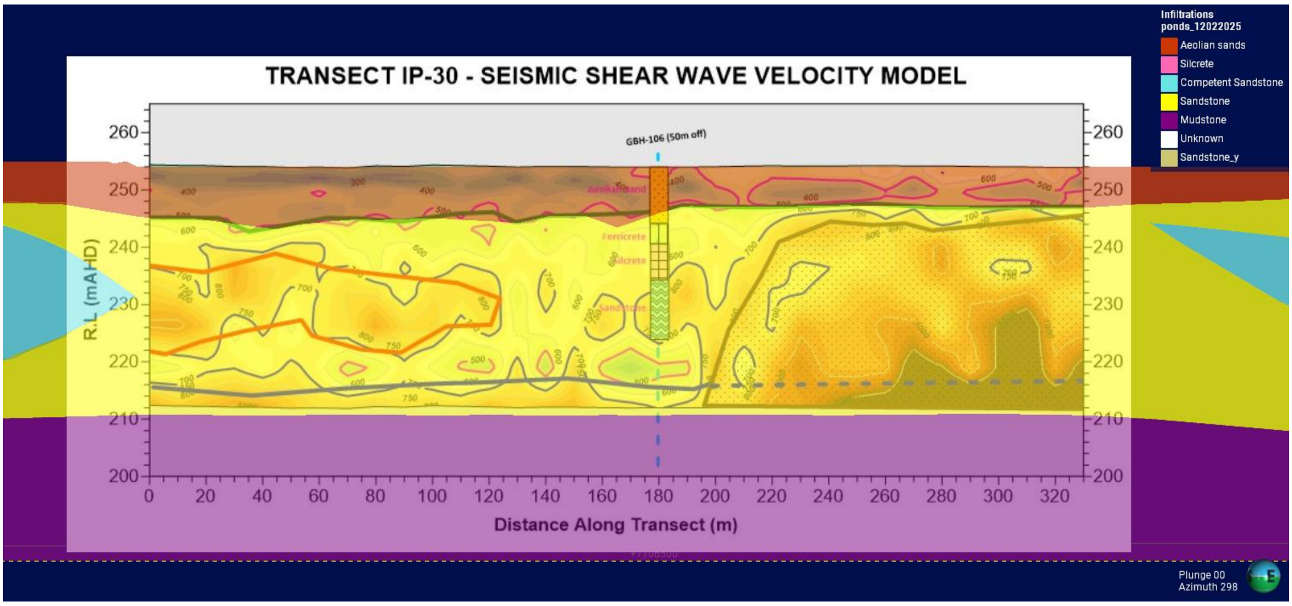

TRANSECT IP-30 - SEISMIC SHEAR WAVE VELOCITY MODEL
Infiltrations ponds_12022025
Aeolian sands
Silcrete
Competent Sandstone
Sandstone
Mudstone
Unknown
Sandstone_y
GBH-106 (50m off)
R.L (mAHD)
Distance Along Transect (m)
Plunge 00
Azimuth 298

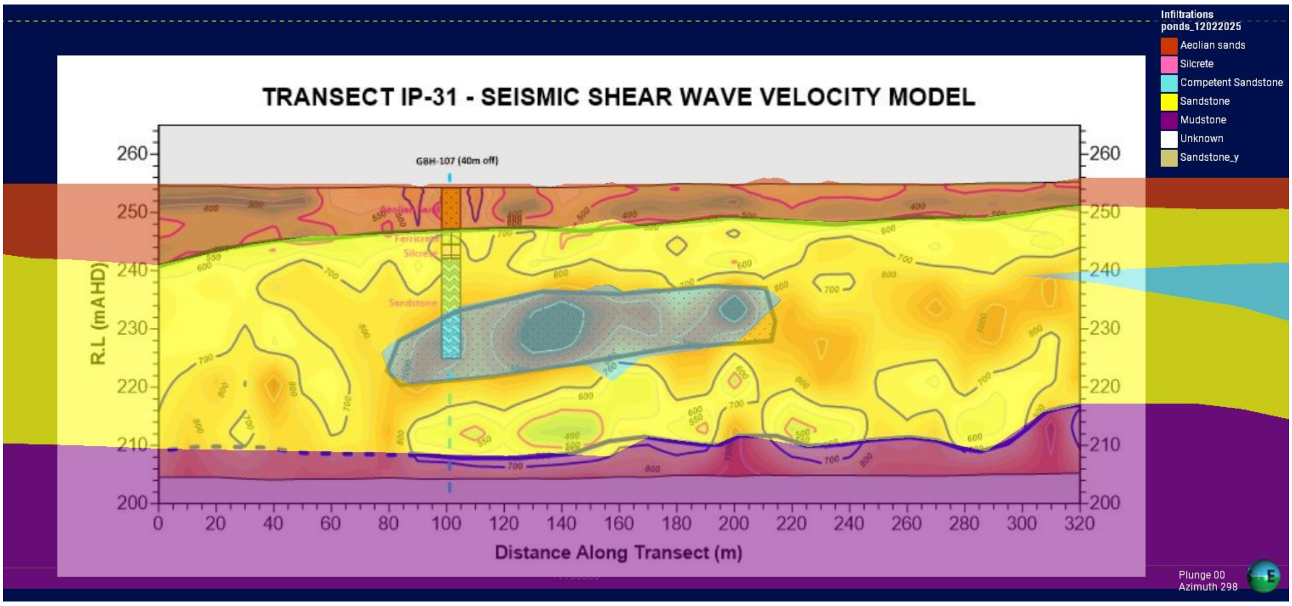

TRANSECT IP-31 - SEISMIC SHEAR WAVE VELOCITY MODEL
Infiltrations ponds_12022025
Aeolian sands
Silcrete
Competent Sandstone
Sandstone
Mudstone
Unknown
Sandstone_y
GBH-107 (40m off)
R.L (mAHD)
Distance Along Transect (m)
Plunge 00
Azimuth 298

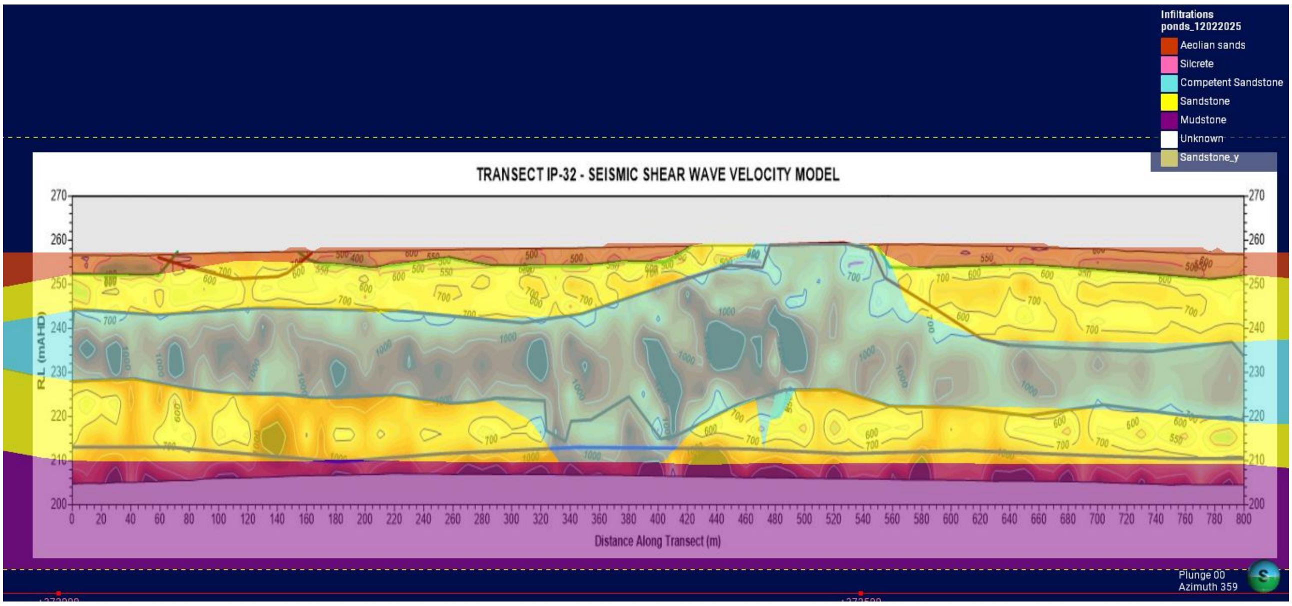

Infiltrations ponds_12022025
Aeolian sands
Silcrete
Competent Sandstone
Sandstone
Mudstone
Unknown
Sandstone_y
TRANSECT IP-32 - SEISMIC SHEAR WAVE VELOCITY MODEL
R.L (mAHD)
Distance Along Transect (m)
Plunge 00
Azimuth 359

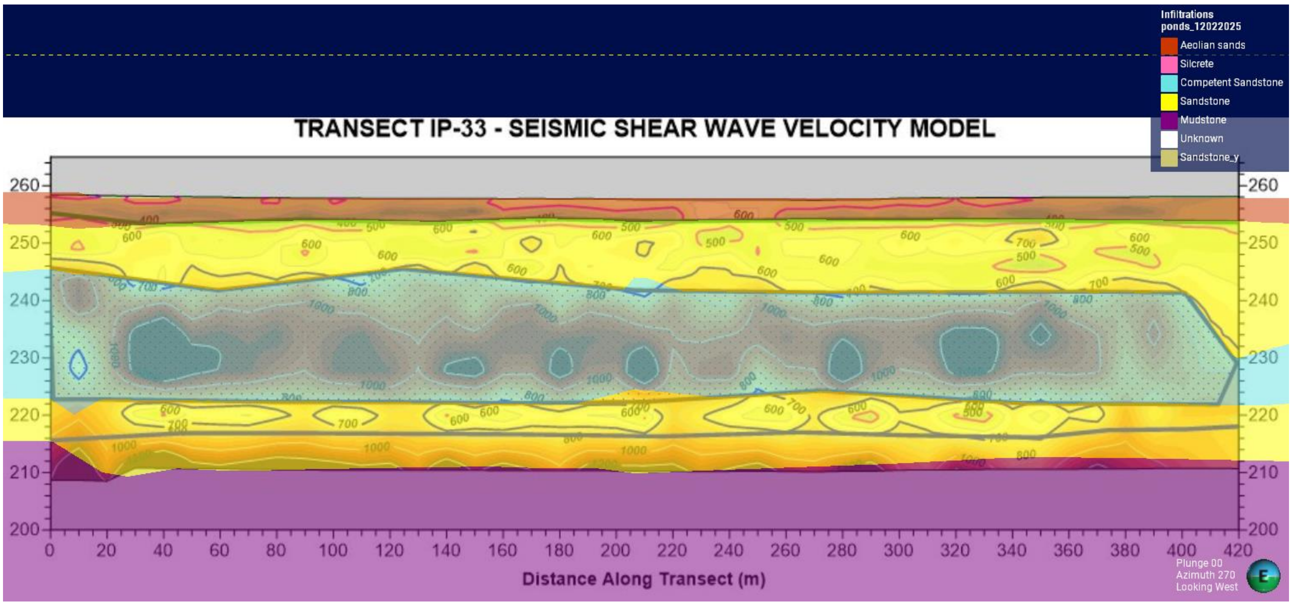

Infiltrations ponds_12022025
Aeolian sands
Silcrete
Competent Sandstone
Sandstone
Mudstone
Unknown
Sandstone_y
TRANSECT IP-33 - SEISMIC SHEAR WAVE VELOCITY MODEL
Distance Along Transect (m)
Plunge 00
Azimuth 270
Looking West

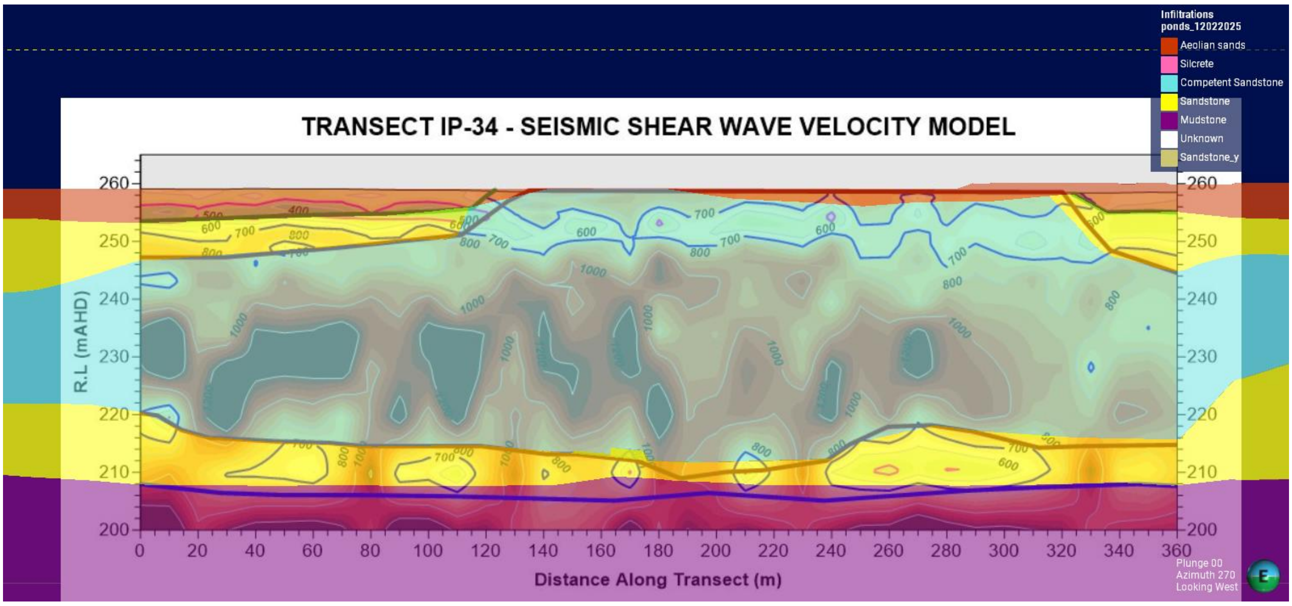

TRANSECT IP-34 - SEISMIC SHEAR WAVE VELOCITY MODEL
Infiltrations ponds_12022025
Aeolian sands
Silcrete
Competent Sandstone
Sandstone
Mudstone
Unknown
Sandstone_y
R.L (mAHD)
Distance Along Transect (m)
Plunge 00
Azimuth 270
Looking West

Appendix B. Hydrogeological Bore Logs

B.1 Pond 1 Borehole Logs

WINU1327 – Composite Bore Log

Project: Winu Hydrogeological Investigation Program Client: Rio Tinto CRS: GDA94 MGA51 Coordinates: 371400.95 mE / 7705738.33 mN Elevation: 254.61 m AHD (RL = TOC)	Construction start date: 22/10/2024 Construction end date: 07/11/2024 Inclination: -90° Depth drilled: 50 m BGL	Final airlift yield: N/A L/s EC: N/A µS/cm pH: N/A Temp: N/A °C Static Water Level: 42.38 m TOC

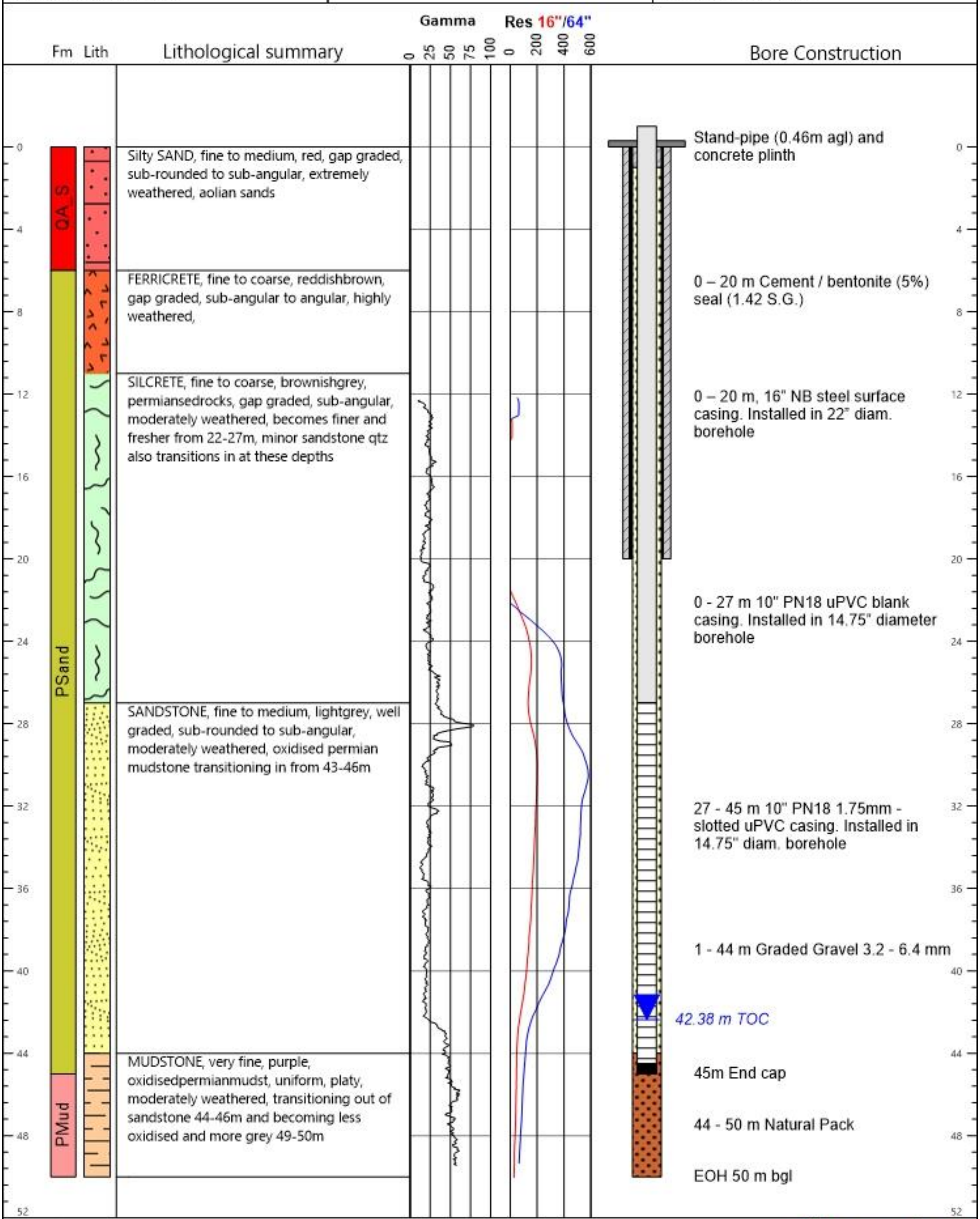

Additional notes:

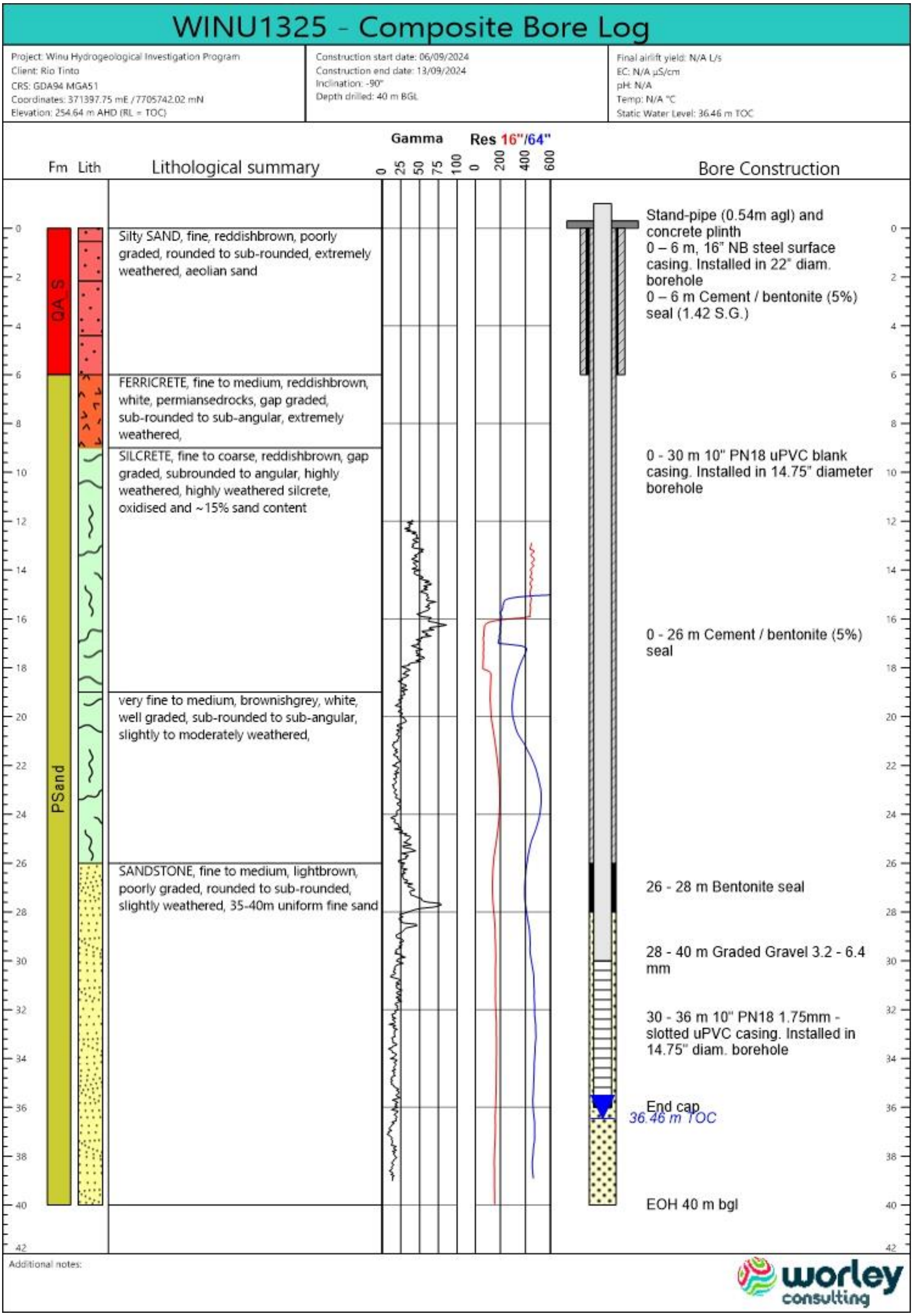

WINU1325 - Composite Bore Log
Project: Winu Hydrogeological Investigation Program
Client: Rio Tinto
CRS: GDA94 MGA51
Coordinates: 371397.75 mE / 7705742.02 mN
Elevation: 254.64 m AHD (RL = TOC)
Construction start date: 06/09/2024
Construction end date: 13/09/2024
Inclination: -90°
Depth drilled: 40 m BGL
Final airlift yield: N/A L/s
EC: N/A µS/cm
pH: N/A
Temp: N/A °C
Static Water Level: 36.46 m TOC
Fm
Lith
Lithological summary
Gamma
0 25 50 75 100
Res 16"/64"
0 200 400 600
Bore Construction
QA_S
PSand
Silty SAND, fine, reddishbrown, poorly graded, rounded to sub-rounded, extremely weathered, aeolian sand
FERRICRETE, fine to medium, reddishbrown, white, permiansedrocks, gap graded, sub-rounded to sub-angular, extremely weathered,
SILCRETE, fine to coarse, reddishbrown, gap graded, subrounded to angular, highly weathered, highly weathered silcrete, oxidised and ~15% sand content
very fine to medium, brownishgrey, white, well graded, sub-rounded to sub-angular, slightly to moderately weathered,
SANDSTONE, fine to medium, lightbrown, poorly graded, rounded to sub-rounded, slightly weathered, 35-40m uniform fine sand
Stand-pipe (0.54m agl) and concrete plinth
0 – 6 m, 16" NB steel surface casing. Installed in 22" diam. borehole
0 – 6 m Cement / bentonite (5%) seal (1.42 S.G.)
0 - 30 m 10" PN18 uPVC blank casing. Installed in 14.75" diameter borehole
0 - 26 m Cement / bentonite (5%) seal
26 - 28 m Bentonite seal
28 - 40 m Graded Gravel 3.2 - 6.4 mm
30 - 36 m 10" PN18 1.75mm - slotted uPVC casing. Installed in 14.75" diam. borehole
End cap
36.46 m TOC
EOH 40 m bgl
0
2
4
6
8
10
12
14
16
18
20
22
24
26
28
30
32
34
36
38
40
42
Additional notes:

WINU1070 – Composite Bore Log

Project: Winu Hydrogeological Investigation Program Client: Rio Tinto CRS: GDA94 MGA51 Coordinates: 371404.19 mE / 7705740.08 mN Elevation: 254.82 m AHD (RL = TOC)	Construction start date: 17/07/2024 Construction end date: 19/07/2024 Inclination: -90° Depth drilled: 46 m BGL	Final airlift yield: N/A L/s EC: N/A µS/cm pH: N/A Temp: N/A °C Static Water Level: 42.38 m TOC

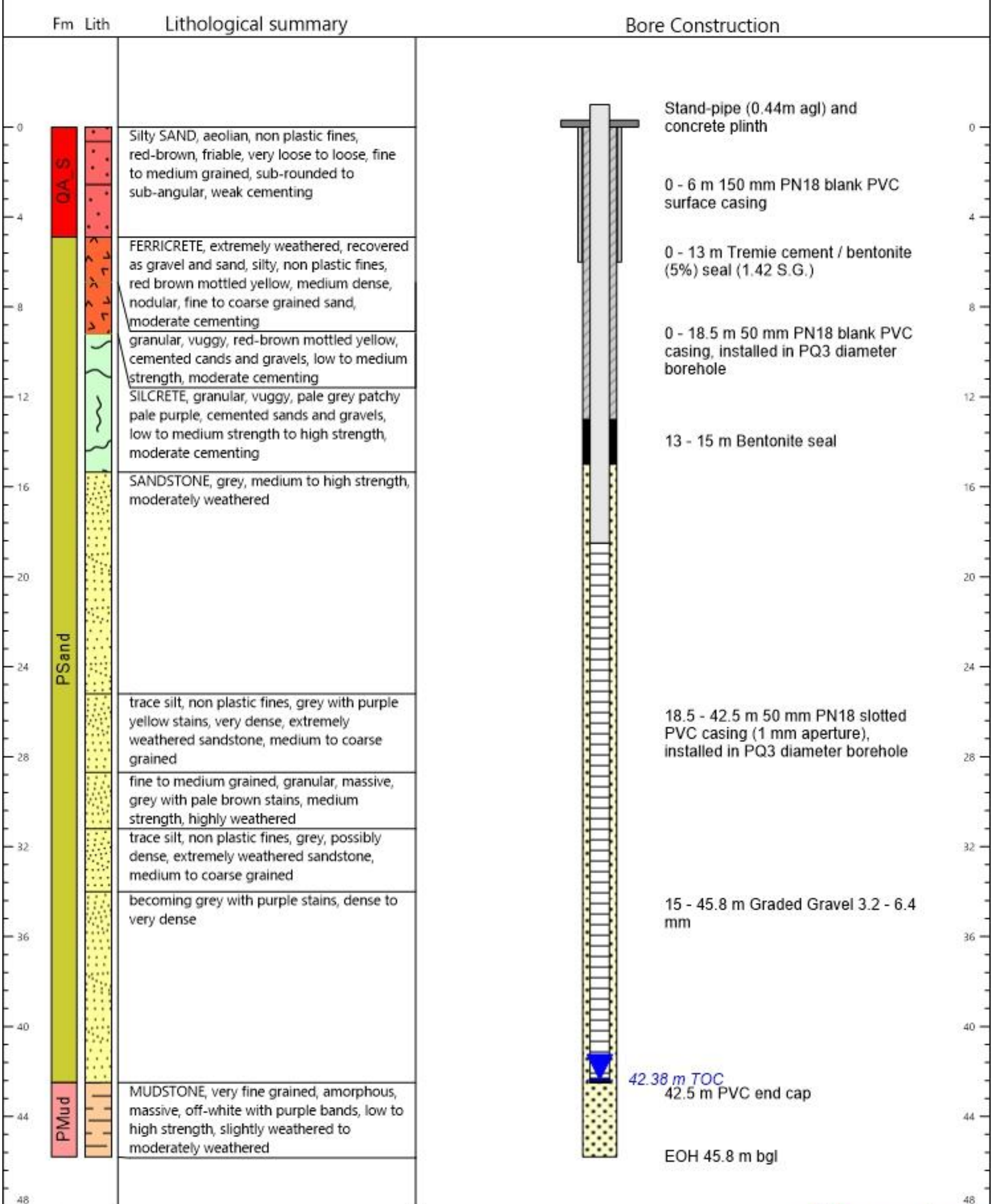

Additional notes:

WINU1071 - Composite Bore Log

Project: Winu Hydrogeological Investigation Program Client: Rio Tinto CRS: GDA94 MGA51 Coordinates: 371391.71 mE / 7705732.84 mN Elevation: 254.68 m AHD (RL = TOC)	Construction start date: 20/07/2024 Construction end date: 21/07/2024 Inclination: -90° Depth drilled: 45 m BGL	Final airlift yield: N/A L/s EC: N/A µS/cm pH: N/A Temp: N/A °C Static Water Level: 42.01 m TOC

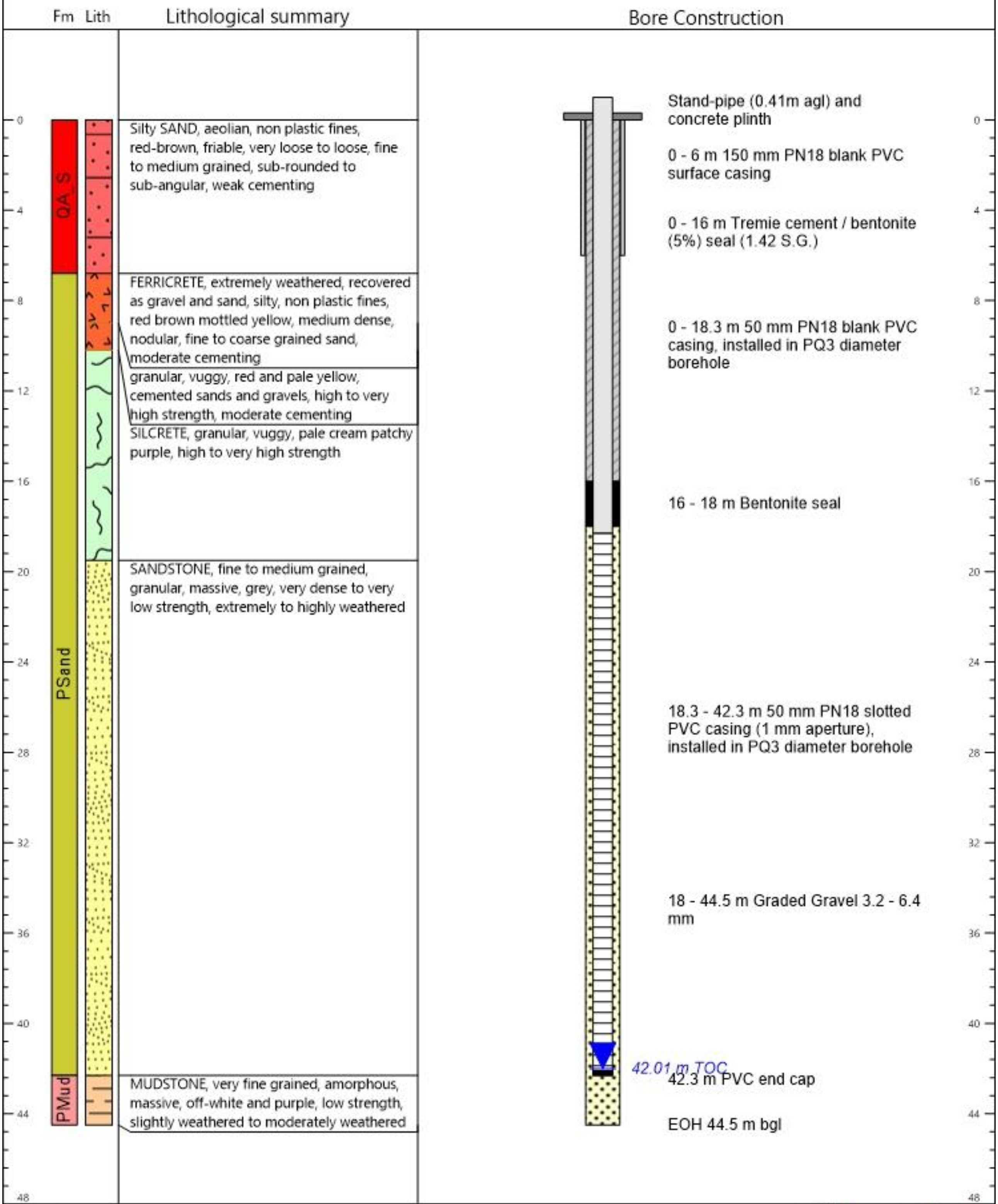

Additional notes:

WINU1072 – Composite Bore Log

Project: Winu Hydrogeological Investigation Program Client: Rio Tinto CRS: GDA94 MGA51 Coordinates: 371445.54 mE / 7705750.00 mN Elevation: 254.99 m AHD (RL = TOC)	Construction start date: 15/07/2024 Construction end date: 16/07/2024 Inclination: -90° Depth drilled: 45 m BGL	Final airlift yield: N/A L/s EC: N/A µS/cm pH: N/A Temp: N/A °C Static Water Level: 42.10 m TOC

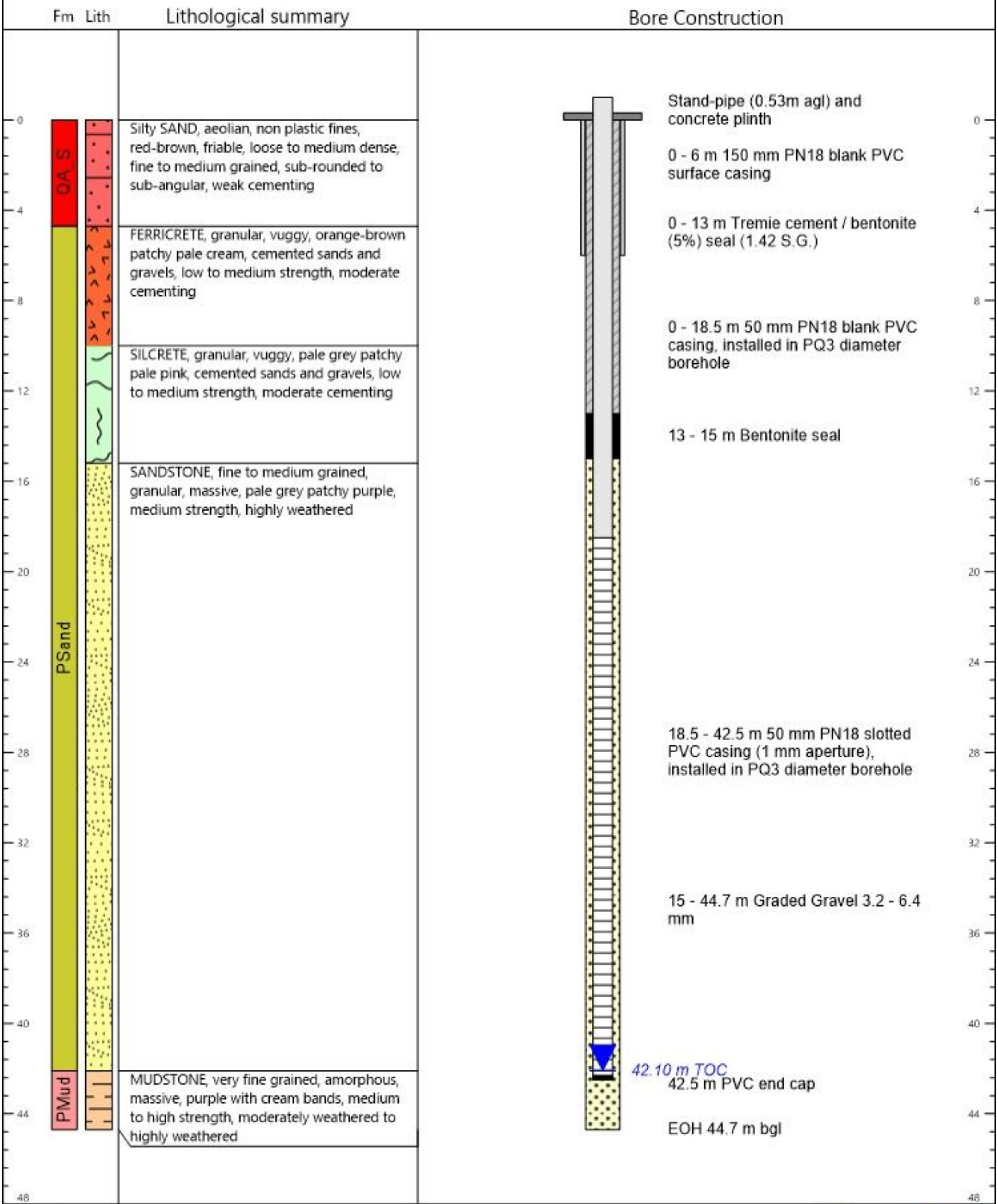

Additional notes:

WINU1073 - Composite Bore Log

Project: Winu Hydrogeological Investigation Program Client: Rio Tinto CRS: GDA94 MGA51 Coordinates: 371348.99 mE / 7705722.86 mN Elevation: 254.74 m AHD (RL = TOC)	Construction start date: 21/07/2024 Construction end date: 23/07/2024 Inclination: -90° Depth drilled: 47 m BGL	Final airlift yield: N/A L/s EC: N/A µS/cm pH: N/A Temp: N/A °C Static Water Level: Dry m TOC

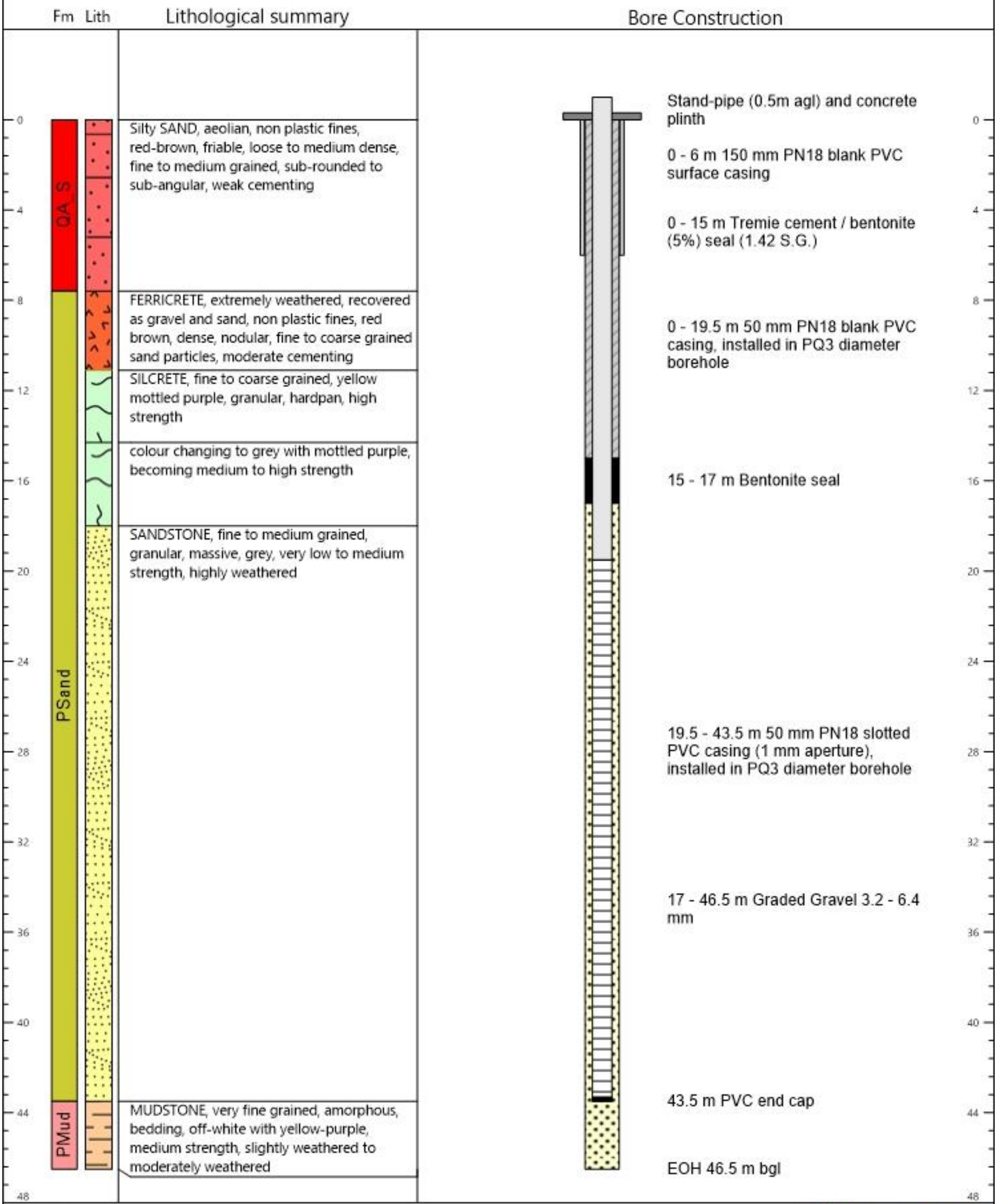

Additional notes:

WINU1317 - Composite Bore Log

Project: Winu Hydrogeological Investigation Program Client: Rio Tinto CRS: GDA94 MGA51 Coordinates: 371403.66 mE / 7705735.12 mN Elevation: 254.69 m AHD (RL = TOC)	Construction start date: 15/09/2024 Construction end date: 16/09/2024 Inclination: -90° Depth drilled: 10 m BGL	Final airlift yield: N/A L/s EC: N/A µS/cm pH: N/A Temp: N/A °C Static Water Level: Dry m TOC

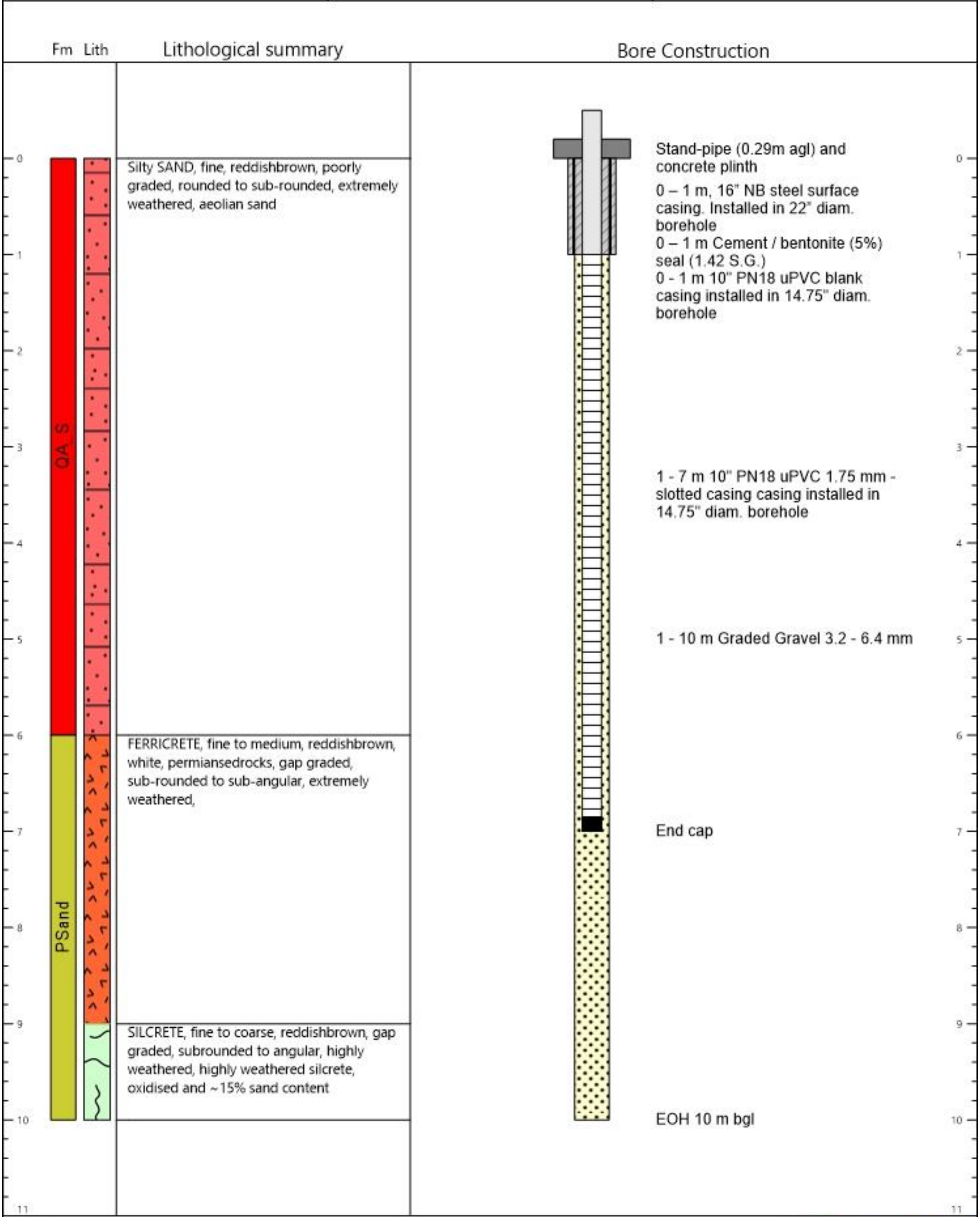

Additional notes:

WINU1075 - Composite Bore Log

Project: Winu Hydrogeological Investigation Program
Client: Rio Tinto
CRS: GDA94 MGA51
Coordinates: 371397.62 mE / 7705737.79 mN
Elevation: 254.76 m AHD (RL = TOC)

Construction start date: 07/08/2024
Construction end date: 07/08/2024
Inclination: -90°
Depth drilled: 11 m BGL

Final airlift yield: N/A L/s
EC: N/A µS/cm
pH: N/A
Temp: N/A °C
Static Water Level: 7.61 m TOC

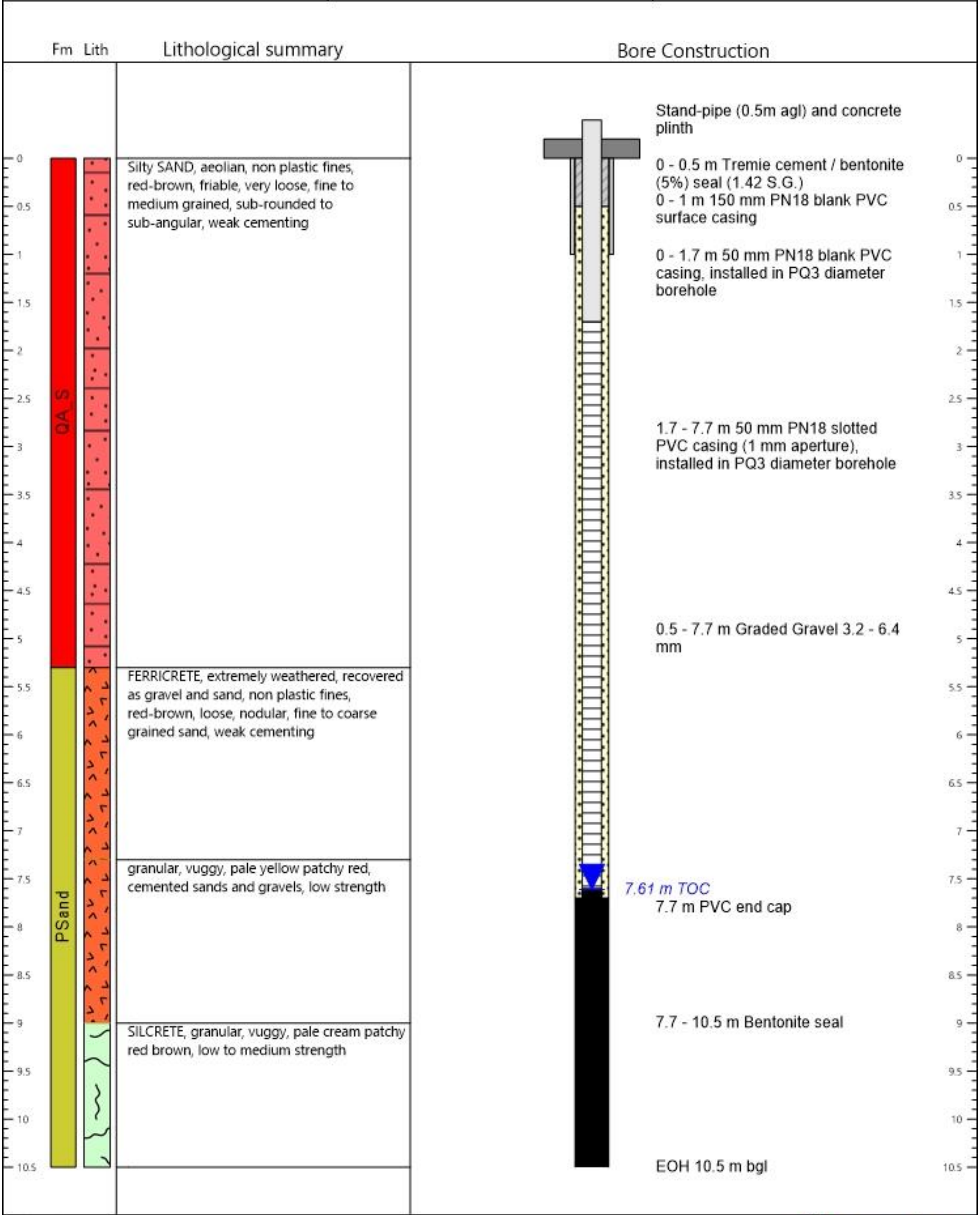

Additional notes:

WINU1076 - Composite Bore Log

Project: Winu Hydrogeological Investigation Program	Construction start date: 06/08/2024	Final airlift yield: N/A L/s
Client: Rio Tinto	Construction end date: 06/08/2024	EC: N/A µS/cm
CRS: GDA94 MGA51	Inclination: -90°	pH: N/A
Coordinates: 371409.95 mE / 7705732.69 mN	Depth drilled: 11 m BGL	Temp: N/A °C
Elevation: 254.82 m AHD (RL = TOC)		Static Water Level: 7.49 m TOC

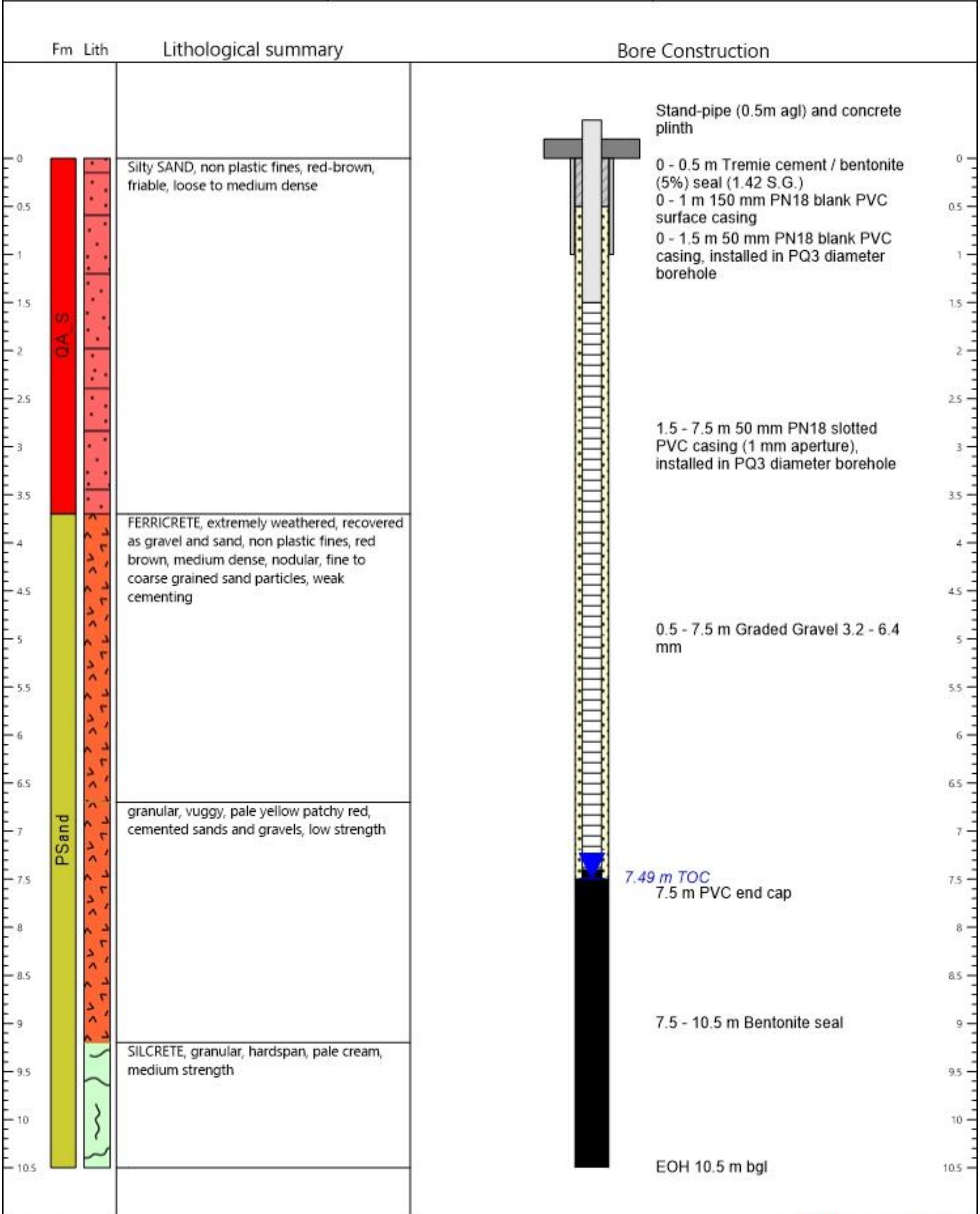

Additional notes:

WINU1077 – Composite Bore Log

Project: Winu Hydrogeological Investigation Program Client: Rio Tinto CRS: GDA94 MGA51 Coordinates: 371375.47 mE / 7705748.27 mN Elevation: 254.78 m AHD (RL = TOC)	Construction start date: 26/07/2024 Construction end date: 05/08/2024 Inclination: -90° Depth drilled: 15 m BGL	Final airlift yield: N/A L/s EC: N/A µS/cm pH: N/A Temp: N/A °C Static Water Level: Dry m TOC

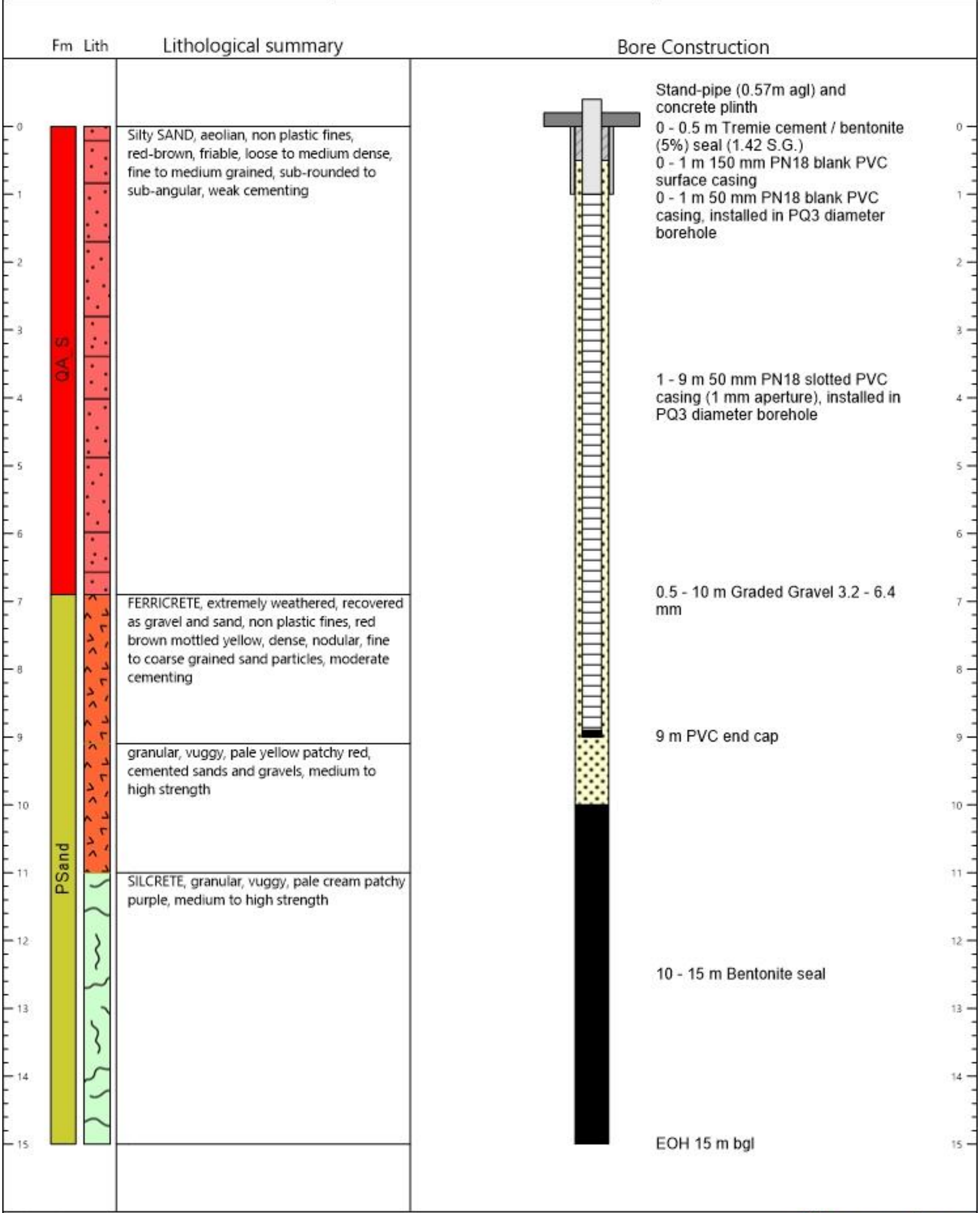

Additional notes:

WINU1078 – Composite Bore Log

Project: Winu Hydrogeological Investigation Program Client: Rio Tinto CRS: GDA94 MGA51 Coordinates: 371429.87 mE / 7705728.97 mN Elevation: 254.90 m AHD (RL = TOC)	Construction start date: 05/08/2024 Construction end date: 05/08/2024 Inclination: -90° Depth drilled: 15 m BGL	Final airlift yield: N/A L/s EC: N/A µS/cm pH: N/A Temp: N/A °C Static Water Level: Dry m TOC

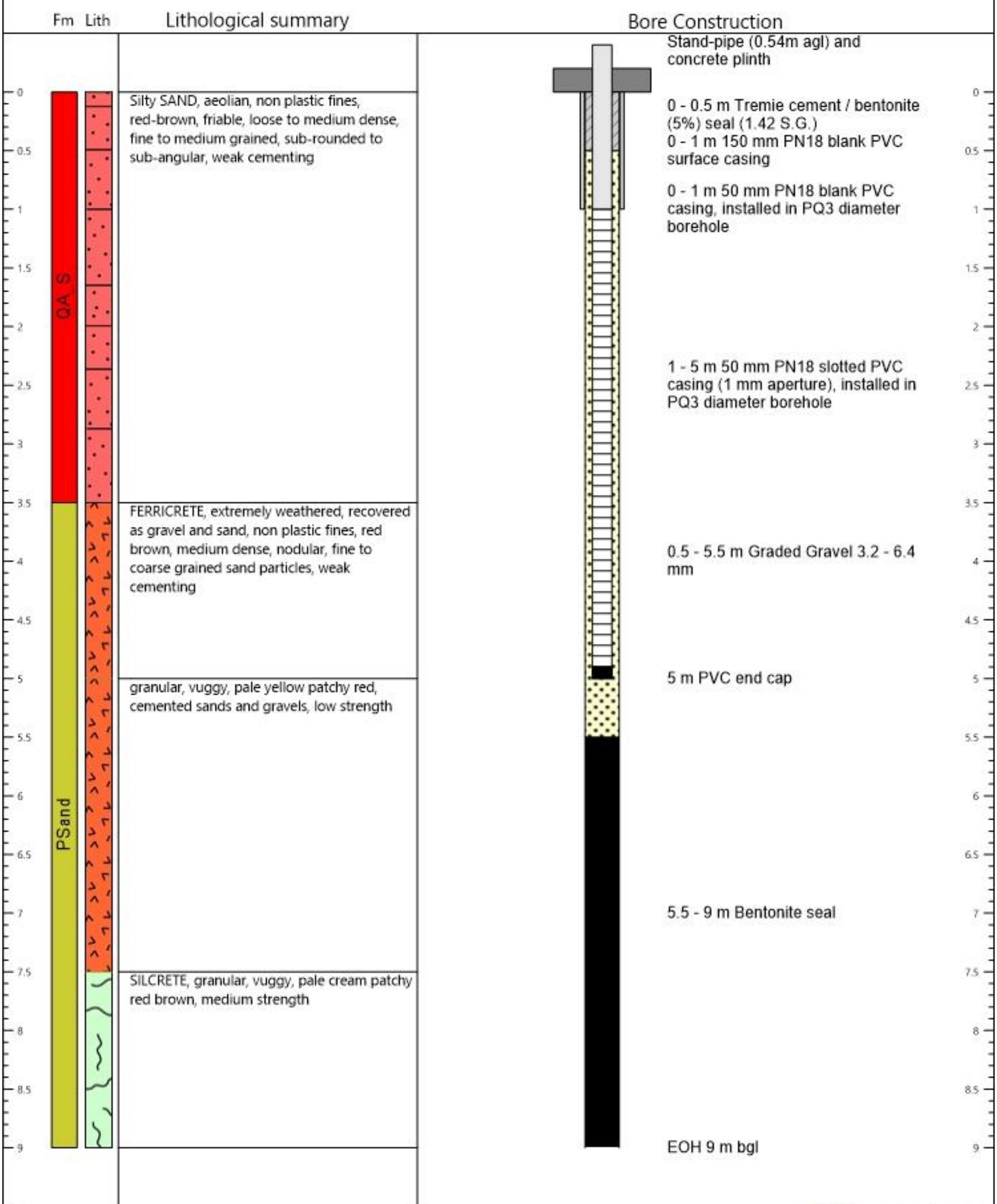

Additional notes:

B.2 Pond 2 Borehole Logs

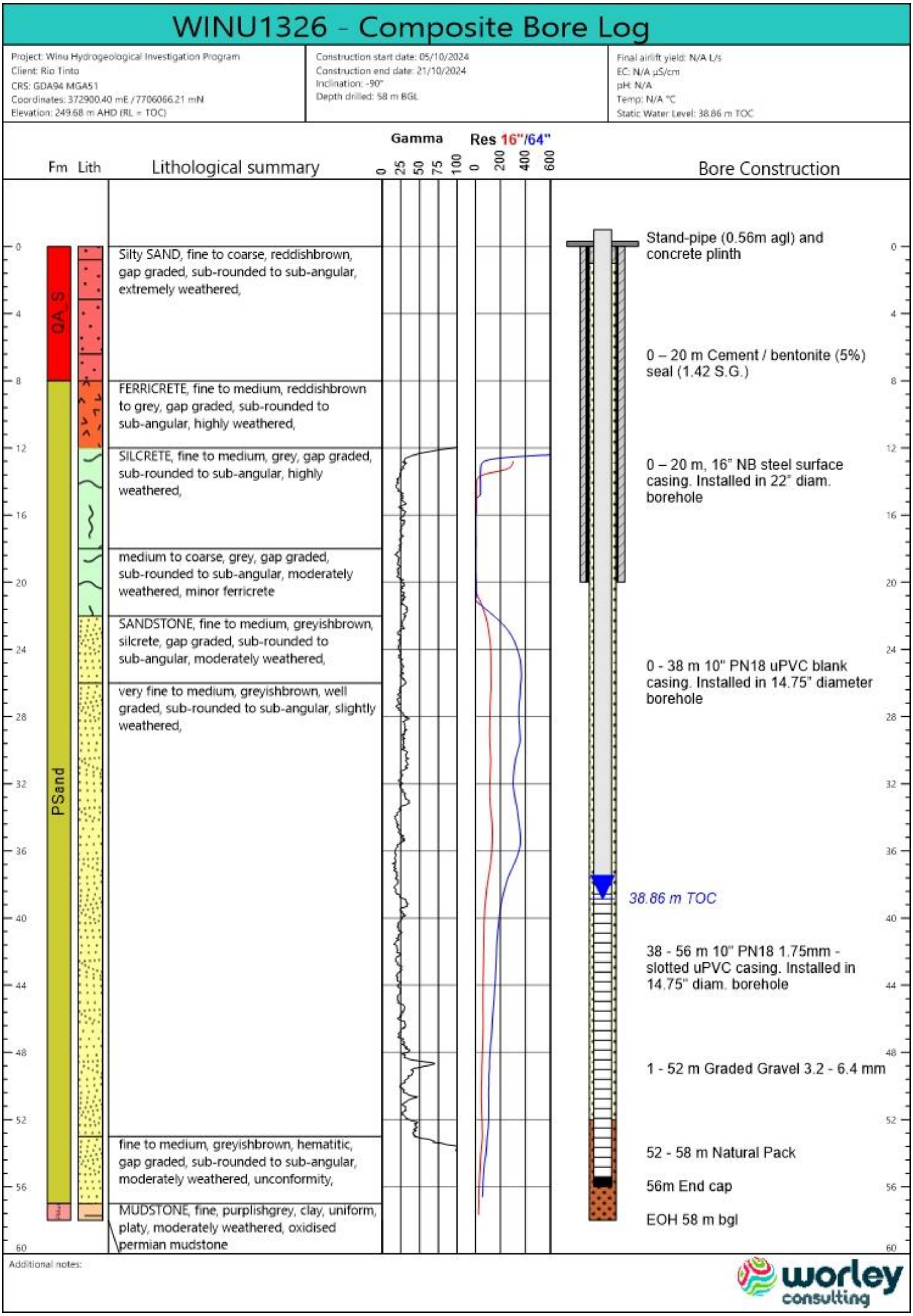

WINU1326 - Composite Bore Log
Project: Winu Hydrogeological Investigation Program
Client: Rio Tinto
CRS: GDA94 MGA51
Coordinates: 372900.40 mE / 7706066.21 mN
Elevation: 249.68 m AHD (RL = TOC)
Construction start date: 05/10/2024
Construction end date: 21/10/2024
Inclination: -90°
Depth drilled: 58 m BGL
Final airlift yield: N/A L/s
EC: N/A µS/cm
pH: N/A
Temp: N/A °C
Static Water Level: 38.86 m TOC
Fm
Lith
Lithological summary
Gamma
Res 16"/64"
Bore Construction
QA_S
PSand
Silty SAND, fine to coarse, reddishbrown, gap graded, sub-rounded to sub-angular, extremely weathered,
FERRICRETE, fine to medium, reddishbrown to grey, gap graded, sub-rounded to sub-angular, highly weathered,
SILCRETE, fine to medium, grey, gap graded, sub-rounded to sub-angular, highly weathered,
medium to coarse, grey, gap graded, sub-rounded to sub-angular, moderately weathered, minor ferricrete
SANDSTONE, fine to medium, greyishbrown, silcrete, gap graded, sub-rounded to sub-angular, moderately weathered,
very fine to medium, greyishbrown, well graded, sub-rounded to sub-angular, slightly weathered,
fine to medium, greyishbrown, hematitic, gap graded, sub-rounded to sub-angular, moderately weathered, unconformity,
MUDSTONE, fine, purplishgrey, clay, uniform, platy, moderately weathered, oxidised permian mudstone
Stand-pipe (0.56m agl) and concrete plinth
0 – 20 m Cement / bentonite (5%) seal (1.42 S.G.)
0 – 20 m, 16" NB steel surface casing. Installed in 22" diam. borehole
0 - 38 m 10" PN18 uPVC blank casing. Installed in 14.75" diameter borehole
38.86 m TOC
38 - 56 m 10" PN18 1.75mm - slotted uPVC casing. Installed in 14.75" diam. borehole
1 - 52 m Graded Gravel 3.2 - 6.4 mm
52 - 58 m Natural Pack
56m End cap
EOH 58 m bgl
Additional notes:

WINU1318 – Composite Bore Log

Project: Winu Hydrogeological Investigation Program Client: Rio Tinto CRS: GDA94 MGA51 Coordinates: 372897.13 mE / 7706070.72 mN Elevation: 249.75 m AHD (RL = TOC)	Construction start date: 23/09/2024 Construction end date: 29/09/2024 Inclination: -90° Depth drilled: 34 m BGL	Final airlift yield: N/A L/s EC: N/A µS/cm pH: N/A Temp: N/A °C Static Water Level: Dry m TOC

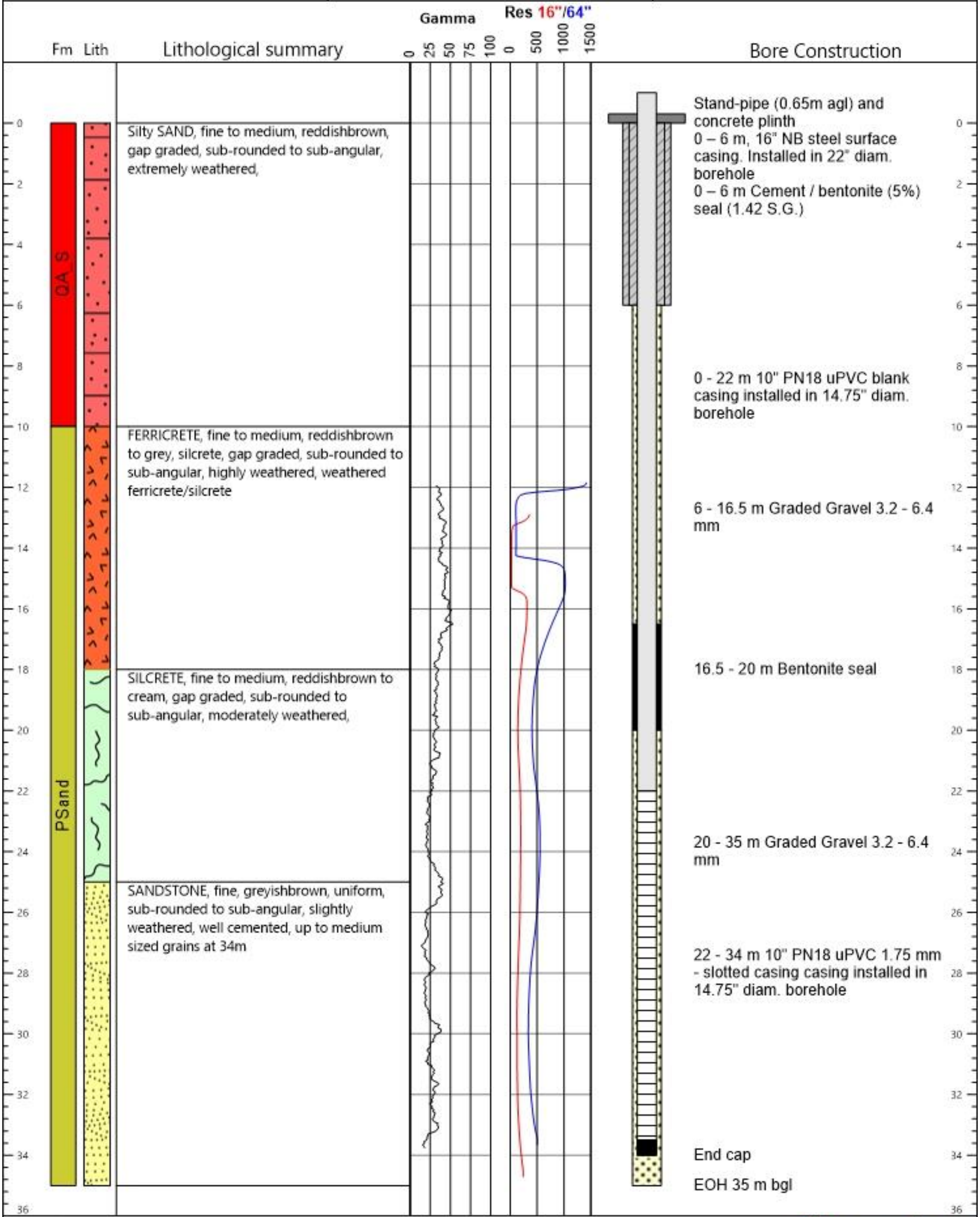

Additional notes:

WINU1551 – Composite Bore Log

Project: Winu Hydrogeological Investigation Program Client: Rio Tinto CRS: GDA94 MGA51 Coordinates: 372889.45 mE / 7706071.03 mN Elevation: 249.87 m AHD (RL = TOC)	Construction start date: 03/09/2024 Construction end date: 04/09/2024 Inclination: -90° Depth drilled: 53 m BGL	Final airlift yield: N/A L/s EC: N/A µS/cm pH: N/A Temp: N/A °C Static Water Level: 38.85 m TOC

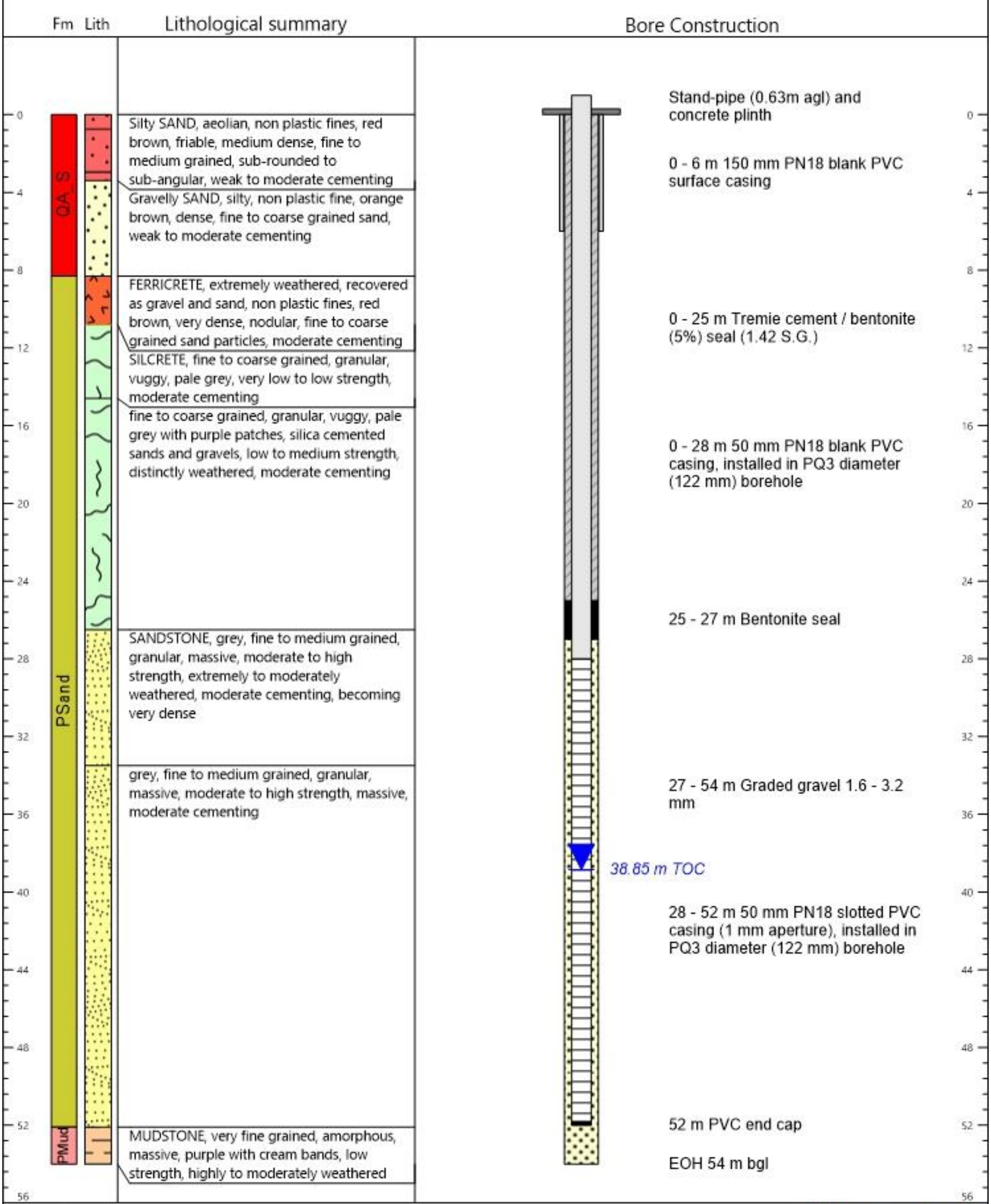

Additional notes:

WINU1552 - Composite Bore Log

Project: Winu Hydrogeological Investigation Program Client: Rio Tinto CRS: GDA94 MGA51 Coordinates: 372861.52 mE / 7706083.33 mN Elevation: 250.10 m AHD (RL = TOC)	Construction start date: 01/09/2024 Construction end date: 02/09/2024 Inclination: -90° Depth drilled: 51 m BGL	Final airlift yield: N/A L/s EC: N/A µS/cm pH: N/A Temp: N/A °C Static Water Level: 39.54 m TOC

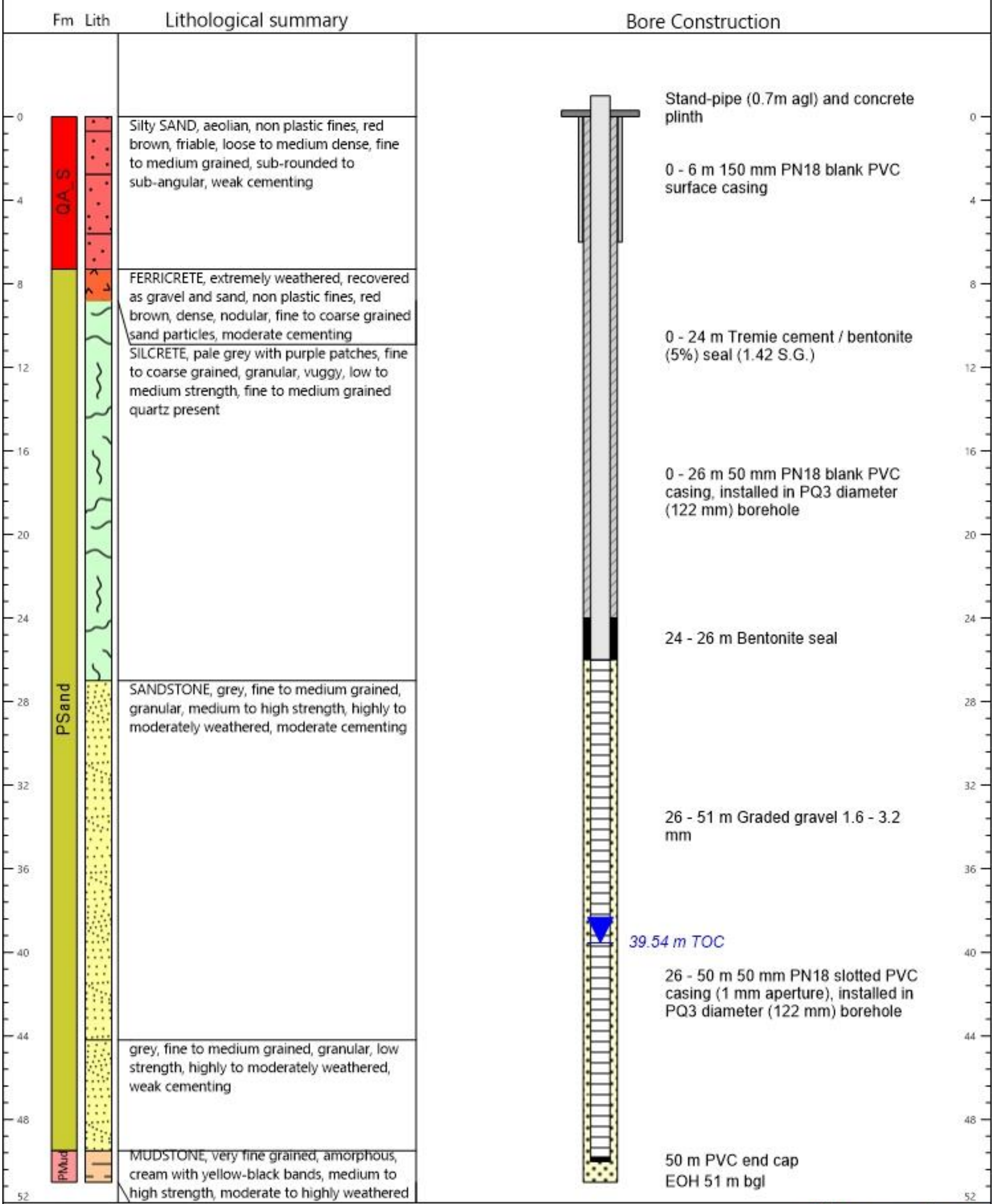

Additional notes:

WINU1553 - Composite Bore Log

Project: Winu Hydrogeological Investigation Program Client: Rio Tinto CRS: GDA94 MGA51 Coordinates: 372906.07 mE / 7706066.33 mN Elevation: 249.76 m AHD (RL = TOC)	Construction start date: 04/09/2024 Construction end date: 09/09/2024 Inclination: -90° Depth drilled: 53 m BGL	Final airlift yield: N/A L/s EC: N/A µS/cm pH: N/A Temp: N/A °C Static Water Level: 38.61 m TOC

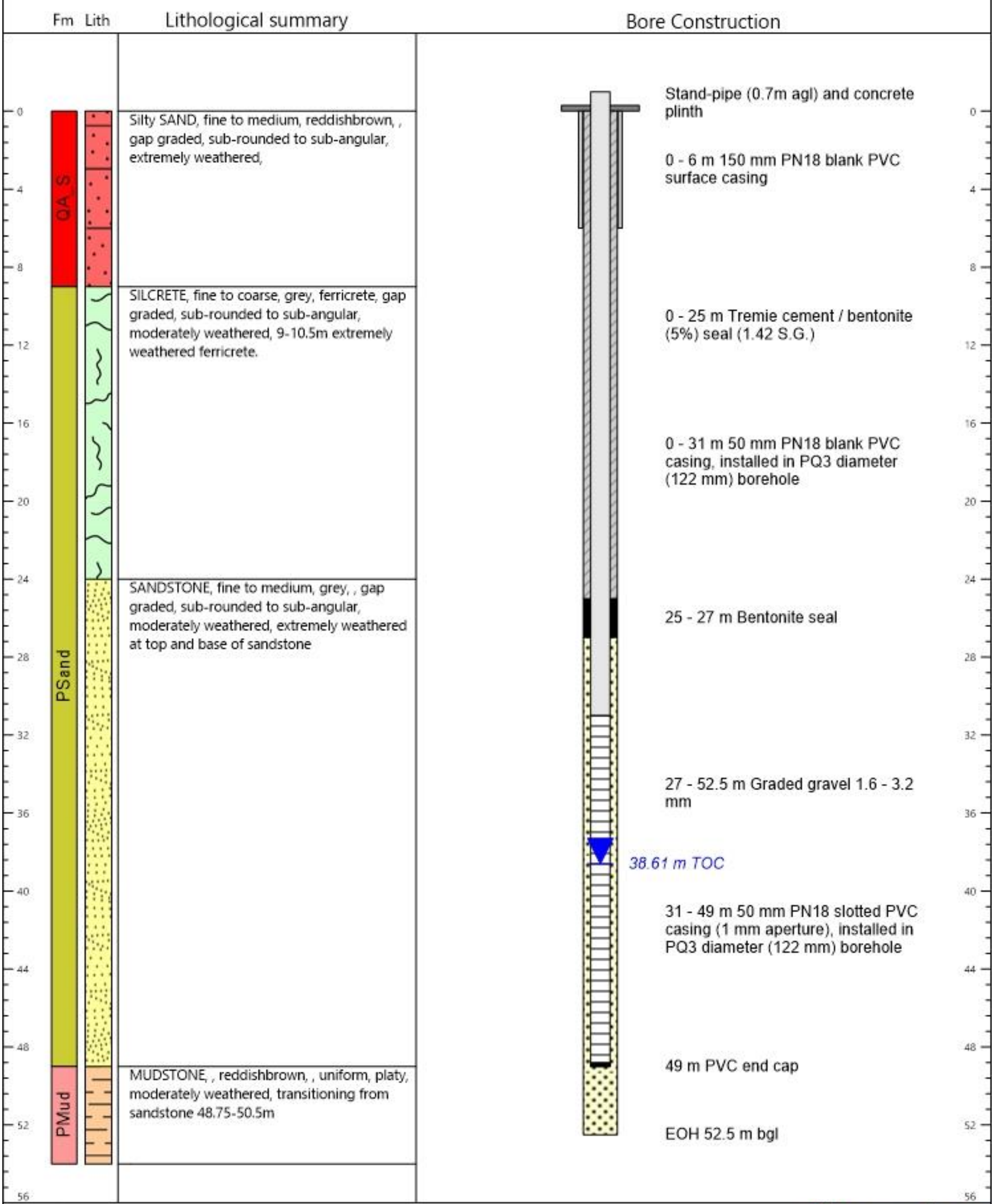

Additional notes:

WINU1554 – Composite Bore Log

Project: Winu Hydrogeological Investigation Program Client: Rio Tinto CRS: GDA94 MGA51 Coordinates: 372936.30 mE / 7706051.84 mN Elevation: 249.49 m AHD (RL = TOC)	Construction start date: 15/09/2024 Construction end date: 16/09/2024 Inclination: -90° Depth drilled: 54 m BGL	Final airlift yield: N/A L/s EC: N/A µS/cm pH: N/A Temp: N/A °C Static Water Level: 38.73 m TOC

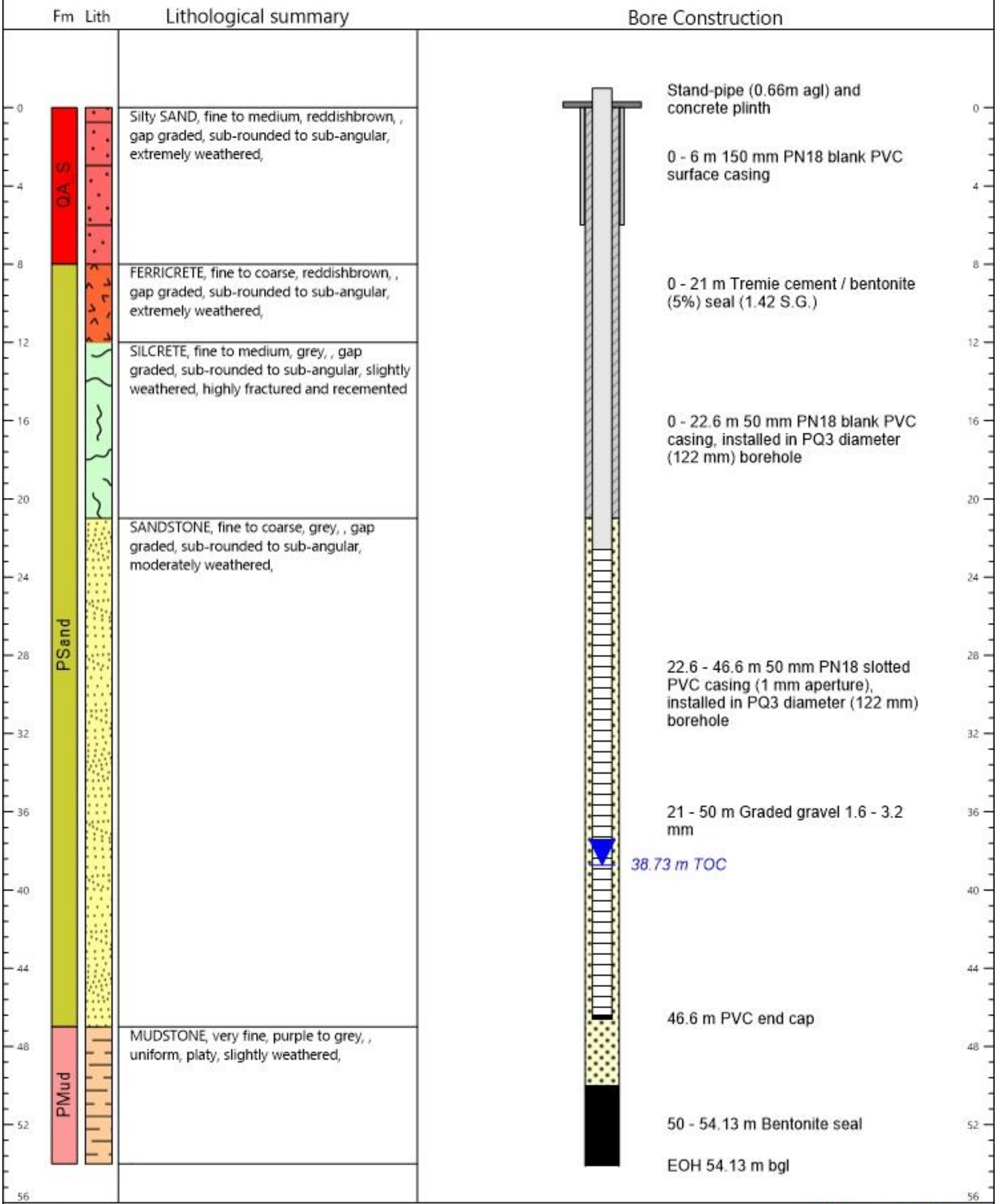

Additional notes:

WINU1319 - Composite Bore Log

Project: Winu Hydrogeological Investigation Program Client: Rio Tinto CRS: GDA94 MGA51 Coordinates: 372898.42 mE / 7706067.41 mN Elevation: 249.67 m AHD (RL = TOC)	Construction start date: 28/09/2024 Construction end date: 02/10/2024 Inclination: -90° Depth drilled: 15 m BGL	Final airlift yield: N/A L/s EC: N/A µS/cm pH: N/A Temp: N/A °C Static Water Level: Dry m TOC

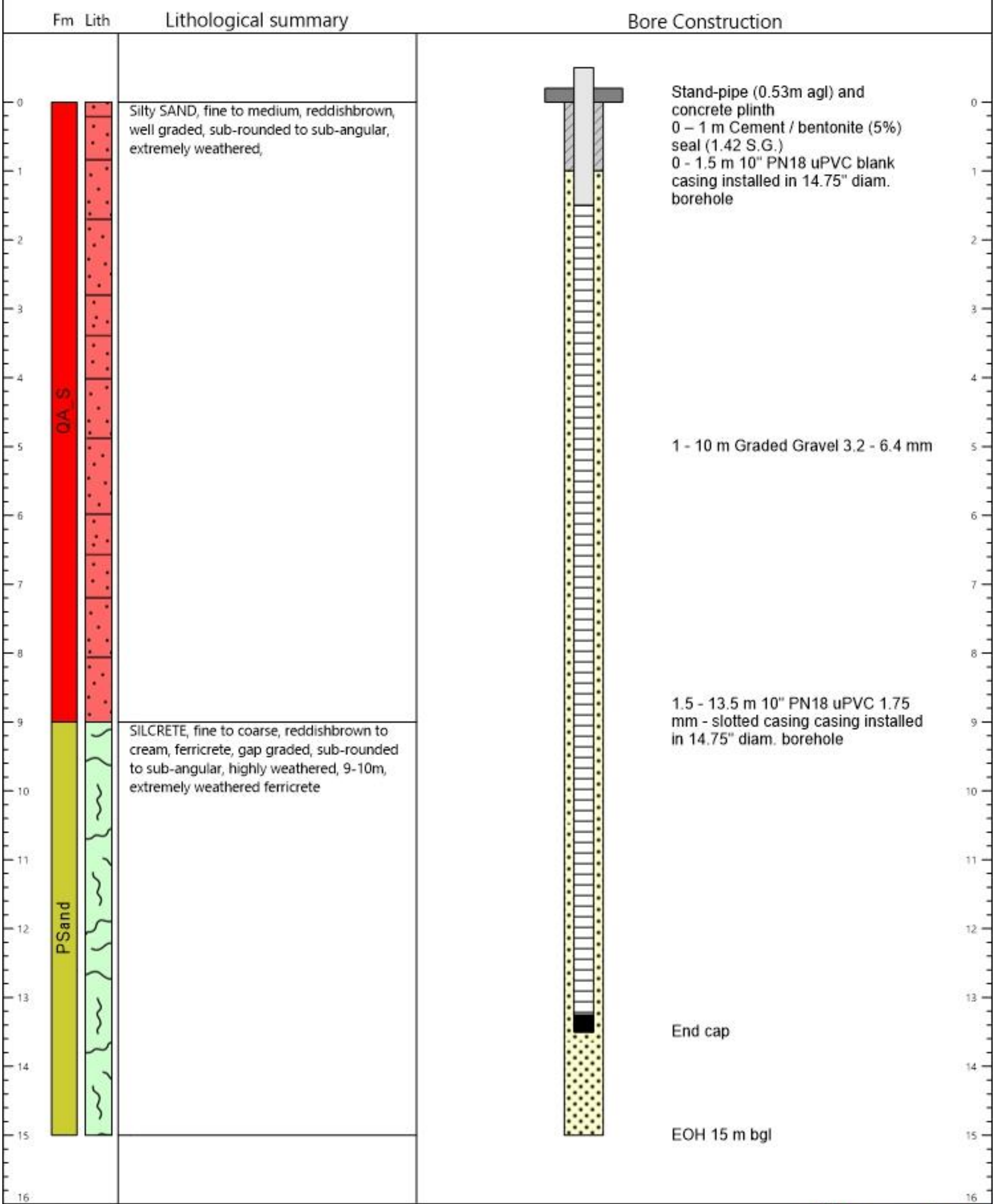

Additional notes:

WINU1555 - Composite Bore Log

Project: Winu Hydrogeological Investigation Program Client: Rio Tinto CRS: GDA94 MGA51 Coordinates: 372904.59 mE / 7706063.33 mN Elevation: 249.77 m AHD (RL = TOC)	Construction start date: 10/09/2024 Construction end date: 10/09/2024 Inclination: -90° Depth drilled: 15 m BGL	Final airlift yield: N/A L/s EC: N/A µS/cm pH: N/A Temp: N/A °C Static Water Level: 11.91 m TOC

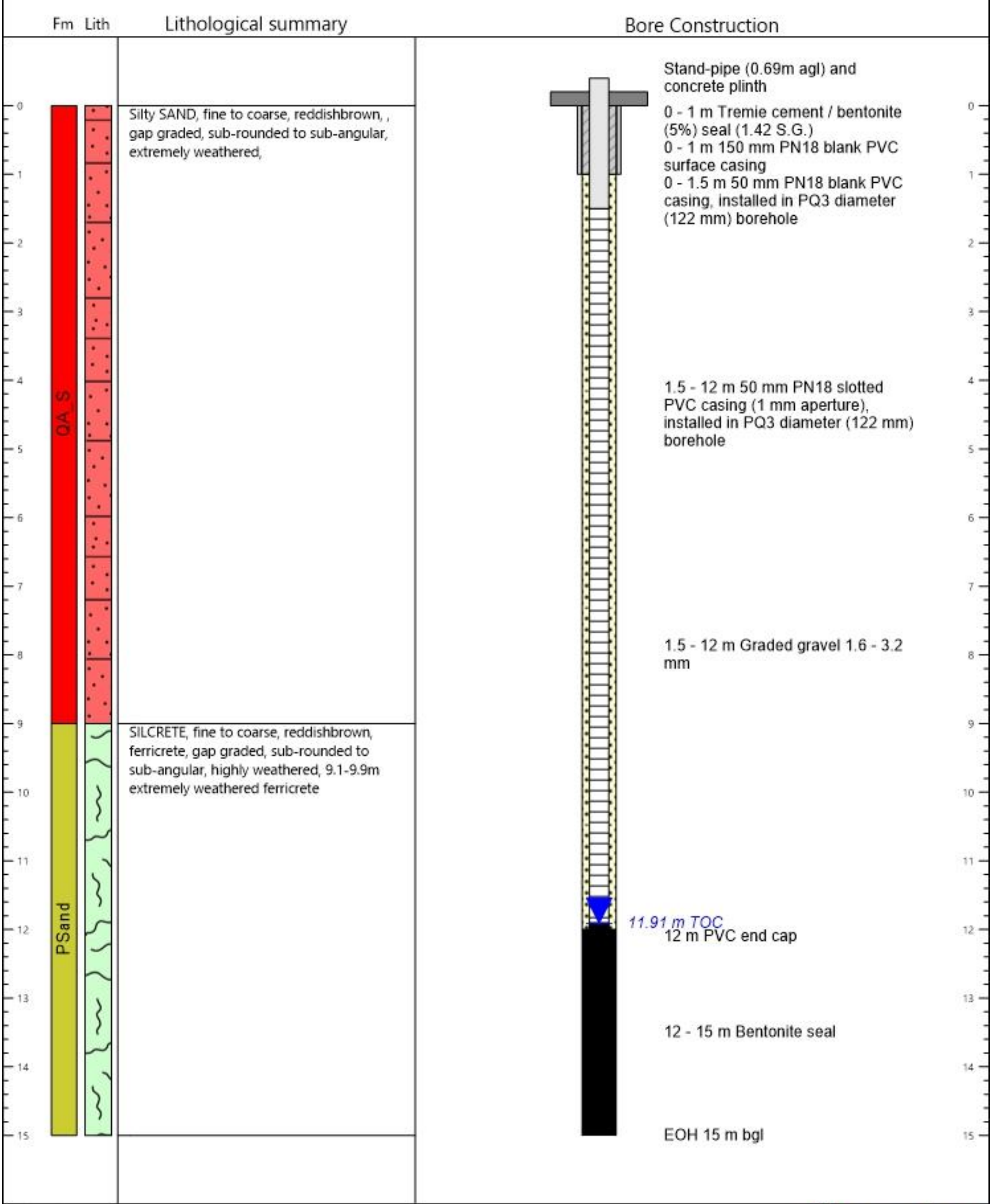

Additional notes:

WINU1556 – Composite Bore Log

Project: Winu Hydrogeological Investigation Program Client: Rio Tinto CRS: GDA94 MGA51 Coordinates: 372919.95 mE / 7706054.81 mN Elevation: 249.63 m AHD (RL = TOC)	Construction start date: 12/09/2024 Construction end date: 13/09/2024 Inclination: -90° Depth drilled: 15 m BGL	Final airlift yield: N/A L/s EC: N/A µS/cm pH: N/A Temp: N/A °C Static Water Level: 13.35 m TOC

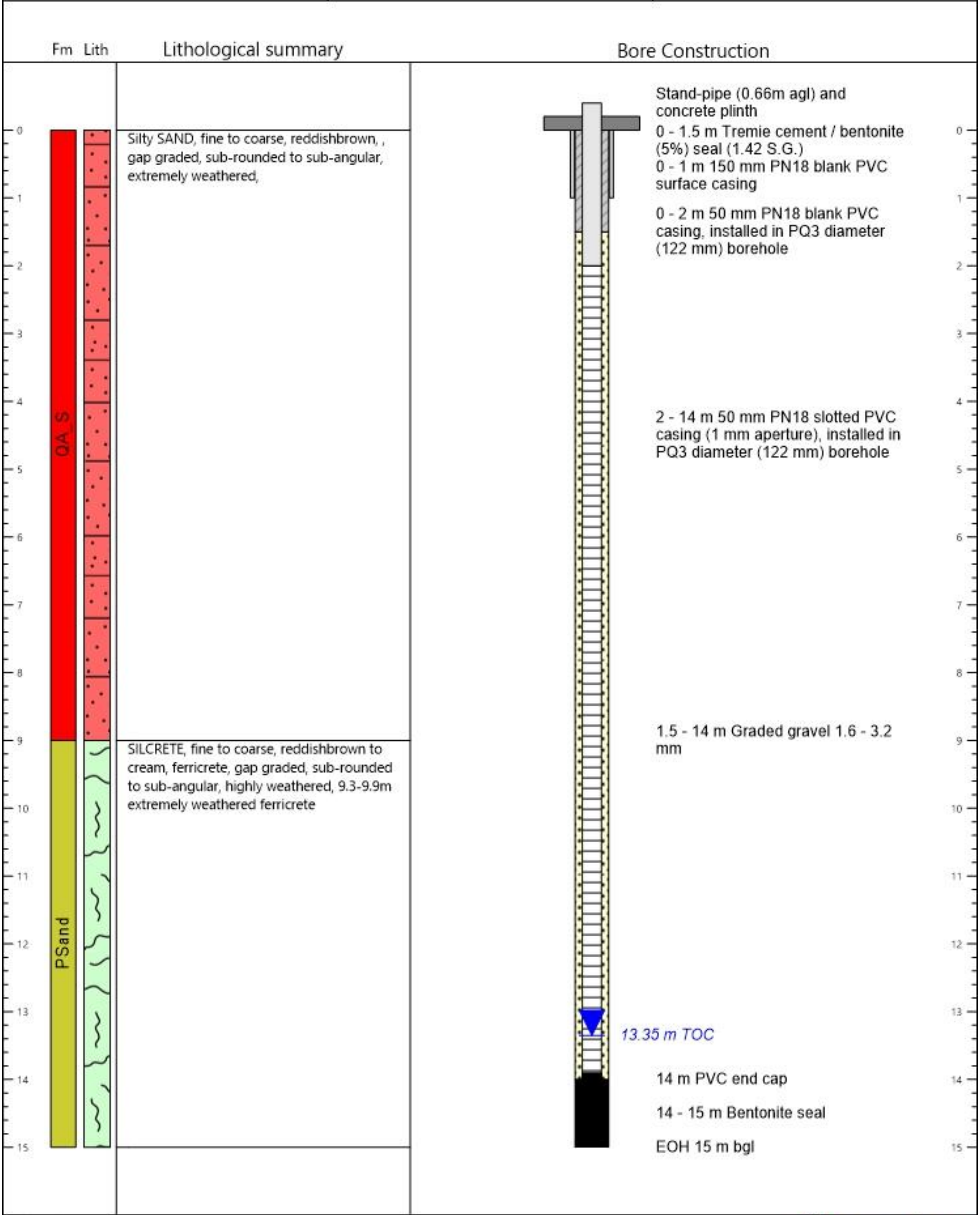

Additional notes:

WINU1557 - Composite Bore Log

Project: Winu Hydrogeological Investigation Program Client: Rio Tinto CRS: GDA94 MGA51 Coordinates: 372893.54 mE / 7706073.85 mN Elevation: 249.82 m AHD (RL = TOC)	Construction start date: 14/09/2024 Construction end date: 15/09/2024 Inclination: -90° Depth drilled: 15 m BGL	Final airlift yield: N/A L/s EC: N/A µS/cm pH: N/A Temp: N/A °C Static Water Level: 10.82 m TOC

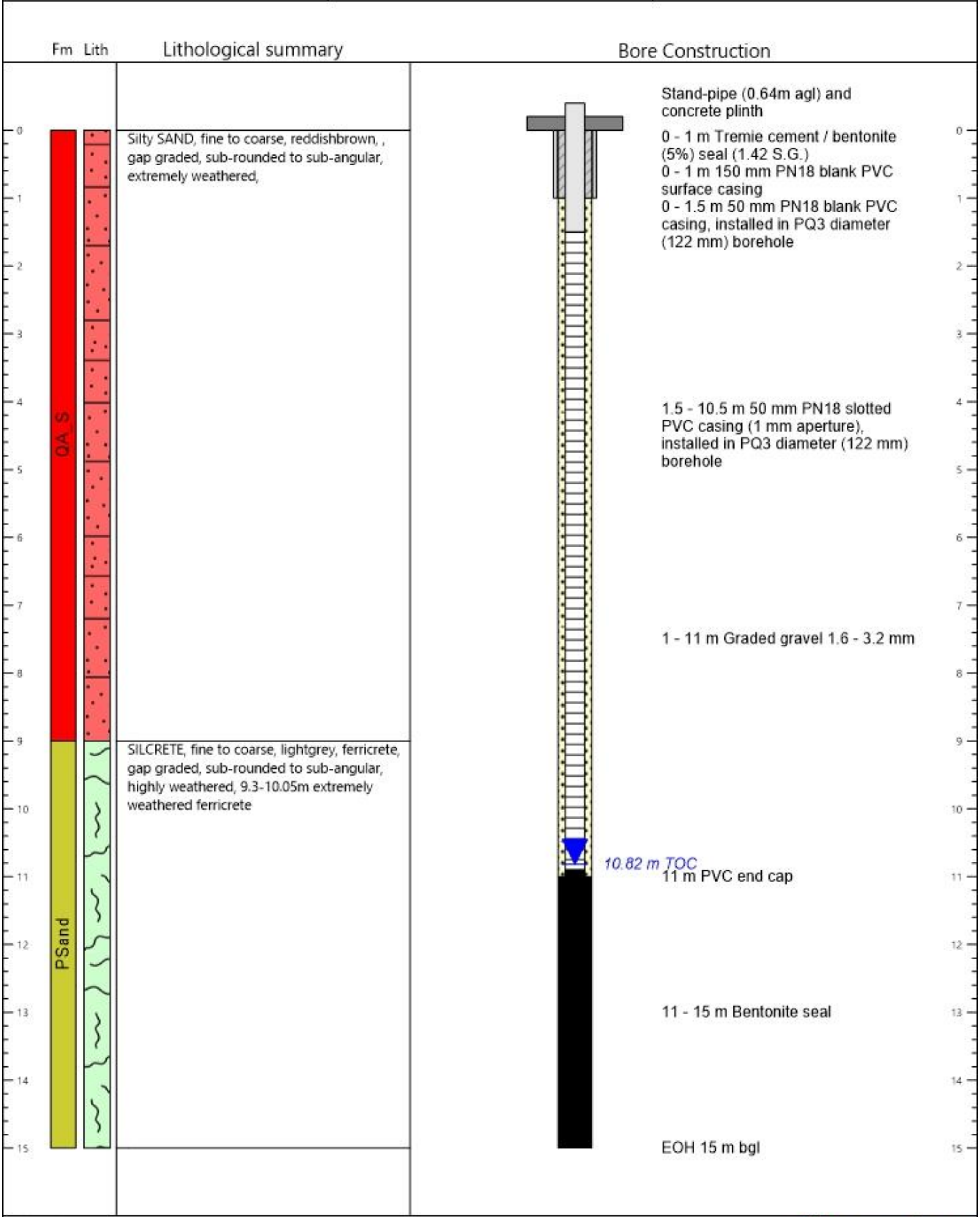

Additional notes:

WINU1558 – Composite Bore Log

Project: Winu Hydrogeological Investigation Program Client: Rio Tinto CRS: GDA94 MGA51 Coordinates: 372880.54 mE / 7706083.08 mN Elevation: 249.88 m AHD (RL = TOC)	Construction start date: 13/09/2024 Construction end date: 14/09/2024 Inclination: -90° Depth drilled: 15 m BGL	Final airlift yield: N/A L/s EC: N/A µS/cm pH: N/A Temp: N/A °C Static Water Level: 11.55 m TOC

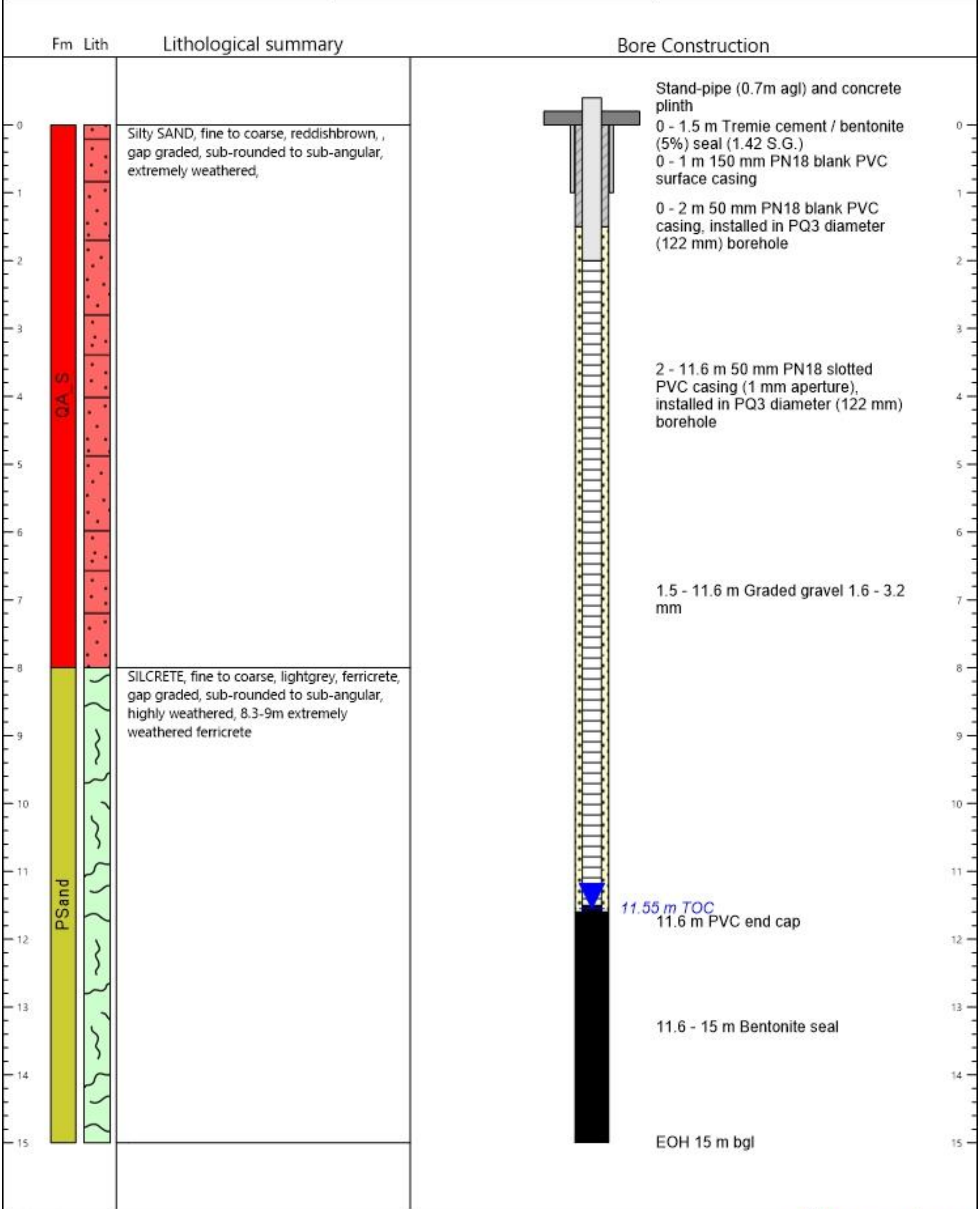

Additional notes:

Appendix C. Uncertainty Analysis Hydrographs

C1 Uncertainty MAR

WINU1071

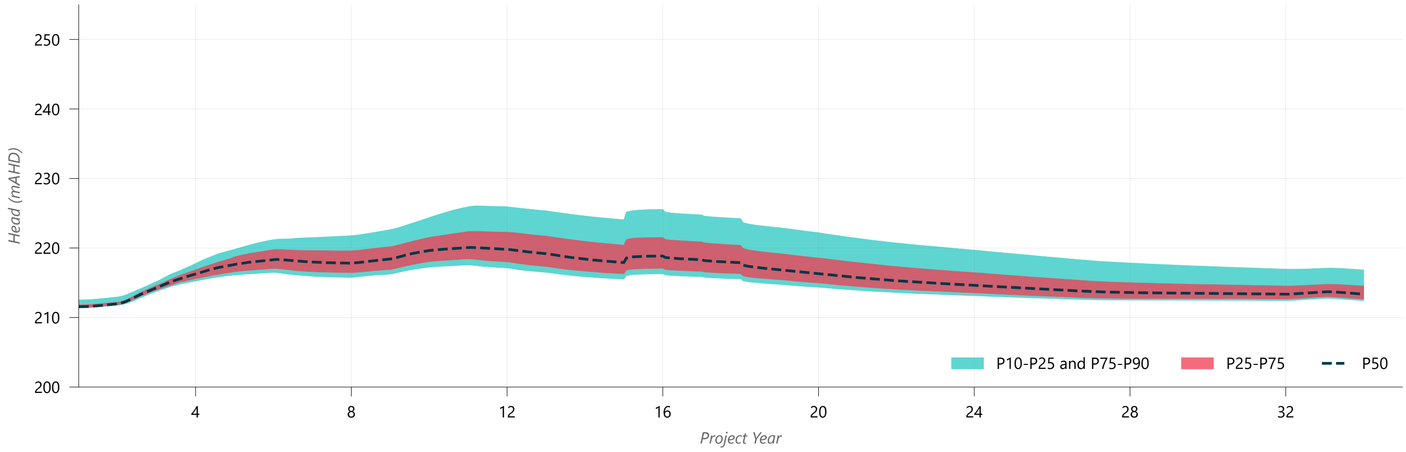

WINU1072

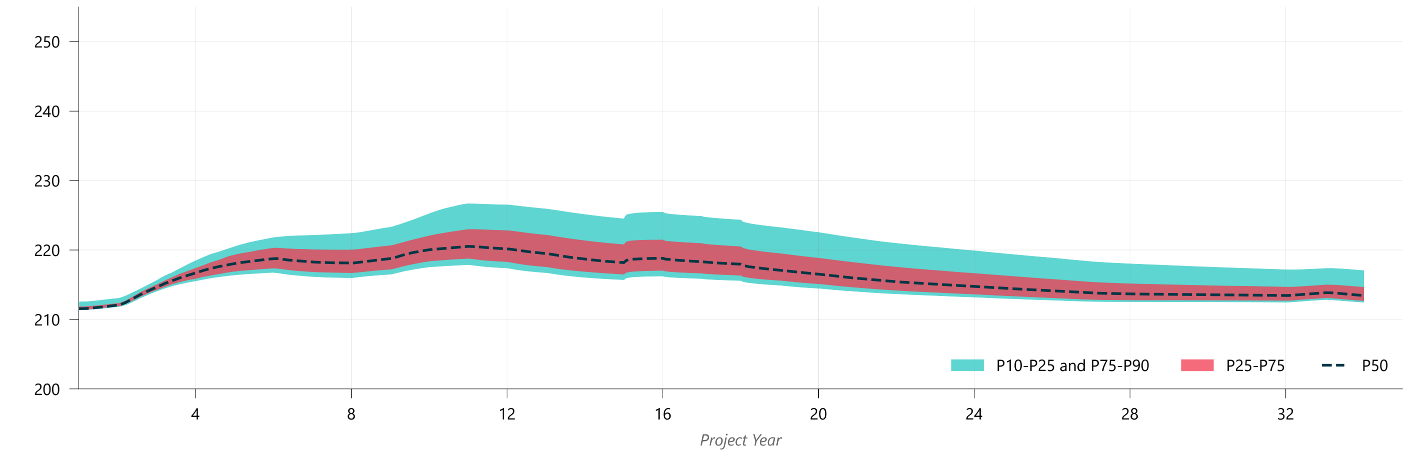

WINU1073

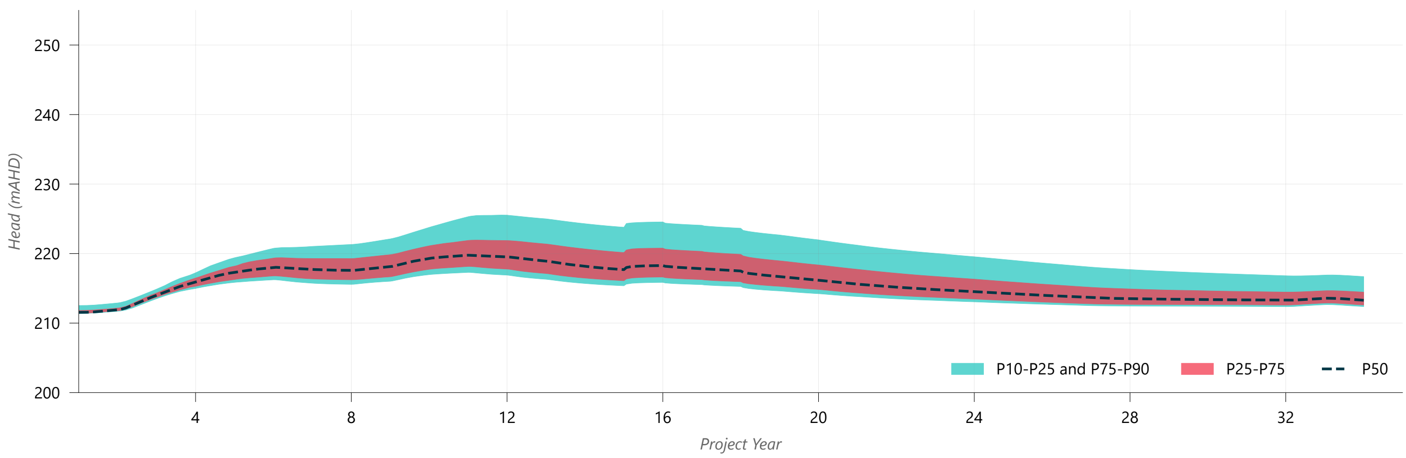

WINU1318

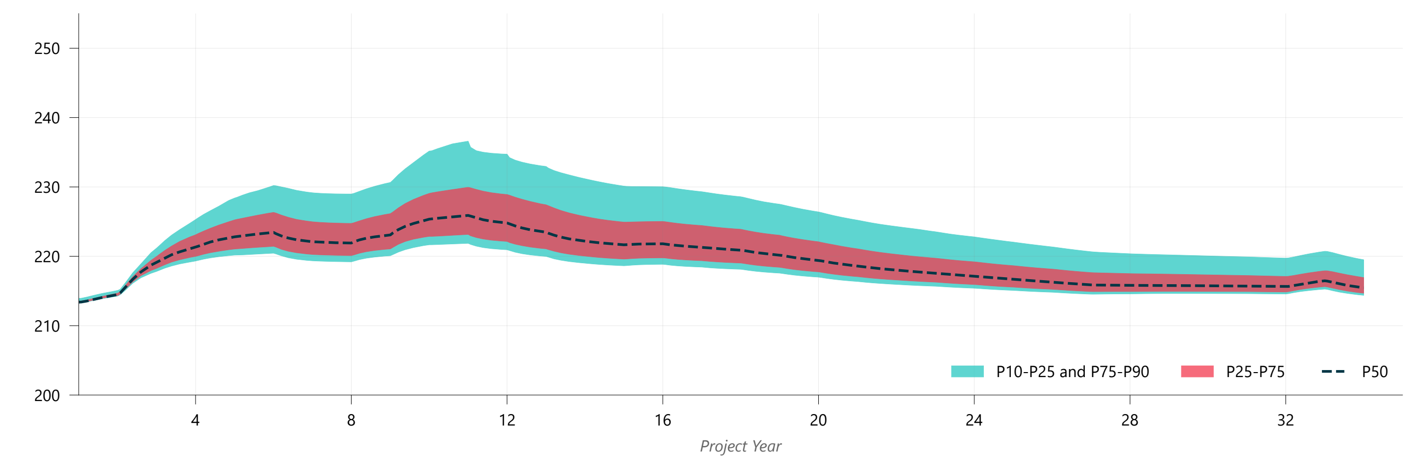

WINU1325

WINU1326

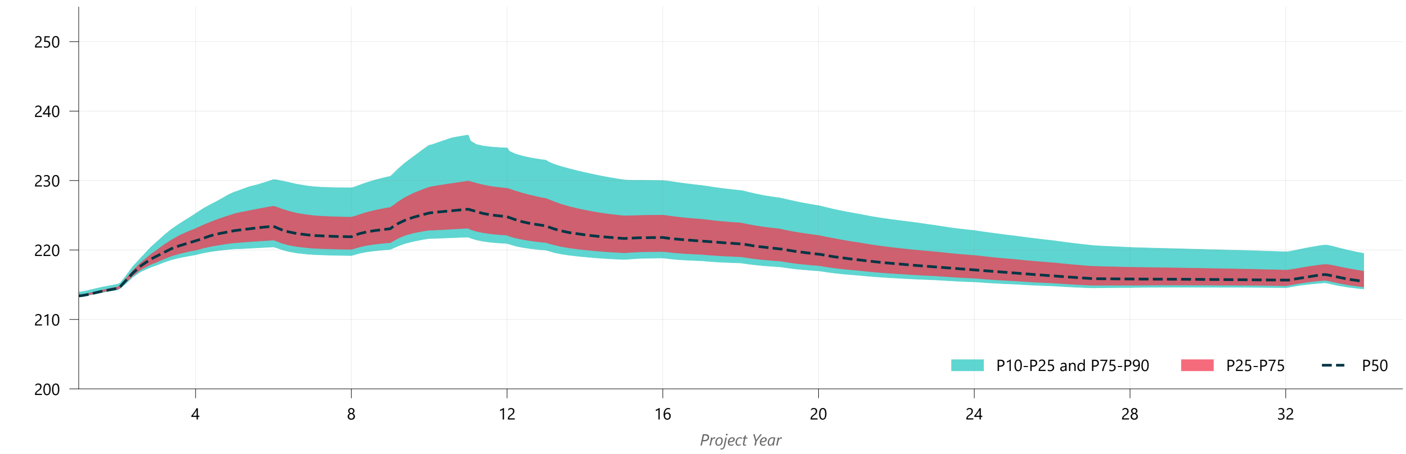

WINU1327

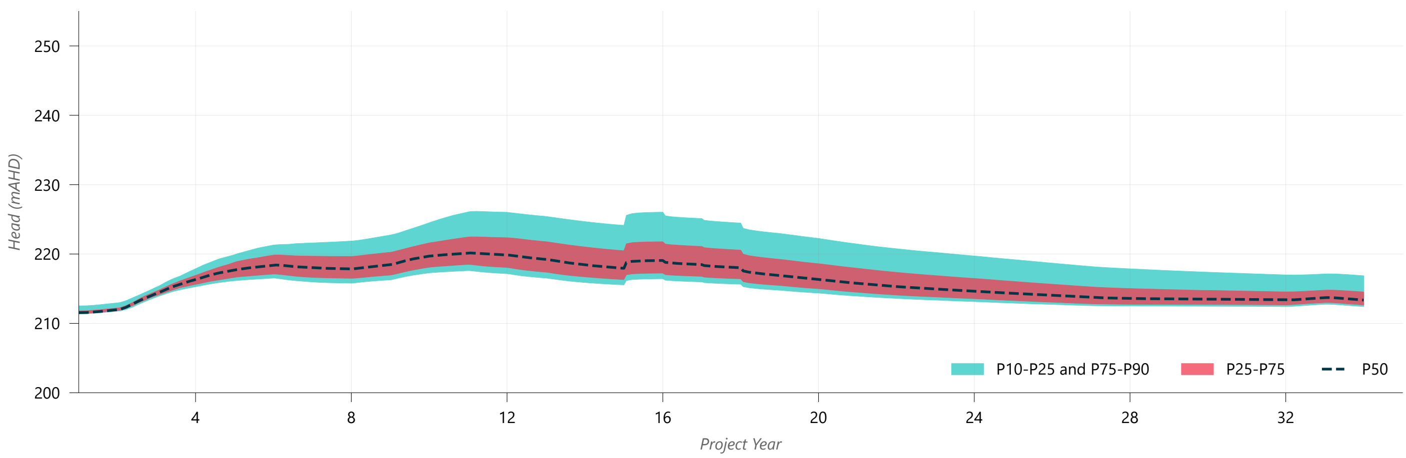

WINU1551

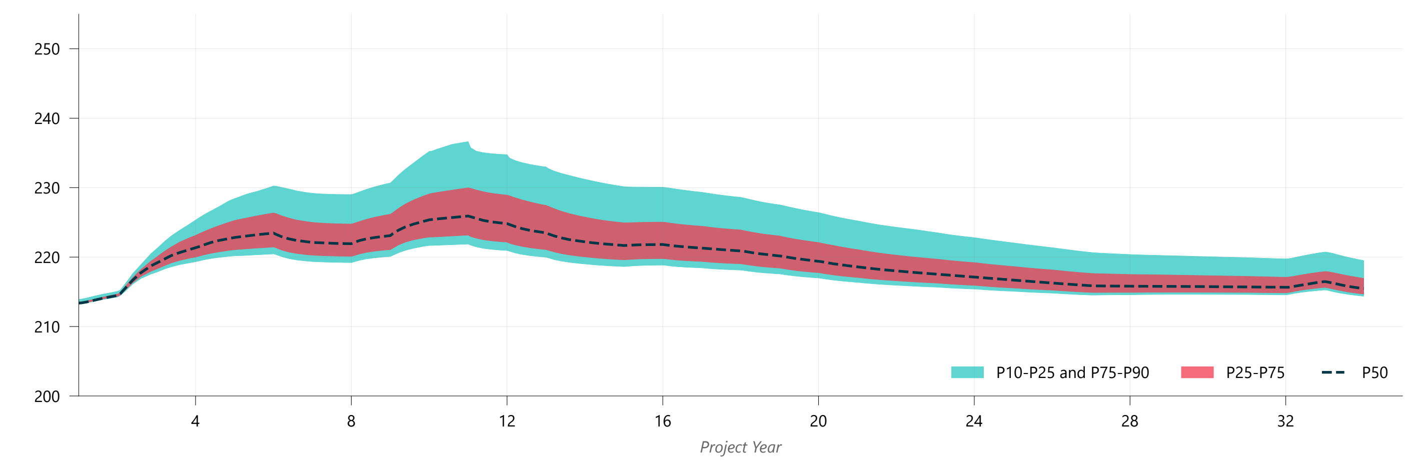

WINU1552

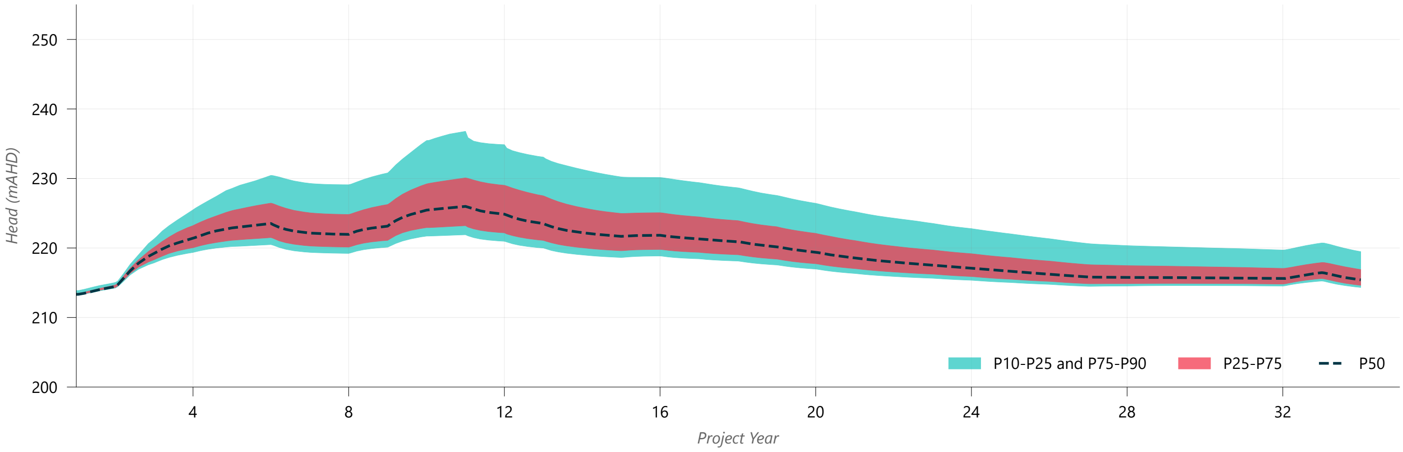

WINU1553

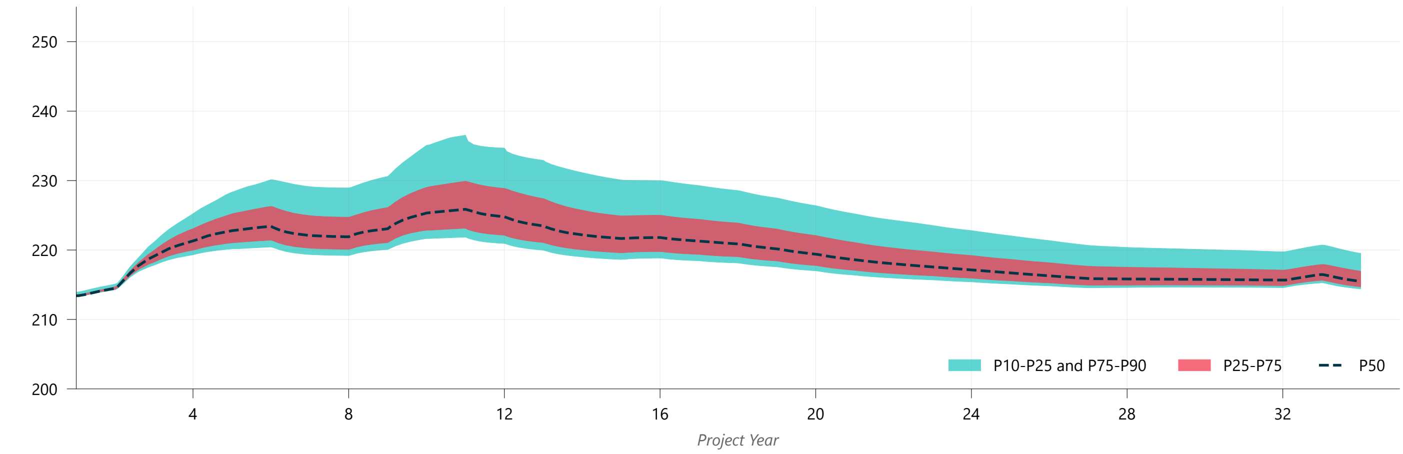

WINU1554

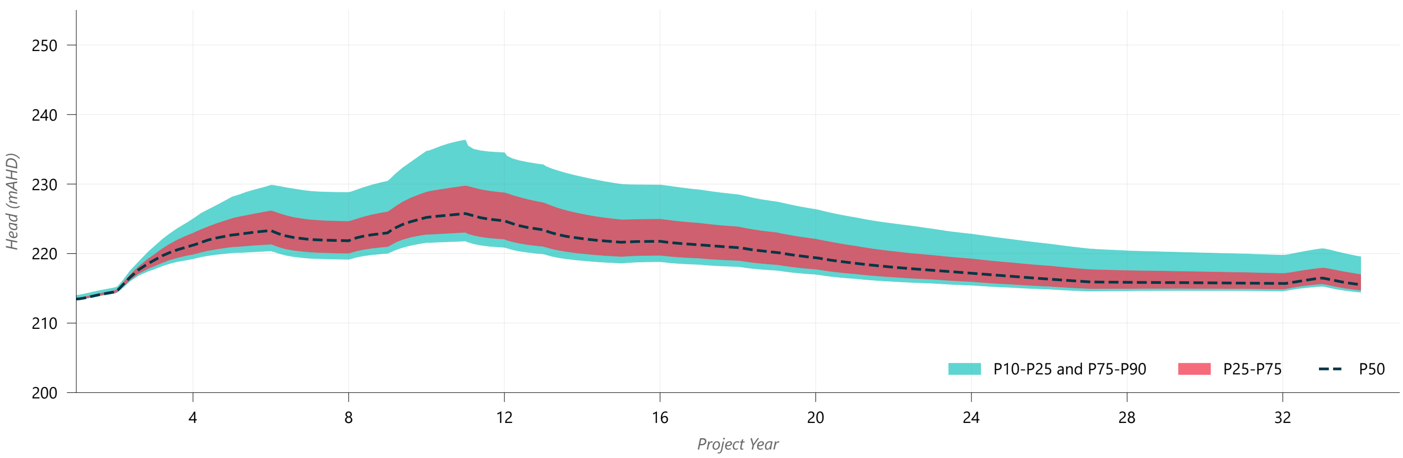

C2 Uncertainty Ponds

WINU1071

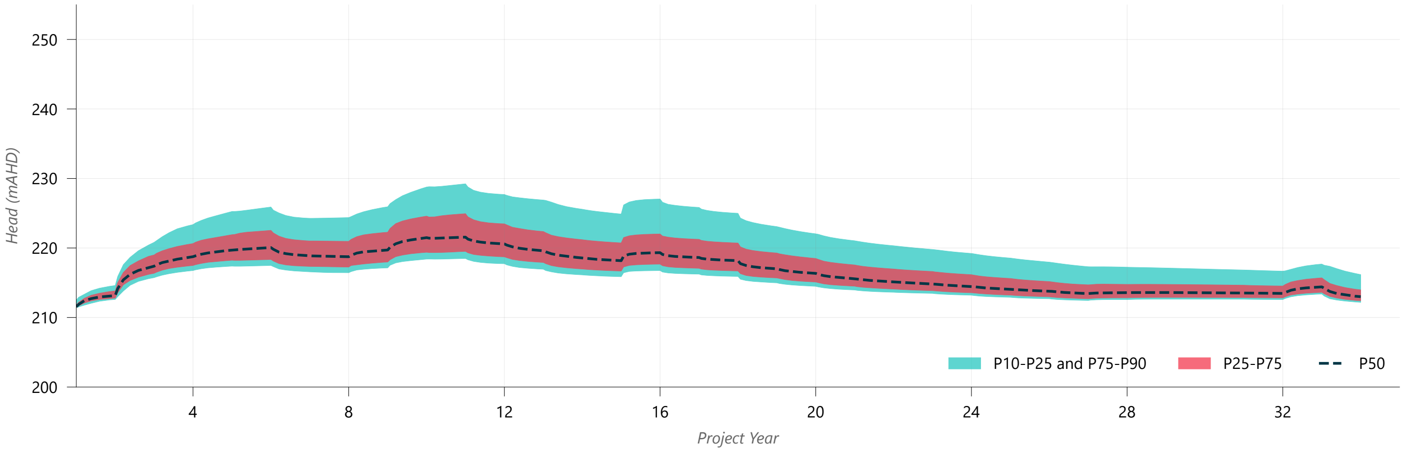

WINU1072

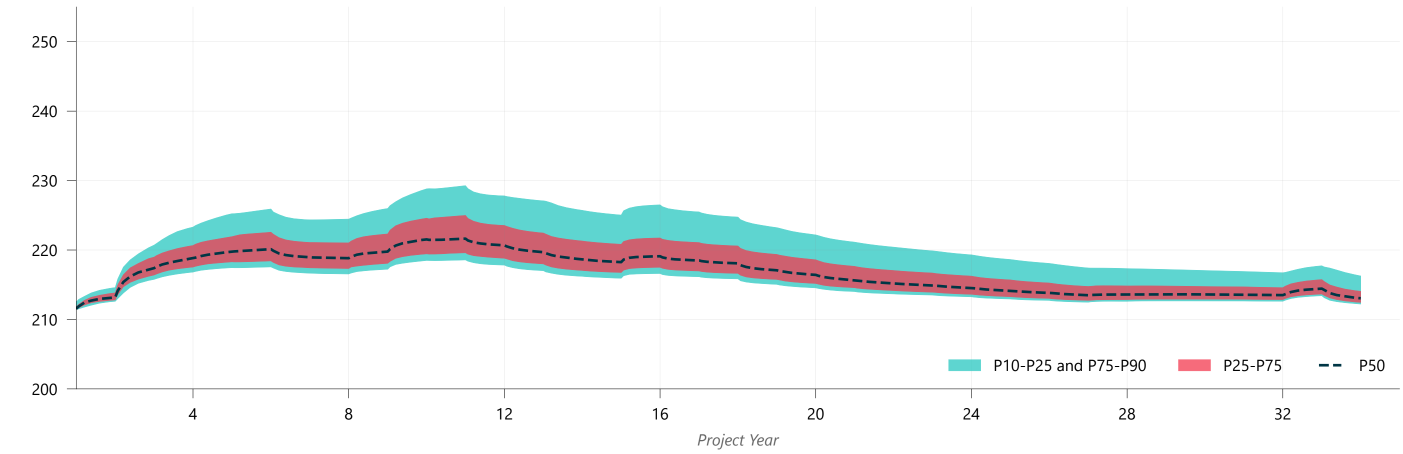

WINU1073

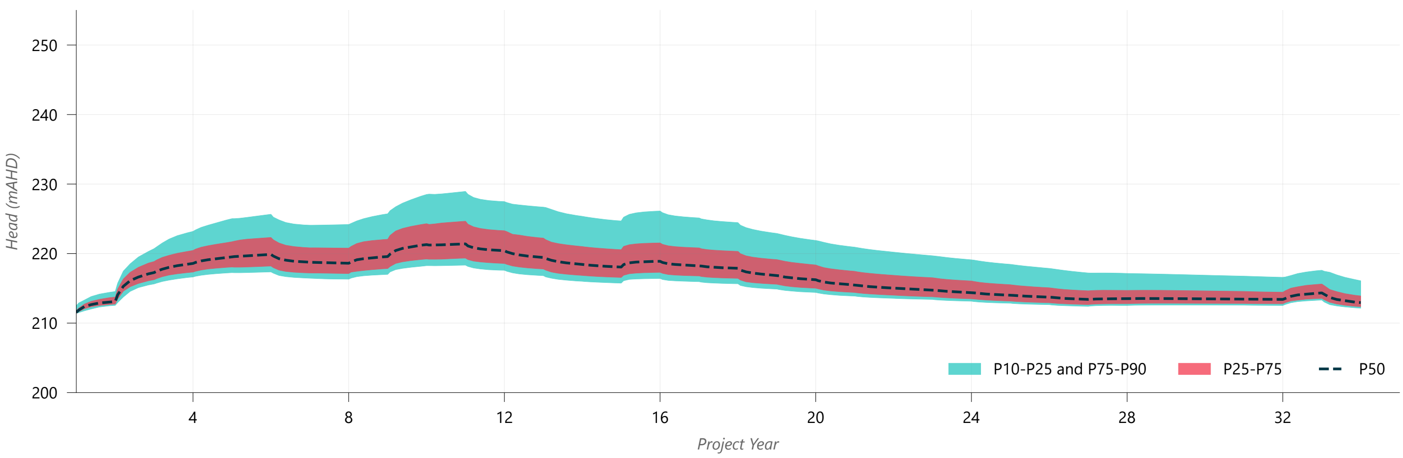

WINU1318

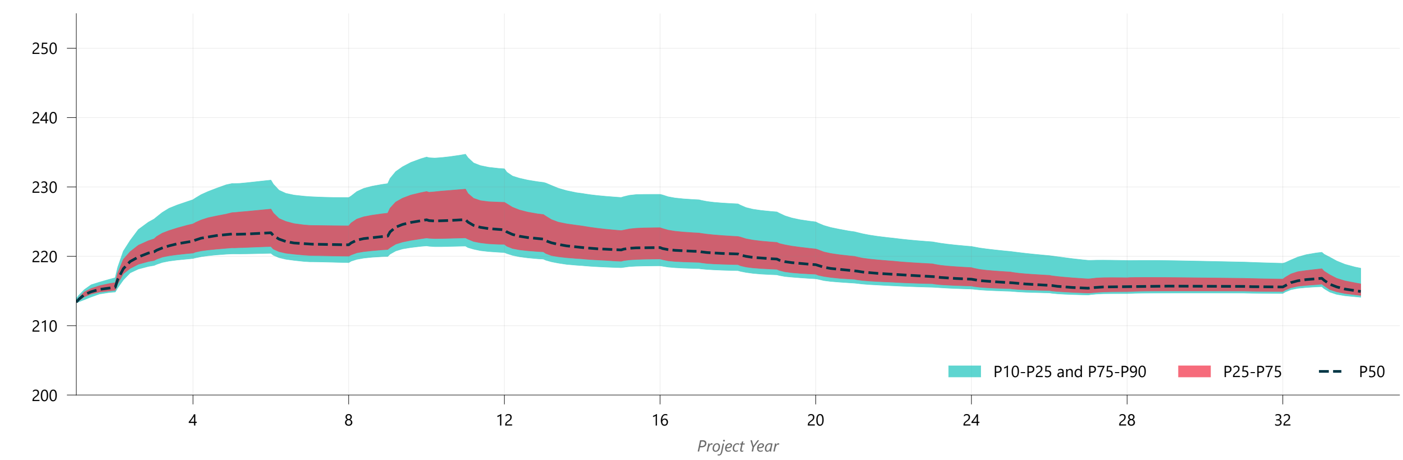

WINU1325

WINU1326

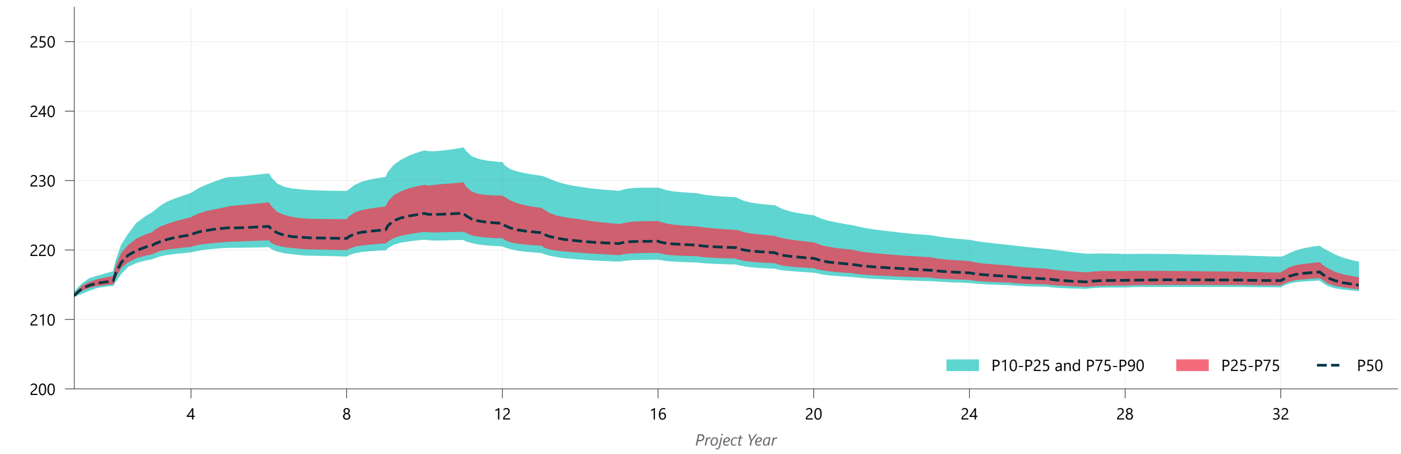

WINU1327

WINU1551

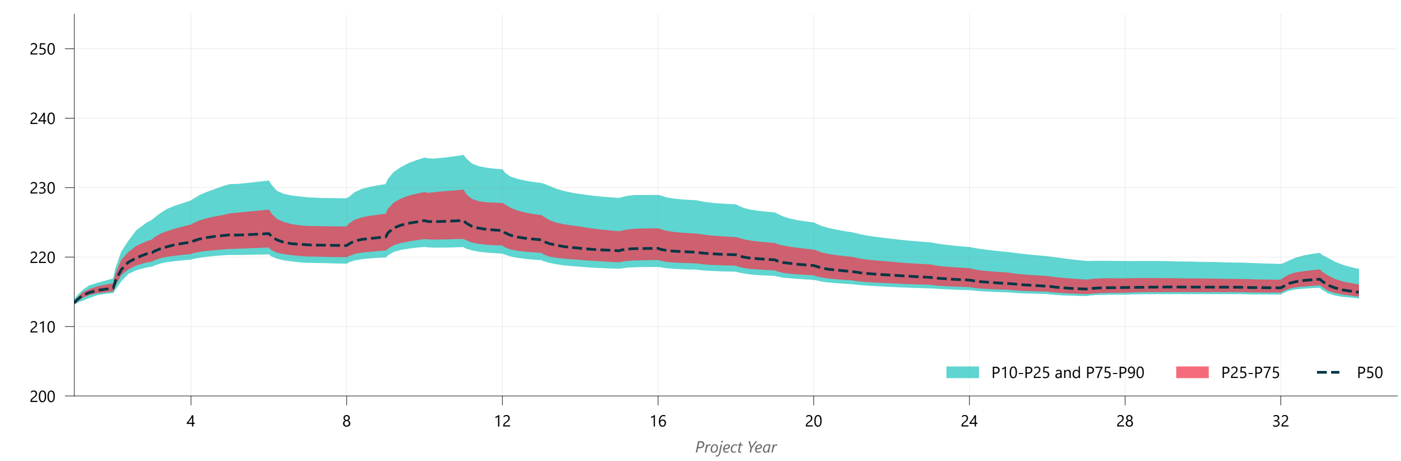

WINU1552

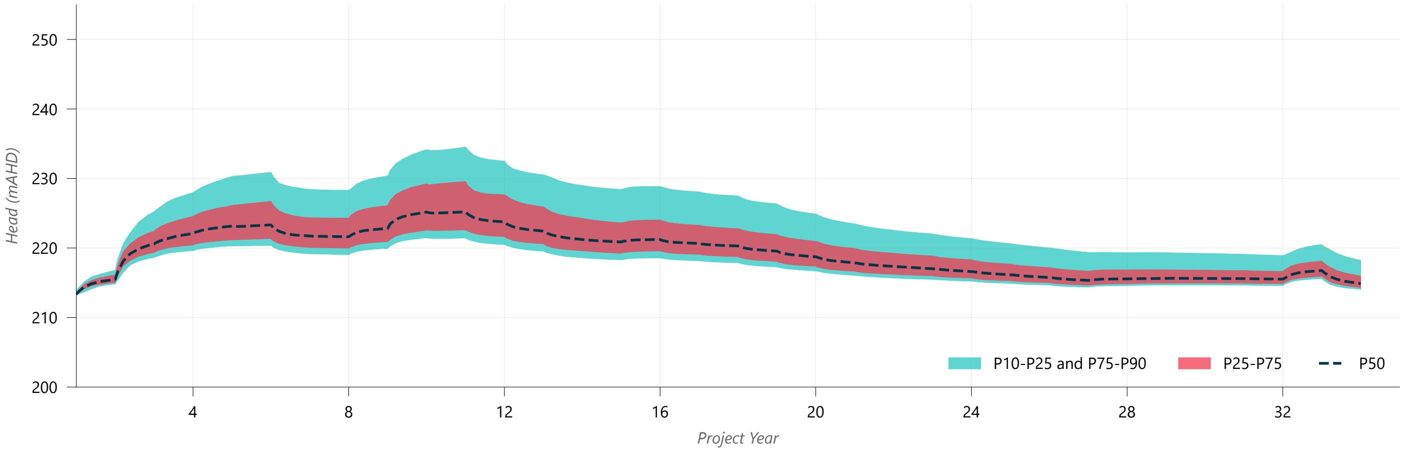

WINU1553

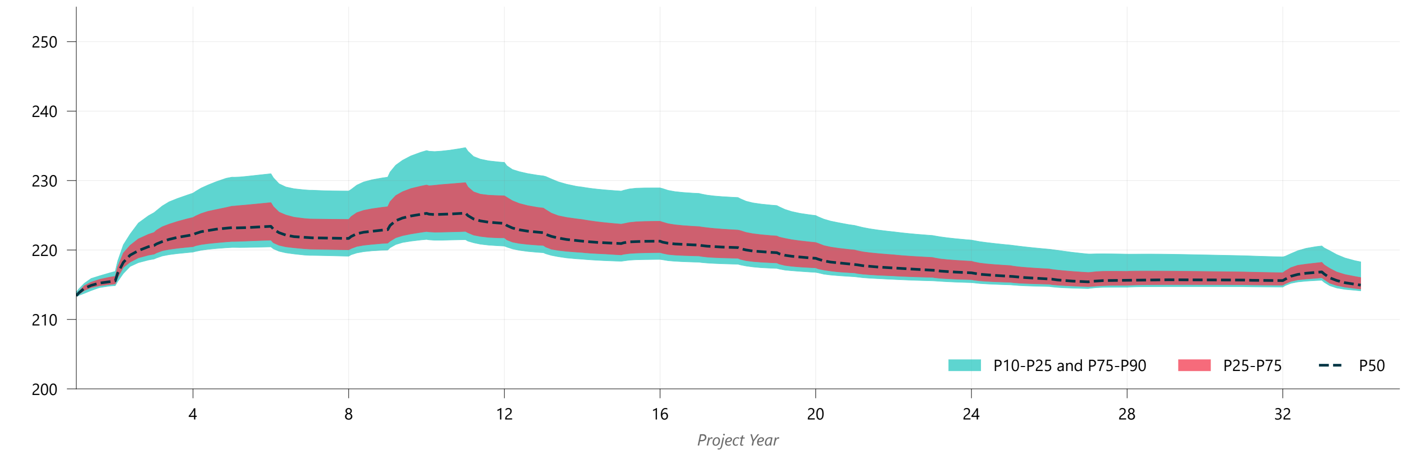

WINU1554